

Inês de Sousa Bernardino

Investigation of the dorsal stream hypothesis in Williams syndrome

Tese de Doutoramento em Ciências da Saúde, ramo de Ciências Biomédicas orientada por Miguel Castelo-Branco e Marieke van Asselen e apresentada à Faculdade de Medicina da Universidade de Coimbra

2013



UNIVERSIDADE DE COIMBRA

**Investigation of the dorsal stream hypothesis
in Williams syndrome**

Inês de Sousa Bernardino

2013

The studies presented in this thesis were carried out at the Visual Neuroscience Laboratory at IBILI (Institute for Biomedical Imaging and Life Sciences), Faculty of Medicine, University of Coimbra, Portugal, and were supported by a personal fellowship from the Portuguese Foundation for Science and Technology (SFRH/BD/41401/2007) and by grants from the Portuguese Foundation for Science and Technology [Grant numbers PTDC/SAU-NEU/68483/2006, PTDC/SAU-ORG/118380/2010, PIC/IC/82986/2007 and PTDC/SAU-NSC/113471/2009].

Cover design: João Castelhana and Inês Bernardino

ISBN: 978-989-20-3790-5

Copyright © 2013 Inês Bernardino

FCT
Fundação para a Ciência e a Tecnologia
MINISTÉRIO DA CIÊNCIA, TECNOLOGIA E ENSINO SUPERIOR

POPH
PROGRAMA OPERACIONAL POTENCIAL HUMANO


UNIÃO EUROPEIA
Fundo Social Europeu

Universidade de Coimbra

Faculdade de Medicina



**Investigation of the dorsal stream hypothesis
in Williams syndrome**

Thesis to obtain a Ph.D. degree in Health Sciences in the domain of Biomedical Sciences,
supervised by Miguel Castelo-Branco and Marieke van Asselen presented at the Faculty
of Medicine of the University of Coimbra

Tese de Doutoramento em Ciências da Saúde, ramo de Ciências Biomédicas orientada
por Miguel Castelo-Branco e Marieke van Asselen e apresentada à Faculdade de
Medicina da Universidade de Coimbra

Inês de Sousa Bernardino

2013

Supervised by: Miguel Castelo-Branco, Ph.D.

Co-Supervised by: Marieke van Asselen, Ph.D.

Para a Rosalia, a Joaquina e o António

“Quem te falou numa verdade enganou-te, há mais verdades escondidas por aí...”

In Lídia, Anaquim

Contents

Abbreviations	VIII
Summary	XI
Sumário	XIV
Introduction	
<i>Chapter 1</i>	
General Introduction	20
Aims and outline of the thesis	46
Methods	
<i>Chapter 2</i>	
Neuroscientific tools for brain function investigation: electroencephalography and functional magnetic resonance imaging	58
Results	
<i>Chapter 3</i>	
Williams syndrome as a clinical model to study the neural correlates of visual coherence: A direct comparison of local-global visual integration in WS and Autism	76
<i>Chapter 4</i>	
Dorsal-ventral stream dissociation in Williams Syndrome: a novel experimental paradigm exploring egocentric and allocentric spatial representations	104
<i>Chapter 5</i>	
Reorganization of 3D visual processing in Williams syndrome: an electrophysiological approach of coherence perception	124
<i>Chapter 6</i>	
Functional reorganization of the visual dorsal stream in Williams syndrome as probed by 3D visual coherence: an fMRI approach	146
Concluding Remarks	
<i>Chapter 7</i>	
Discussion and conclusions	171
List of Publications	181
Agradecimentos	182
Curriculum Vitae	184

Abbreviations

2D	Two-Dimensional
3D	Three-Dimensional
4D	Four-Dimensional
ADHD	Attention Deficit and Hyperactivity Disorder
ADI-R	Autism Diagnostic Interview-Revised
ADOS	Autism Diagnostic Observation Schedule
ANOVA	Analysis of Variance
ASD	Autism Spectrum Disorders
ASD_ID	ASD patients with Intellectual Disability
ASD_noID	ASD patients without Intellectual Disability
BOLD	Blood-Oxygen-Level-Dependent contrast
C_ID	Intellectual quotient matched control group
cIPS	Caudal Intraparietal Sulcus
CSD	Current Source Density
C_TD	Chronological-age matched control group
CTRL	Control Group
DNA	Deoxyribonucleic Acid
DSM-IV-TR	Diagnostic and Statistical Manual of Mental Disorders IV
DTI	Diffusion Tensor Imaging
EEG	Electroencephalography
<i>ELN</i>	Elastin gene
EOG	Electrooculogram
EPI	Echo Planar Imaging
ERP	Event-Related Potential
ERPs	Event-Related Potentials
f	Feminine
FA	Flip Angle
FFA	Fusiform Face Area
FFT	Fast Fourier Transform
FISH	Fluorescent <i>in situ</i> Hybridization
fMRI	Functional Magnetic Resonance Imaging

IX

FOV	Field of View
FSIQ	Full-scale Intellectual Quotient
GABA	γ -Aminobutyric Acid
GC	Ganglion Cells
GLM	General Linear Model
Hb	Deoxyhaemoglobin
HbO ₂	Oxyhaemoglobin
HDR	Hemodynamic Response
HEOG	Horizontal Electrooculogram
hMT+	Human Motion Area (Medial Temporal)
ICA	Independent Component Analysis
IP	Intraparietal Area
IPS	Intraparietal Sulcus
IQ	Intellectual Quotient
ISI	Interstimulus Interval
L	Left
LCR	Low-Copy Repeat
LGN	Lateral Geniculate Nucleus
LH	Left Hemisphere
LO	Lateral Occipital Cortex
LOC	Lateral Occipital Complex
M	Magnocellular
m	Masculine
Mb	Megabyte
MEG	Magnetoencephalography
MPRAGE	Magnetization-Prepared Rapid-Acquisition Gradient Echo
MR	Magnetic Resonance
MRI	Magnetic Resonance Imaging
MST	Medial Superior-Temporal area
MTG	Middle Temporal Gyrus
O ₂	Oxygen
OFC	Orbitofrontal Cortex

X

P	Parvocellular
PEA	Perturbações do Espectro do Autismo
PIQ	Performance Intelligence Quotient
PPA	Parahippocampal Place Area
ppaf	Projected power accounted for
PSA	Parietal Shape Area
R	Right
RCPM	Ravens Coloured Progressive Matrices
RFX	Random Effects
RH	Right Hemisphere
RMF	Ressonância Magnética Funcional
ROI	Region of Interest
SE	Standard Error of the mean
SFM	Structure-From-Motion
sLORETA	Standardized Low Resolution Brain Electromagnetic Tomography
STS	Superior Temporal Sulcus
SVAS	Supravalvular Aortic Stenosis
SVPS	Supravalvular Pulmonary Stenosis
SW	Síndrome de Williams
TD_NVMA	Non-Verbal Mental Age matched control group
TD_CA	Chronological Age-matched control group
TE	Echo Time
TR	Repetition Time
VBM	Voxel-Based Morphometry
VEOG	Vertical Electrooculogram
VIQ	Verbal Intelligence Quotient
VMI	Visuo-Motor Integration Test
WAIS-III	Wechsler Adult Intelligence Scale, 3rd ed.
WCC	Weak Central Coherence
WISC-III	Wechsler Intelligence Scale for Children, 3rd. ed.
WS	Williams Syndrome
WSCP	Williams Syndrome Cognitive Profile

Summary

Williams syndrome (WS) is a rare genetically based neurodevelopmental condition associated with a unique combination of sensory, cognitive and neuroanatomical characteristics. This condition is, therefore, an outstanding model to understand cognition because it provides a rare opportunity to investigate genes, brain and behaviour relationships. WS has captured the interest of cognitive neuroscientists in the last decades, mainly because of its intriguing cognitive profile characterized by surprising spared language and face abilities contrasting with severe deficits in visuospatial skills and visual coherence. These patients tend to exhibit a visual bias towards local processing while failing to achieve global coherence from the integration of local cues. Functional dissociations in the cognitive domain have been concomitantly investigated at the neural level in particular in which concerns both dorsal and ventral visual processing pathways. However, the existing literature on this topic has not yet settled this issue and the neurophysiological and neuroanatomical correlates of such impairments remain unclear.

The main focus of this thesis is the investigation of multiple levels of visual processing along dorsal and ventral visual pathways in WS, from the point of view of functional dissociations. These include dorsal vs. ventral, local vs. global, ego vs. allocentric processing dichotomies and their relationships. This is particularly relevant, since this condition is a neurobiological model of a split between ventral and dorsal visual processing pathways with a generalized deficit in dorsal pathway. The combination of multiple methodological modalities such as psychophysics, electrophysiology and neuroimaging tools is conducted in this thesis to allow a better characterization of the visuospatial impairments in WS and elucidate on how the neural correlates of such vulnerabilities relate to dorsal and ventral functioning.

In the first study of this thesis, visual coherence perception in WS was comprehensively investigated by probing the local-global visual processing under different task conditions (Navon hierarchical figures under perception, memory and visuoconstructive conditions) and performing a direct comparison to autism spectrum disorders (ASD) in which visual coherence weakness was also suggested, along with local vs. global and dorsal stream deficits. We confirmed the WS group as a clinical model of impaired visual coherence. These impairments were shown in WS to a larger extent than in ASD which may suggest the involvement of the dorsal visual stream (more impaired in WS than in ASD) in such perceptual mechanisms.

We further investigated the dorsal vs. ventral stream dissociation in WS by employing a novel paradigm in which dichotomic egocentric (associated with dorsal stream) and allocentric (associated with ventral stream) spatial frames of reference were investigated. A computer judgment task as well as a more ecological 3D judgment task (using a board) was used. Our findings confirmed dorsal stream vulnerability in the WS group as assessed by egocentric spatial judgments. We also found unexpected impaired allocentric spatial judgments in WS suggesting that ventral visual stream may also be compromised.

Given that the aforementioned findings confirm WS as a suitable clinical model of coherence impairment and dorsal stream vulnerability (alongside with possible slightly affected ventral stream function), we conducted two additional studies to investigate neural correlates of visual coherence impairment in WS. These studies were accomplished using electroencephalogram (EEG) and functional magnetic resonance imaging (fMRI). We used a three-dimensional (3D) structure-from-motion (SFM) task in order to assess coherent perception in which we parametrically modulated depth information. EEG data revealed distinct patterns across groups, suggesting functional reorganization in WS. We observed a novel component P200 present only in the clinical group as well as differential neural sources in occipital sites in contrast to parietal sources in controls. The fMRI study, due to its higher spatial resolution, allowed us to pinpoint the neural correlates of such reorganization. Individuals with WS recruited more medial areas (cuneus, precuneus and retrosplenial cortex) in response to 3D coherent stimuli, high-level visual object categories and simple coherent motion in contrast with typically developing controls who showed, as expected, more lateral areas (caudal intraparietal sulcus and lateral occipital cortex/hMT+). This shift to the midline we observed in the WS group pattern of activation suggests a substantial reorganization of dorsal stream regions with predominant motion processing occurring in the medial part of this visual pathway. We did not identify significant group differences regarding the ventral visual modulation. However, subtle alterations in the pattern of activation across groups were found indicating that ventral visual stream may not be as preserved as traditionally defined.

In sum, the work presented in this thesis demonstrate visual coherence impairments in WS which are associated with dorsal stream dysfunction as was assessed by multiple visual levels. The substantial reorganization of dorsal stream observed in our EEG and fMRI studies may contribute to alterations in the ventral visual stream which already demonstrated slight vulnerabilities. These findings improve our knowledge concerning the nature of

XIII

functional dissociations (dorsal/ventral, ego/allo and local/global) in WS and provide insight on the mechanisms of visual processing within the dorsal stream.

Sumário

O Síndrome de Williams (SW) é uma perturbação genética rara do neurodesenvolvimento caracterizada por alterações sensoriais, cognitivas e neuroanatômicas. Esta patologia constitui, por isso, um modelo ímpar para investigar a natureza modular (ou não) dos processos cognitivos, dado que proporciona uma oportunidade rara de estudo das relações entre genes, cérebro e comportamento. O SW tem suscitado interesse no domínio das neurociências cognitivas, devido ao seu perfil cognitivo peculiar, caracterizado por funções preservadas no domínio da linguagem e do reconhecimento facial em oposição a consideráveis défices de coerência visual e de perceção visuo-espacial. No SW verifica-se um viés a favor do processamento visual local, falhando ao mesmo tempo na integração desta informação local que é determinante para a perceção de coerência global. Estas dissociações funcionais no domínio cognitivo têm sido estudadas a par com dissociações ao nível do funcionamento neuronal particularmente no que diz respeito às vias de processamento visual dorsal e ventral. Contudo, o debate persiste e os correlatos neuroanatômicos e neurofisiológicos destes défices não estão ainda estabelecidos.

O foco desta tese prende-se com a investigação de múltiplos níveis de processamento visual associados às vias dorsal e ventral no SW, com especial enfoque nas dissociações funcionais encontradas nesta patologia. Nestas incluem-se as dicotomias funcionais entre as vias dorsal vs. ventral, o processamento local vs. global e as representações egocêntricas vs. alocêntricas, bem como as relações entre eles. O estudo destas dicotomias é relevante no SW pois este é um modelo neurobiológico de dissociação entre as vias visuais ventral e dorsal, caracterizada por um défice acentuado desta última. Nesta tese foram usadas de forma complementar múltiplos métodos tais como a psicofísica, eletrofisiologia bem como neuroimagem funcional com vista a melhor caracterizar os défices visuo-espaciais no SW e elucidar em que medida os seus correlatos neuronais se prendem com o funcionamento das vias dorsal e ventral.

Neste trabalho, a coerência visual foi extensivamente investigada no SW através da avaliação do processamento visual local e global sob várias condições experimentais (perceção, memória e capacidade visuo-construtiva) comparando com as perturbações do espectro do autismo (PEA), que têm sido associadas a défices de coerência visual, do processamento local vs. global e do funcionamento da via dorsal. O nosso primeiro estudo confirmou o SW como um modelo clínico de coerência visual diminuída, mostrando que

estes défices são mais severos nesta patologia do que nas PEA sugerindo o envolvimento da via dorsal (mais afectada no SW) neste tipo de processamento.

O estudo da dissociação entre as vias dorsal e ventral no SW foi aprofundado, no segundo estudo, usando um novo paradigma experimental no qual investigámos representações espaciais egocêntricas (associadas à via dorsal) e allocêntricas (associadas à via ventral) no SW. Desenvolvemos uma tarefa experimental em computador e outra utilizando um tabuleiro (com maior validade ecológica). Ambos os tipos de representação espacial se mostraram alteradas no grupo de SW. Para além de confirmarem défices na via visual dorsal no SW (representações egocêntricas), os nossos resultados revelaram alterações inesperadas nas representações espaciais allocêntricas sugerindo que a via ventral pode também estar afetada nesta condição.

Uma vez confirmado que o grupo de SW constitui um modelo clínico de coerência visual diminuída e alterações da via dorsal, realizámos dois estudos adicionais, com vista a estabelecer os correlatos neuronais dos défices de coerência visual no SW. Devido ao seu carácter complementar, estes estudos usaram respetivamente eletroencefalografia (EEG) e ressonância magnética funcional (RMF).

A percepção de coerência foi avaliada com uma tarefa de percepção de estrutura tridimensional através do movimento na qual modulámos a informação de profundidade. Os dados de EEG revelaram padrões distintos entre os grupos, sugerindo uma organização neuronal alternativa no SW. Um novo componente, o P200, foi observado somente para este grupo e foram observadas diferentes fontes neuronais, sobretudo localizadas no lobo occipital por contraste às fontes parietais encontradas nos controlos. A elevada resolução espacial da RMF permitiu ao estudo subsequente uma melhor localização dos correlatos neuronais desta reorganização. Verificou-se que, enquanto os controlos ativam as áreas dorso-laterais esperadas (sulco intraparietal caudal e córtex occipital lateral/hMT+), os indivíduos com SW recrutam áreas mais mediais (cuneus, precuneus e córtex retrosplenial) em resposta aos estímulos coerentes em 3D, mas também a imagens estáticas de várias categorias visuais e movimento coerente simples (2D). A ativação em zonas mais mediais do cérebro observada no grupo de SW sugere uma reorganização substancial das regiões da via dorsal, com o processamento de movimento a ocorrer na parte medial desta via. Não encontramos diferenças entre os grupos no que respeita à via ventral, não obstante ligeiras alterações nos padrões de ativação entre os grupos que poderão indicar que esta via não está tão preservada quanto o esperado.

O trabalho aqui apresentado demonstra défices de coerência visual no SW que estão associados à disfunção da via dorsal, avaliada em múltiplos níveis visuais. A reorganização substancial da via dorsal observada no SW pode levar a alterações na via visual ventral, como sugerido pelos nossos estudos. Estes resultados contribuem para o conhecimento relativo à natureza das dissociações funcionais (dorsal/ventral, ego/alo e local/global) no SW e proporcionam um avanço no nosso entendimento dos mecanismos de processamento visual que ocorrem na via dorsal.

INTRODUCTION

CHAPTER I

General Introduction

*“It makes me feel special to have Williams, you know? (...) because if I didn't have it, then what would I be like?
(...) Would I be different to other people? Would I have friends like these people, or what would I be doing? I really
don't know.”*

(Jeremy Vest - Williams syndrome patient)

In this introductory chapter, the central clinical and neurocognitive characteristics of WS will be described as well as the current knowledge regarding the nature of neuroanatomical and neurophysiological functioning in this condition. In addition, a close look into the parallel organization of the visual system will be provided with a focus on the characterization of both ventral and dorsal visual processing pathways. The different experimental paradigms employed to investigate this topic will be discussed along with further implications for the understanding of the pathophysiology of visuospatial impairments in WS and their neural substrates. The final part of this chapter will present the general outline of this thesis and elucidate its main objectives.

Historical overview

The first references to a combination of clinical features consistent with the diagnosis of WS were provided in early reports describing children who had idiopathic infantile hypercalcaemia, short stature and congenital malformations (Fanconi, Girardet, Schlesinger, Butler, & Black, 1952). Despite these first sparse descriptions, WS was firstly described as a clinical entity in 1961 by John Williams, a New Zealand cardiologist who identified four children sharing a specific form of heart defect (supravalvular aortic stenosis - SVAS), mental retardation and peculiar facial features.

“The presence of supravalvular aortic stenosis in mentally retarded patients with the unusual facial features here detailed may constitute a syndrome that has not previously been described” (Williams, Barratt-Boyes, & Lowe, 1961, p.1317).

Concurrently, Beuren, Apitz and Harmjanz also described four children with the same characteristics identified by Williams (Beuren, Apitz, & Harmjanz, 1962). For this reason, WS is sometimes also referred to as Williams-Beuren syndrome.

In the mid-1980s, an increasing interest on this condition emerged in the scientific community and significant advances were made towards understanding the neuropsychological, neurobiological and psycho-educational features of WS. The pioneering work of Bellugi and colleagues in 1988 (Bellugi, Sabo, & Vaid, 1988a) highlighted some clear-cut dissociations in the cognitive architecture of this condition, well summarized in the statement that “Williams syndrome represents a clear dissociation between intact language

abilities and severe cognitive deficits” (Mervis, 2003, p. 2). This led to an ample discussion on the relevance of this disease model for the debate concerning the modularity of mind. Many researchers either in favour or against the modular organization perspective have devoted substantial attention to the WS neurocognitive profile.

Etiology: genetic basis

Until the 1990s, the etiology of WS was unknown and it was not even determined whether it has a genetic basis. In the early 1990s, reports of parent–to-child transmission and monozygotic twin concordance for WS came out and provided the first hint for the putative genetic basis of WS (Morris, Thomas, & Greenberg, 1993; Murphy, Greenberg, Wilson, Hughes, & DiLiberti, 1990). The classification of this condition as a genetic disorder occurred in 1993 when Ewart et al. (1993) discovered that WS is related to the elastin gene (*ELN*) deletion, after being established that the disruption of *ELN* at 7q11.23 is associated with SVAS. This finding was extensively confirmed (Lowery et al., 1995; Nickerson, Greenberg, Keating, McCaskill, & Shaffer, 1995) and a growing body of research has been dedicated to the study of the molecular basis of the WS cognitive and neuroanatomical phenotype (Antonell et al., 2010; Cusco et al., 2008).

It is now well accepted that WS results from a hemizygous microdeletion in a single copy region of the long arm of chromosome 7 (7q11.23) involving the *ELN* gene. As a result, the definitive diagnostic of WS is performed by a laboratory test named fluorescent *in situ* hybridization (FISH), in which a DNA (deoxyribonucleic acid) probe for the *ELN* gene is labelled with a brightly coloured fluorescent dye (Lowery et al., 1995). The common microscopic deletion on chromosome 7 is detectable by the FISH test in more than 90% of the WS individuals (Nickerson et al., 1995). Deletions occur sporadically, although some cases with autosomal dominant inheritance have been reported, and are independent of the parental origin of the disease-transmitting chromosome (Perez Jurado, Peoples, Kaplan, Hamel, & Francke, 1996).

The common microdeletion is composed by a single copy gene region of approximately 1.5 million base (Mb) pairs of DNA flanked by three large low-copy-repeat sequences (LCR), organized in LCR blocks A, B and C. The breakpoints in the typical WS deletion are located in the inner duplicated regions within the centromeric and medial LCR block B. Although nearly 20 genes have been mapped within this deleted region, a genotype-

phenotype correlation has been established for only a few, with *ELN*, *LIMK1*, *GTF2I*, *GTF2IRD1*, and *CYLN2* being the most investigated (see Figure 1.1). The study of “atypical” WS deletions (deletion-sizes ranging from ~0.2Mb to ~2.5Mb) as well as experiments with mice models have been crucial to determine the role of the deleted genes in the WS phenotype (Gagliardi, Bonaglia, Selicorni, Borgatti, & Giorda, 2003; Osborne, 2010).

The *ELN* was the first deleted gene identified and its haploinsufficiency has been suggested to cause connective-tissue abnormalities and cardiovascular diseases such as SVAS and supravalvular pulmonary stenosis (SVPS), frequently found in WS (Ewart et al., 1993).

The *LIMK1* is an *ELN* neighbouring gene and encodes LIM-kinase1 protein. This protein is highly expressed in neurons and has been suggested as the candidate gene underlying the visuospatial difficulties found in these patients (Frangiskakis et al., 1996; Meng et al., 2002). However, the contribution of this gene to the WS cognitive profile remains inconclusive, since patients with very small or atypical deletions including only *ELN* and *LIMK1* do not show visuospatial impairments (Gagliardi et al., 2003).

Additionally, evidences have been gathered suggesting that the loss of genes such as *CYLN2*, *GTF2I* and *GTF2IRD1* may contribute to the unique behavioural and cognitive pattern of this disorder. *CYLN2* was proposed to be one of the major candidates for motor and cognitive deficits in WS (van Hagen et al., 2007). Disruption of the *GTF2IRD1* in mice resulted in reduced fear and aggression as well as increased social behaviour which is in accordance with the personality profile of WS (Morris et al., 2003). More recently, a study of a larger 1.8Mb microdeletion encompassing an additional gene, the transcription factor *GTF2IRD2*, demonstrated that the deletion of this gene may be associated with pronounced impairments in spatial functioning, social reasoning, cognitive flexibility and executive functioning (Porter et al., 2012). Finally, haploinsufficiency of *BAZ1B* has been associated with hypercalcaemia in individuals with WS (Schubert, 2009).

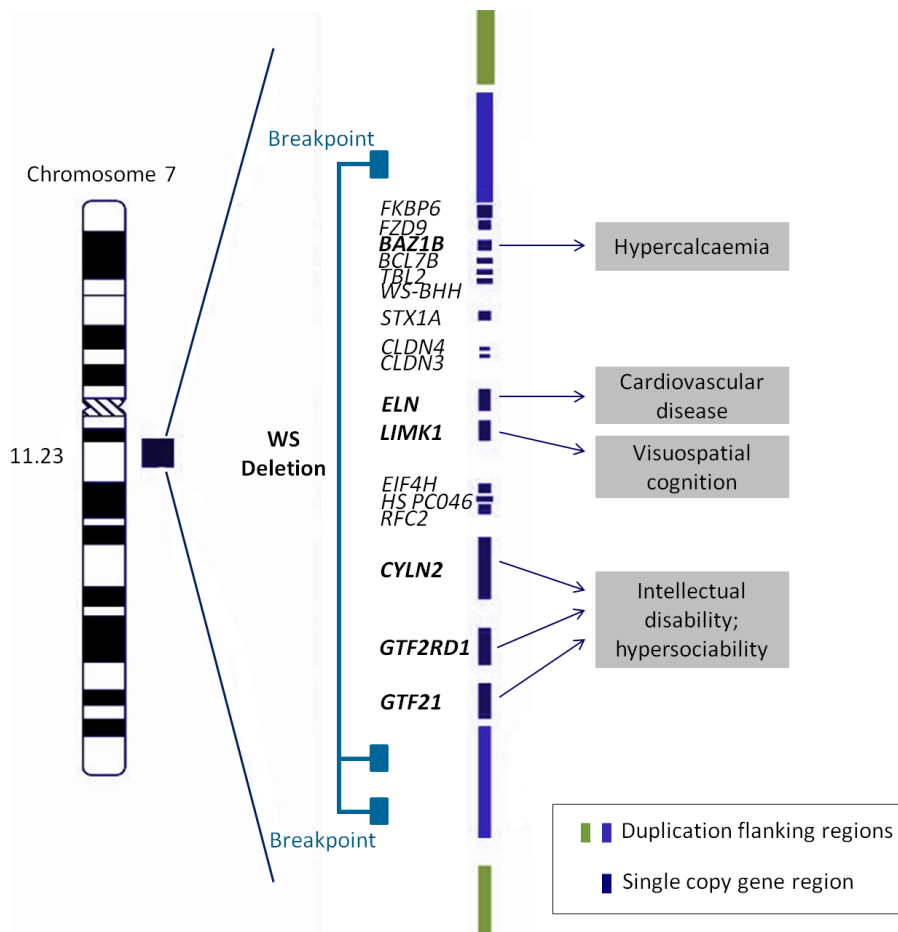


Figure 1.1. Summary of single genes within the region of chromosome 7, band 7q11.23. The common deleted region in WS is represented by a solid dark blue square and is expanded to the right to show the single genes flanked by duplicated regions. The contribution of some mapped genes to explain specific characteristics of WS phenotype is also illustrated. (Adapted from Antonell, Del Campo, Flores, Campuzano, & Perez-Jurado, 2006; Korenberg, Bellugi, Salandanan, Mills, & Reiss, 2003).

Despite the intense effort that has been made to establish genotype-phenotype correlations, the contribution of several identified genes remains undefined. The cognitive and behaviour features of the WS phenotype, such as intellectual disability, visuospatial perception, language abilities and overfriendliness traits are harder to investigate using knockout mice and are often suggested to result from a co-action of several genes.

Williams syndrome phenotype

WS is a multisystem disorder accompanied by an extended cluster of phenotypic characteristics which involve physical, clinical, behavioural, neurological and mainly neurocognitive alterations (Table 1.1 summarizes the common WS phenotypic features).

This condition has an estimated prevalence of 1/20.000 to 1/50.000 births (Morris, Demsey, Leonard, Dilts, & Blackburn, 1988) although more recently a prevalence as high as 1/7500 births was found, suggesting that WS may be under diagnosed (Stromme, Bjornstad, & Ramstad, 2002). WS is present at birth, affects boys and girls equally and has been identified in many different countries all around the world.

The WS physical phenotype includes facial dimorphism, typically described as an “elfin-like” appearance which comprises a long forehead, salient eyes, a short-upturned nose, wide mouth with pronounced lips, full lower cheeks and a small chin. Frequently, these individuals have a small head, a long neck and prominent pointed ears. Individuals with WS exhibit a small stature and intrauterine growth retardation is usually present. Although the gestation period tends to be nearly normal (38.6 ± 3.2 weeks), the weight along with the height at birth are usually low (2.77 ± 0.5 Kg and 47.2 ± 2.6 cm, respectively) (Carrasco, Castillo, Aravena, Rothhammer, & Aboitiz, 2005).

WS is associated with a constellation of health problems affecting several organ systems. Congenital heart disease, namely SVAS and peripheral pulmonary artery stenosis, is one of the most common health problems found in this disorder occurring in approximately 85% of the individuals with WS (Carrasco et al., 2005). During infancy, additional medical problems can include feeding difficulty, stomach pain, hernias, renal abnormalities, high levels of calcium in the blood (transient infantile hypercalcaemia) and incessant crying. As children get older, they reveal hoarse voice, physical and mental retardation and disturbed fine motor control (Semel & Rosner, 2003). Ophthalmological difficulties like hypermetropia, reduced stereo acuity and strabismus are also common. In adults, hypertension is frequent as well as gastrointestinal diseases and urinary tract problems (Morris et al., 1988). Moreover, WS involves delay in the acquisition of motor abilities, clumsiness, difficulties in gross and fine motor coordination in addition to oromotor and oculomotor impairments (Gagliardi, Martelli, Burt, & Borgatti, 2007). An extreme sensitivity to certain sounds (hyperacusis) particularly from machines, fireworks and bursting balloons is observed in 85-95% of WS individuals and may be associated with a high-frequency

hearing loss caused by a deficiency in the acoustic reflex resulting from auditory nerve dysfunction (Gothelf, Farber, Raveh, Apter, & Attias, 2006).

Regarding the socio-emotional phenotype, WS show a singular set of attributes frequently described as a ‘cocktail-party’ personality profile which contrasts with severe behavioural problems and psychiatric symptoms. WS individuals are repeatedly described as hypersocial, talkative, friendly even with unfamiliar people and highly empathic in their responses to the others. However, this is an incomplete and oversimplified description as it neglects important developmental changes observed in this disorder. Most individuals with WS show dysfunction in the social domain characterized by high levels of anxiety, fears, distractibility and attentional problems, impulsivity, poor adaptability, low frustration tolerance and emotional disorders (Semel & Rosner, 2003). In addition, psychiatric disorders such as depression, obsessive compulsive symptoms, panic attacks, and post-traumatic stress disorder have been clinically observed in this population (Smoot, Zhang, Klaiman, Schultz, & Pober, 2005). Within the spectrum of psychiatric disorders, Attention Deficit Hyperactivity Disorder (ADHD) and specific phobias are the most prevalent comorbidities and are present in 64.7% and 53.8% of individuals with WS, respectively (Leyfer, Woodruff-Borden, Klein-Tasman, Fricke, & Mervis, 2006). WS can be also associated with Autism Spectrum Disorders (ASD) including behavioural characteristics that fit in the autistic symptomatic triad like social communication impairments or restricted and stereotyped behaviours or interests (e.g. hypersensitivity to sounds, picky eating, obsessive and perseverating attitudes) (Tordjman et al., 2012). Importantly, the presence of developmental disability in this condition may explain the majority of the observed psychiatric symptoms. Specific phobias, mainly from noises, obsessive-compulsive symptoms and stereotypic behaviours were the only psychiatric signs that were found to be more prevalent in WS than in idiopathic developmental disability (Green et al., 2011)

Williams syndrome cognitive profile

WS is commonly described as involving mild to moderate intellectual disability which is present in 75% of the individuals while the remaining 25% have learning disabilities (Mervis & Klein-Tasman, 2000). The mean Intellectual Quotient (IQ) of individuals with WS lies between 50 and 60 although some individuals are located in the severely retarded or borderline normal range (range of 40-100) (Martens, Wilson, & Reutens, 2008). These IQ

scores have been replicated even using different full-scale IQ measures. Increases and decreases in IQ scores along age were found to occur at rates comparable to the normative sample indicating that the pattern of strengths and weaknesses that are part of the phenotype variability in WS is maintained through adulthood (Searcy et al., 2004). Some studies have revealed significant discrepancies between verbal intelligence quotient (VIQ) and performance intelligence quotient (PIQ) in the WS population (Udwin & Yule, 1991). However, these differences have not been consistently found across the studies (Bellugi, Lichtenberger, Jones, Lai, & St George, 2000) and were not reported in a Portuguese WS group of patients (Sampaio et al., 2009). It is, however, important to note that although the IQ scores provide an overall perspective of the cognitive functioning of the individuals with WS, they may not accurately reflect their variability in the cognitive domain.

The first insight into the WS cognitive profile was accomplished by Bellugi and colleagues (1988a) who reported remarkable strengths in language and facial processing abilities contrasting with profound weaknesses in visuospatial construction abilities. Later, Mervis et al (2000) outlined the Williams Syndrome Cognitive Profile (WSCP) that specifies the criteria needed to fit the WS cognitive phenotype. The first criterion refers to the expected strengths in either auditory rote memory or language, while the second reflects the expected weakness in visuospatial construction. The remaining criteria rely on the relative impairment in visuospatial construction in contrast to overall intellectual ability and auditory short-term memory. This profile revealed high sensitivity and specificity scores (0.88 and 0.93, respectively).

Based on the first descriptions of Bellugi and colleagues (1988), WS was defined as a paradigm case of the modularity of mind providing a strong demonstration of the independence of language and other cognitive modules. This modular approach states that language is a module which is biologically programmed and develops independently of other cognitive abilities. The researchers who adopted this perspective as well as those who took the opposite direction found in WS an outstanding clinical model to investigate the modularity of mind. As a result, research on WS has been conducted concerning three overlapping clusters: language development, other aspects of cognition, particularly visuospatial domain, and interpersonal relations/personality (Mervis, 2003).

Table 1.1. Summary of the common WS phenotypic features

<p>Cardiovascular</p> <ul style="list-style-type: none"> - Vascular stenosis (SVAS, SVPS) - Hypertension 	<p>Auditory</p> <ul style="list-style-type: none"> - Hyperacusis - High-frequency hearing loss
<p>Neurological</p> <ul style="list-style-type: none"> - Hypotonia - Hyperreflexia - Cerebellar signs (poor balance) - Poor gross and fine motor coordination 	<p>Ophthalmologic</p> <ul style="list-style-type: none"> - Strabismus - Altered visual acuity - Reduced stereopsis
<p>Personality and behaviour</p> <ul style="list-style-type: none"> - Friendly personality - Impulsivity and attention deficit - Anxiety and specific phobias - Obsessive-compulsive traits - Stereotyped behaviours or interests 	<p>Facial Features</p> <ul style="list-style-type: none"> - Salient eyes - Short-upturned nose - Wide mouth - Full prominent lips - Prominent pointed ears
<p>Development and cognition</p> <ul style="list-style-type: none"> - Global cognitive impairment - Unique cognitive profile with strengths in language and weakness in visuospatial cognition 	<p>Other</p> <ul style="list-style-type: none"> - Short stature - Sleep dysregulation - Feeding difficulties

Dissociation between language and visuospatial abilities

Over the years, multiple studies have confirmed Bellugi's finding that language abilities are more preserved than visuospatial constructive abilities in WS. Language in WS was firstly described as being intact, surprisingly well preserved and even considered a strengthened domain. In fact, these individuals tend to be verbally fluent, articulate and extremely interested in conversation. Early studies indicated that WS patients are able to understand grammatical structures and employ a variety of grammatically complex forms (Bellugi, Lai, &

Wang, 1997), demonstrate preserved receptive vocabulary (Bellugi, Bihrlle, Jernigan, Trauner, & Doherty, 1990), know the syntax and semantic use of language (Poher & Dykens, 1996) and exhibit adequate affective language (Reilly, Klima, & Bellugi, 1990). This strength on the language domain was seen as a result of a diverging developmental trajectory whereby the vocabulary skills develop in a higher rate than the visuospatial abilities (Jarrod, Baddeley, & Hewes, 1998).

However, subsequent work has largely challenged the notion of an intact language module independent of the other cognitive domains (for a review see Brock, 2007). The language acquisition in WS was studied in more detail and was found to be delayed and in some cases below the level of matched younger typically developing children, such as in the case of morphological processing, pragmatic abilities, syntactic skills (Volterra, Longobardi, Pezzini, Vicari, & Antenore, 1999) and oral and semantic fluency (Stojanovik, 2006).

Collectively, these findings argue that there is no sustainable evidence for an intact language module in WS and that the language acquisition process in this condition follows a different path as compared to that found in typical development (Karmiloff-Smith, Brown, Grice, & Paterson, 2003). Possibly, the WS overfriendly and communicative interpersonal style may be at least partially masking their difficulties in the language domain.

Disturbed visuospatial construction is considered one of the hallmark characteristics of WS. Several aspects of the visuospatial functioning have been shown to be altered namely perceptual grouping, orientation discrimination, mental imagery, spatial relationships and spatial memory (Martens et al., 2008). In addition, visual search abilities were found to be altered in this condition accompanied by distinct pattern of saccadic eye movements (Montfoort, Frens, Hooge, Haselen, & van der Geest, 2007). These patients also demonstrated impaired drawing abilities which have been explained through disturbances in planning and/or executing motor responses in addition to visuospatial impairments. The visuospatial processing dysfunction in WS has been explained in relation to individuals' visual processing preferences (Bihrlle, Bellugi, Delis, & Marks, 1989; E. K. Farran & Jarrod, 2003). Researchers have suggested that this pattern of visual processing is due to the fact that these patients tend to focus on the details of an image and fail in extracting the global form (E. K. Farran & Jarrod, 2003). Hence, they have difficulties in integrating both local and global levels of information. The pattern of performance exhibited by individuals with WS on block construction tasks, such as the Block Design task of Wechsler intelligence scales illustrated these impairments (Bellugi et al., 2000). However, the local bias hypothesis in WS has been explored through the use of hierarchical stimuli (i.e. figures containing both

local and global levels of information) (Navon, 1977). Several variations to the Navon's original experimental paradigm were employed in order to explore both constructional and perceptive components of visuospatial processing (these studies will be described in the Chapter 3). The visual integration deficits in WS were also shown in tasks requiring perception of coherent motion as well as detection of forms through the perception of global motion (Atkinson et al., 2006; Mendes et al., 2005). Taken together, the mentioned findings suggested the WS as a clinical model of visual integration dysfunction associated with impaired visual coherence. This hypothesis will be further described and explored in the Chapter 3.

The visuospatial impairments observed in individuals with WS have been related to a dysfunction of the dorsal visual pathway, responsible for the flow of motion and spatial information in the visual system. However, the ventral visual pathway, involved on face and object recognition, is considered to be relatively preserved (A. Milner & Goodale, 2008). Indeed, the face processing skills such as face and facial expression recognition seem to be preserved in WS. As an example, individuals with WS seem to be able to process faces holistically (Paul, Stiles, Passarotti, Bavar, & Bellugi, 2002). Despite the normal to near-normal levels of performance on face recognition tasks, there is evidence that these occur through different underlying neural mechanisms (Karmiloff-Smith et al., 2004; D. L. Mills et al., 2000). The functioning of both visual processing pathways, as well as their role on visuospatial and face processing in WS will be addressed below in this introduction chapter.

To complete the characterization of the cognitive phenotype of WS, it is important to mention the recent interest in the study of high level domains such as attention and executive function in this neurodevelopmental disorder. Accordingly, impairments in tasks involving auditory sustained attention, visual selective attention, visual categorization and working memory can be contrasted with relatively preserved performance in visual sustained attention, auditory selective attention and visual inhibition tasks (Carney, Brown, & Henry, 2013; Costanzo et al., 2013).

In summary, the traditionally defined WS cognitive profile which contrasted intact language and face processing abilities to severely impaired visuospatial skills has been slightly modified in order to incorporate new research findings. The overall intelligence level is in the range of mild to moderate mental retardation. Language abilities seem to be atypical in areas such as grammatical comprehension, gender agreement, pragmatics and oral fluency. In addition, visuospatial impairments were extensively confirmed across studies, and may partly be dissected through the recent focus on executive functions.

Brain imaging contributions to understand the WS cognitive phenotype

Brain Anatomy

The study of brain anatomy is important because it provides clues to understand the cognitive phenotype in WS. Neuroanatomical studies using high-resolution magnetic resonance imaging (MRI) have demonstrated distinct brain morphology in individuals with WS when compared to both typically developing individuals and people with other neurodevelopmental disorders.

The most reported brain structure alteration in WS is a reduction in total brain volume (10-13%), which has been consistently found both in *post mortem* (Galaburda, Holinger, Bellugi, & Sherman, 2002) and *in vivo* studies (Jernigan & Bellugi, 1990; Reiss, et al., 2004). This finding explains the distinctive cerebral shape also reported in this condition (Schmitt, Eliez, Bellugi, & Reiss, 2001) since it is suggested to result from greater reductions in the white matter than in grey matter within specific regions (Reiss, et al., 2000).

MRI studies demonstrated that the reduction in the cerebral volume is not uniform through the brain with the posterior cerebrum being more affected, while the frontal and cerebellar structures seem to be preserved (Jernigan & Bellugi, 1990). Thus, there is evidence for a greater ratio of frontal to posterior regional volume in WS (Reiss, et al., 2000), an hypothesis confirmed by voxel-based morphometry (VBM) studies demonstrating reduced grey matter density in superior parietal lobe areas and in occipital regions. These findings were found in WS children (Boddaert et al., 2006) but also in both WS adults with and without intellectual disability (Reiss, et al., 2004; Meyer-Lindenberg et al., 2004). Accordingly, increased gyrification patterns were found in parietal (Schmitt et al., 2002) and occipital regions (Gaser et al., 2006) in addition to *post mortem* evidences showing significant differences in neuronal cell size, packing-density and organization in the peripheral visual cortex of individuals with WS (Galaburda et al., 2002). Such findings of different brain structure in areas underlying visual and visuospatial information processing are in line with the WS cognitive phenotype. Indeed, the grey matter volume in the inferior parietal lobule was found to be correlated to Block design performance measures and the regional grey matter density in the orbitofrontal lobe was found to be correlated with measures of visuospatial integration from the Visuo-motor Integration (VMI) test (Menghini et al., 2011).

Converging findings were provided by analyses of sulcal morphology suggesting the presence of a shortened central sulcus on its dorsal extension failing to reach the

interhemispheric fissure (Galaburda & Bellugi, 2000). This finding brings attention to a possible developmental anomaly affecting the dorsal half of the hemispheres. Sulcal depth reductions were found in the cingulate, anterior and posterior intraparietal sulcus along with increases in hippocampus, superior temporal gyrus and parieto-occipital regions (Van Essen et al., 2006). Atypical Sylvian fissure patterning was found in 24% of the individuals with WS demonstrating a right hemisphere Sylvian fissure that did not ascend to the parietal lobe (Eckert et al., 2006).

Morphological alterations have been found in other brain areas such as basal ganglia and brainstem (Reiss, et al., 2004; Faria et al., 2012), and corpus callosum. Volumetric reductions were found mainly in the posterior component (splenium and isthmus) of corpus callosum in addition to morphological abnormalities including larger blending angle, short length and increased thickness (Sampaio et al., 2012; Schmitt, Eliez, Warsofsky, Bellugi, & Reiss, 2001). Given that the posterior regions of the corpus callosum contain the majority of white matter tracts that bilaterally connect the visual and visual association areas of the brain, these findings might contribute to explain the visuospatial difficulties attributed to WS.

Less consistent findings have been reported for other brain regions with some studies showing increased grey matter volumes and other demonstrating reduced or preserved volumes. This pattern of mixed findings was obtained for areas related to emotion and face processing such as amygdala (Reiss, et al., 2004; Capitao et al., 2011; Galaburda & Bellugi, 2000), anterior cingulate cortex, orbito and medial prefrontal cortex and superior temporal gyrus (Meyer-Lindenberg et al., 2004; A. L. Reiss et al., 2004).

Besides morphometric and volumetric studies, some recent studies used diffusion tensor imaging (DTI) in order to investigate the white matter microstructure in WS (Avery, Thornton-Wells, Anderson, & Blackford, 2012; Faria et al., 2012; Marenco et al., 2007). The abnormal white matter integrity along the superior longitudinal fasciculus was suggested to contribute to the visuospatial impairments in WS given that this structure extends between the posterior parietal and the posterior lateral prefrontal cortex and is thought to have an important role on visuospatial attention and processing (Hoeft et al., 2007).

Functional neuroimaging studies

The functional neuroimaging research in WS has been aimed at investigating the most distinctive and prominent features of the WS phenotype, encompassing three main areas: visuospatial perception, social and emotional cognition and auditory processing.

Regarding the visuospatial domain, an attempt has been made to find the neural correlates of such profound deficits in WS. Studies have focused on the dissociation between the dorsal and ventral visual pathways suggested by psychophysical experiments which argued in favour of a dorsal stream dysfunction in the presence of spared ventral stream functioning (Atkinson et al., 1997; Paul et al., 2002). The functional magnetic resonance imaging (fMRI) studies in WS supported this notion and reported consistent and circumscribed hypoactivation in regions within the dorsal stream immediately adjacent to the intraparietal sulcus (IPS) contrasting with normal ventral stream activation during match-to-similarity and attention to location tasks (Meyer-Lindenberg et al., 2004). The same results were found in a passive face- and house-viewing experimental paradigm (Sarpal et al., 2008). Accordingly, individuals with WS exhibit significant increases in activation in the right fusiform gyrus and several frontal and temporal areas during face and gaze perception whereas the control group mainly activate posterior regions bilaterally including primary and secondary visual cortices (Mobbs et al., 2004). These findings are in line with the brain structural alterations mentioned above indicating volume reductions in the occipital and parietal regions (Boddaert et al., 2006). The evidence of decreased parietal and visual cortical activation in WS individuals was also demonstrated during a task requiring global processing (Mobbs, Eckert, Menon et al., 2007). Interestingly, this pattern of reduced activation in occipital and parietal areas was observed along with increased posterior thalamic activation encompassing the lateral geniculate nucleus (LGN) and the pulvinar (Mobbs, Eckert, Menon et al., 2007). Based on these evidences, the authors suggested the presence of early visual deficits which may begin in the LGN and extend to cortical regions (e.g. V1) that, in turn, may disturb the dorsal pathway functioning. However, in an fMRI-based retinotopic mapping study, the properties of V1 were overall shown to be normal suggesting that the neural changes lying behind the visuospatial impairments in WS arise at later stages in the visual hierarchy (Olsen et al., 2009).

Despite the well established notion of relative preservation of the areas along the ventral visual stream, more recent evidence shed additional light on this evidence by indicating that the proficient face recognition abilities in WS may stem from atypical neural

substrates in the ventral stream. Recent studies demonstrated that the ventral stream topography in WS is characterized by the same level of activation for face stimuli (measured in the fusiform face area -FFA) but reduced activation for house stimuli (measured in the parahippocampal place area – PPA) as compared to both chronological- and mental-aged matched controls (O'Hearn et al., 2011). Likewise, in a methodologically extensive study, the FFA was systematically found to be approximately two times larger (both absolutely and relative to the fusiform gyrus) in the individuals with WS as compared to control participants (Golarai et al., 2010). Complementary functional connectivity analysis revealed a reduction in functional connectivity between PPA and pivotal parietal regions such as IPS and between FFA and amygdala and prefrontal cortex (Sarpal et al., 2008). Taken together, these findings suggest that even though tasks recruiting the ventral stream areas achieve normal or near-normal performance levels, the pattern of functional activation within the ventral stream is slightly different in the WS groups. The interactions between ventral areas and the neural systems known to be affected in this condition (e.g. IPS) are altered. However, this is an open question which requires additional research regarding the ventral stream functioning in WS and highlights the need to investigate dorsal-ventral streams interconnections as they are pivotal for a proper characterization of the visuospatial impairments present in this disorder.

Concerning the neural basis of emotional and social cognition in WS, the first study on this topic reported reduced amygdala and prefrontal regions (particularly orbitofrontal cortex - OFC) activations in response to threatening faces whereas increased activation was identified in response to threatening scenes (Meyer-Lindenberg, Hariri et al., 2005). Afterwards, results from the same cohort of participants demonstrated persistent enhanced activation of the amygdala to non-social scenes irrespective of the cognitive load (Munoz et al., 2010). The amygdala reactivity to social stimuli, especially to faces, was shown to be increased for positive emotional facial expressions (happy) and attenuated or even absent response to negative (fearful) (Haas et al., 2009; Mimura et al., 2010) or neutral facial expressions (Paul et al., 2009) in WS. When using novel control groups (healthy participants with inhibited temperament vs. individuals with uninhibited temperament) in order to isolate the influence of the WS distinctive behavioural traits (e.g. hypersociability) on the amygdala response, prior findings of heightened amygdala response to non-social fear images were corroborated, suggesting that this pattern of activation is distinctive in the WS group (Thornton-Wells, Avery, & Blackford, 2011). Collectively, these findings of abnormal amygdala and OFC activation in response to social and non-social stimuli have been seen as neural mechanisms underlying the complex constellation of social and emotional

abnormalities found in WS especially the lack of fear of strangers and social disinhibition (Meyer-Lindenberg, Hariri et al., 2005). Accordingly, response inhibition was explored in WS as measured by a Go/NoGo task with individuals with WS demonstrating significant reduced activity in cortical and subcortical areas involved in behavioural inhibition such as the striatum, dorsolateral prefrontal and dorsal anterior cingulate cortices (Mobbs, Eckert, Mills et al., 2007). These findings suggest that the frontostriatal systems in addition to the OFC/amygdala neural system may be critical to better understand the distinctive aspects of the social cognition in this condition.

So far, only two studies have examined the neural correlates of the unique auditory and musical phenotype of individuals with WS. The first study investigated music and noise auditory processing and found a different pattern of activations in the WS group when compared to age-matched controls (Levitin et al., 2003). Both groups exhibited significant bilateral temporal lobe activation (e.g. superior temporal and middle temporal gyri) for music compared to noise though the WS group displayed significant lower levels than controls. Interestingly, individuals with WS activated a wide set of neural structures such as amygdala, cerebellum and brain stem. These findings were replicated in a recent study that found further surprising activations in the occipital and early visual areas in response to musical and other auditory stimuli (Thornton-Wells et al., 2010), suggesting different mechanisms of cross-modal integration of information from different sensory modalities in WS.

Electrophysiological studies

The studies using electroencephalography (EEG) to investigate the neural correlates of specific cognitive characteristics in the WS population are still scarce and have particularly focused on face processing and language abilities.

Indeed, although face processing constitutes an area of proficiency within the WS cognitive profile, EEG evidences have demonstrated abnormal cerebral specialization. The first study investigating the functional organization of WS brain systems linked to face recognition indicated that WS participants exhibited the same pattern of neural responses (small negativity at 100 msec - N100- and an atypically large negativity at 200 msec – N200) for both upright and inverted photographic faces in contrast with what was observed in control participants (D. L. Mills et al., 2000). These findings were recently replicated in a study revealing the absence of face inversion effect in WS with a possible relation to the

severity of the dorsal visual stream deficit (Nakamura et al., 2013). Accordingly, other study (Grice et al., 2001) exploring the brain responses to upright and inverted faces revealed that despite normal behavioural performance, the face orientation did not modulate the gamma-band activity in the WS group in contrast to what was observed in the control group. Moreover, the expected gamma-band bursting pattern was not observed in the WS group, with gamma-band activity being smeared across longer time intervals similar to that observed in very young infants (before 8 months of age) (Csibra, Davis, Spratling, & Johnson, 2000). These results suggested abnormal oscillatory patterning within the gamma-band range in WS which might be expected in this condition given the mentioned deficits in coherent perception. Additional studies reinforced the notion of disordered perceptual processing in WS by demonstrating an abnormal pattern of neural responses in an illusory contour perception task (Kanizsa Square illusion) (Grice et al., 2003) and also in a global-local experimental paradigm using hierarchical figures (Key & Dykens, 2011).

Language abilities were also investigated using the EEG technique and by employing tasks with auditory sentences. Abnormalities in the early event-related potential (ERP) components including small N100 amplitude and more positive amplitude at 200msec (P200) during auditory sentences processing were found in the WS group as compared to the control participants (D. Mills et al., 2003; Neville, Mills, & Bellugi, 1994). The N400 component related to semantic integration was also found to be altered in individuals with WS (Neville et al., 1994; St. George, Mills, & Bellugi, 2000). A recent study replicated these findings in a Portuguese WS sample (Pinheiro, Galdo-Alvarez, Sampaio, Niznikiewicz, & Goncalves, 2010).

Despite these evidences of distinct neural correlates in WS as measured by EEG studies, more studies are needed in order to characterize the neural underpinnings of other important features within the WS cognitive phenotype such as visuospatial perception.

In sum, this first part of the introductory chapter was aimed at characterizing the WS cognitive phenotype and emphasizes the evidence for a profound visuospatial dysfunction in this disorder which has implications in a wide set of perceptual functions such as visual coherence, spatial information and motion processing. The scarce studies investigating the neural correlates of such impairments were described and highlighted the need to conduct both functional neuroimaging and electrophysiological studies in the same cohort of participants, testing the same visual stimuli and using appropriate control groups in order to better characterize and understand the neural basis of visuospatial impairment.

Visual system: parallel visual pathways

The visual system is one of the most studied systems in neuroscience. The interest in studying the visual system comes from the fact that it is central in which concerns human interaction with the world. Advances in the neuroscientific research of the visual system are important in themselves but also represent a significant opportunity to model and understand brain function as a whole (Goebel, Muckli, & Kim, 2004).

Visual information processing begins in the eye, in which the light enters through the cornea and passes through the lens until it reaches the neural retina and crosses ganglion cell, bipolar and photoreceptor layers of the retina.

The main role of the eye in the process of vision is to project an upside down picture of the external world onto the retina. The visual information is then processed by the retina before it is sent to the brain. The light has to pass all the five different layers of the retina until reach the photoreceptors located at the back of the retina. This helps to explain the relatively poor optical design properties of the eyes, in evolutionary terms. It is therefore in the photoreceptors that optical information is transduced into electrical signals (i.e. neuronal code) that are communicated to the bipolar cells, which relay the message to the retinal ganglion cells.

Three retinal ganglion cells types can be distinguished: midget, parasol and small and large bistratified. Parasol ganglion cells (or M-cells) are considered to be the origin of the magnocellular pathway and are more sensitive to contrast and respond strongly to movement but are not sensitive to wavelength. In turn, midget ganglion cells (or P-cells) constitute the parvocellular pathway and are not sensitive to movement but are primarily responsible for seeing detail and colour. The M population tends to exhibit lower spatial and higher temporal resolution and faster conduction speeds than the P population. Finally, small and large bistratified ganglion cells make part of the koniocellular pathway which has been seen as a system sharing functional aspects with the P and M pathways. Although the three streams flow separately from retina to cortex, there is evidence of some interactions among the streams and their messages are combined in the cortex to help form unified percepts (Kaplan, 2004).

The axons of retinal ganglion cells leave the eye in a bundle called optic nerve, meeting at the optic chiasm (from here the optic nerve is now called optic tract) in which some axons cross over the opposite hemisphere meaning that each optic tract contains the information of the contralateral visual field. The optic nerve/tract is made out of ganglion myelinated

axons that transmit to the neurons on the Lateral Geniculate Nucleus (LGN) located in the thalamus. The LGN can be divided in six different layers. The first and second layers are called magnocellular (M) layers (M-type ganglion cells) whereas the four others constitute the parvocellular (P) layers. The LGN is the major visual subcortical center relaying information from both eyes to the primary visual cortex (also known as striate cortex, area V1 or, less precisely, area 17 according to Brodman terminology) where different features of the visual world such as colour, form and motion signals are first processed in a parallel way in separated cortical areas before being redistributed to higher areas in the brain.

Given the work of Livingstone and Hubel in the 1980s (Livingstone & Hubel, 1988), increasing evidence has been gathered concerning the parallel processing of different attributes such as form, colour and motion within the different layers of V1. The neuronal projections from LGN terminate in sublayer 4C of the striate cortex. M pathway projects essentially to layer 4C α which projects to layer 4B and then to higher areas V2, V3 and MT/V5. P pathway projects to layer 4C β which projects to layer 4A and then projects to V2 and V4 (Livingstone & Hubel, 1988). The K pathway project to the blobs in layers 2 and 3 in V1 and from there to V2. The early visual system architecture is summarized in Figure 1.2.

The way whereby visual information is redistributed in V1 to other extrastriate areas was extensively investigated and the anatomical and physiological studies in Old World monkeys were able to identify an important principle of cortical organization which states that extrastriate visual areas are organized into hierarchical, parallel processing streams.

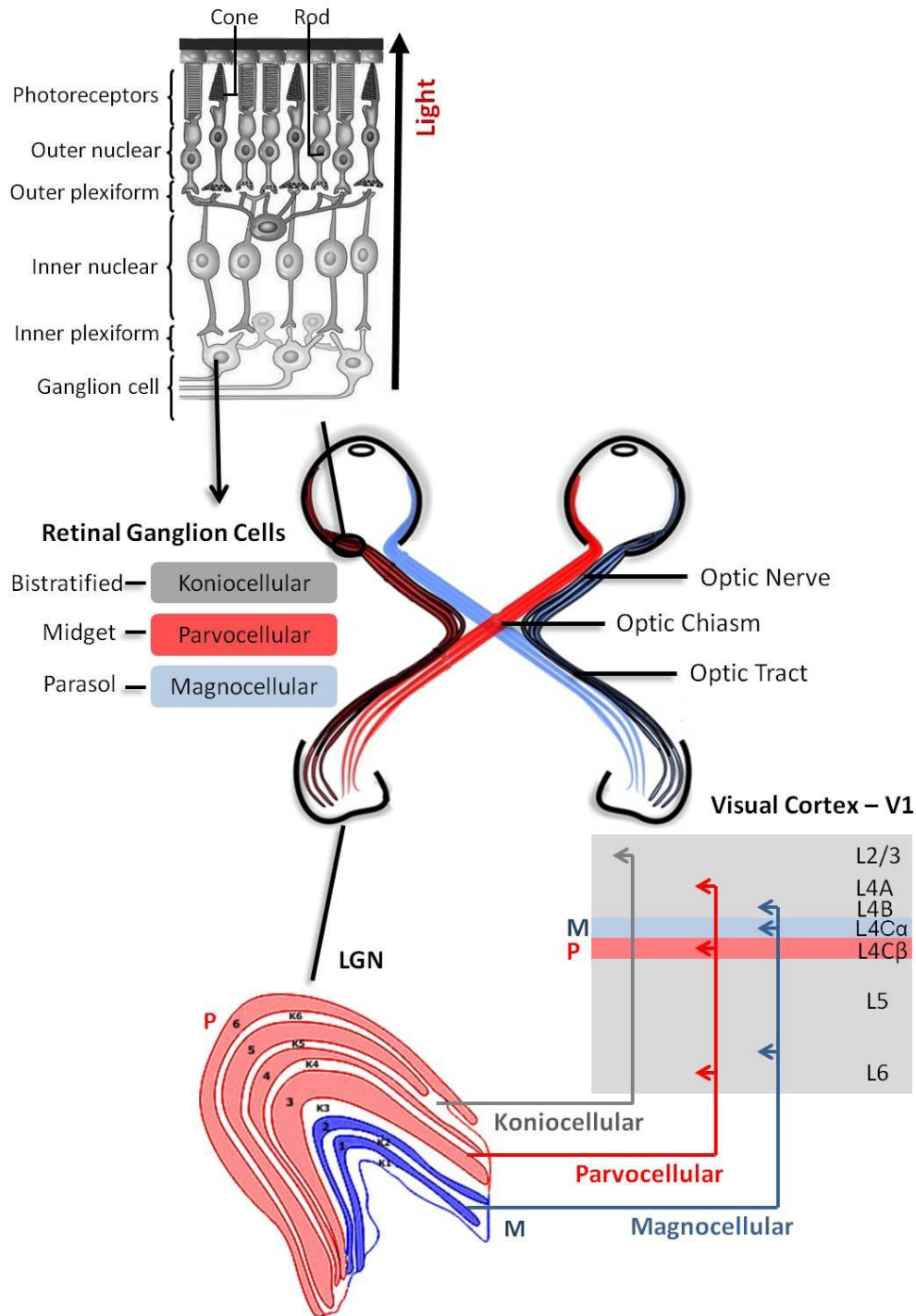


Figure 1.2. Illustration of the visual system architecture from the retina to the primary visual cortex. The visual information is encoded in the retina which transduces the optical information into an electrochemical signal that is relayed from photoreceptors to bipolar and then retinal ganglion cells (GC) (midget, parasol and small and large bistratified). Parasol GC project to the magnocellular layers of the lateral geniculate nucleus (LGN) which extend to layer 4C α of the primary visual cortex (V1) (represented in blue). Midget GC project to the parvocellular layers of the LGN which convey information to 4C β layer of V1 (represented in red). Small and large bistratified GC project to the koniocellular layers of the LGN which, in turn, extends to the layers 2/3 in V1. (Adapted from Hofer, Karaus, & Frahm, 2010; Thomson, 2010; Van Hooser & Nelson, 2005).

The conceptualization of two different visual streams acquired another form with the model proposed by Ungerleider and Mishkin (Ungerleider & Mishkin, 1982). They proposed the existence of two different visual pathways: the ‘where’ or dorsal visual pathway which processes spatial information, object location and motion cues processing and the ‘what’ or ventral visual pathway, devoted to the processing of important features relevant to object identification such as shape and colour (illustrated in Figure 1.3). According to their model, both dorsal/ventral visual streams originate in the primary visual cortex (V1), encompass several extrastriate areas and show functional relationships with the magnocellular/parvocellular division earlier in the visual pathway.

The dorsal visual pathway receives predominant input from the M pathway and projects to the dorsolateral occipital cortex and regions on the posterior parietal lobe encompassing areas V1, V2, dorsal V3 (V3d), middle temporal area (MT/V5), medial superior-temporal area (MST) and intraparietal area (IP). On the other hand, the ventral visual pathway gathers input from the P pathway and extends to the inferotemporal areas of the temporal lobe comprising areas V1-V4 and areas along the posterior and anterior inferior temporal lobe, such as FFA, PPA and lateral occipital complex (LOC)(Ungerleider & Haxby, 1994). The dorsal and ventral visual pathways are illustrated in Figure 1.3.

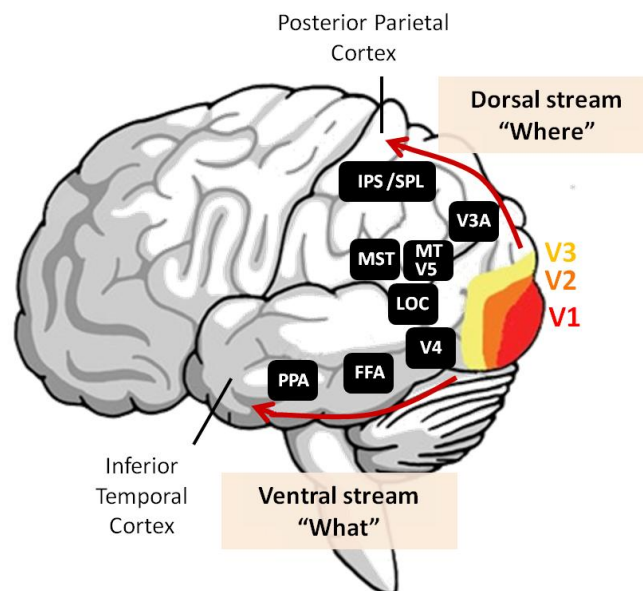


Figure 1.3. Dorsal and Ventral parallel visual pathways. Visual processing in the brain is handled, in part, by two processing streams extending from primary visual cortex: the dorsal visual pathway (‘Where’) which projects from V1 to the parietal cortex and is responsible for the processing of spatial information; and the ventral visual pathway (‘What’) which spreads from V1 to the temporal lobe and is responsible for object identification as well as shape and face processing. (Adapted from Goebel et al., 2004)

These cortical projections are modelled in terms of a hierarchical framework meaning that low-level inputs from lower cortical areas are transformed into more abstract representations through successive processing states in higher cortical areas. At the earliest stage of visual perception the V1 neurons are tuned to several features such as orientation, spatial and temporal frequency (Hubel & Wiesel, 1968), direction of motion (Carandini, Movshon, & Ferster, 1998), binocular depth (Cumming & DeAngelis, 2001) and colour selectivity (Horwitz & Hass, 2012). Within the dorsal visual pathway, V1 cells are sensitive to direction of motion information which is subsequently received by V3 and V5. In turn, MT/V5 activates specially in response to fronto-parallel motion whereas MST cells have a central role in global motion perception (Van Essen, Maunsell, & Bixby, 1981). Along the ventral visual pathway, V1 acts as a spatiotemporal filter whereas V2 responds to illusory and second-order contours (von der Heydt, Peterhans, & Baumgartner, 1984) and V4 cells encode curved shapes and extract objects from the background on the basis of differences in shape or colour being important in global form perception (Desimone & Schein, 1987). Additionally, inferior temporal regions respond selectively to global object features such as shape (e.g. faces) (Kanwisher, McDermott, & Chun, 1997).

Despite this cortical organization was primarily identified in the non-human primate brain, initial focal human lesion studies suggested that a similar pattern of organization in the human visual cortex, in terms of the dorsal vs. ventral visual dichotomy for visual information processing (Damasio, Damasio, & Van Hoesen, 1982; Zihl, von Cramon, Mai, & Schmid, 1991). The findings derived from lesions studies in humans also led to some alterations to the 'What' and 'Where' model. Thus, this model was slightly changed by Goodale and Milner (Goodale & Milner, 1992) to incorporate the distinction between vision for perception and vision for action. This new perspective was mainly formulated on the basis of evidence gathered from case studies on a single patient, D.F., which exhibited damage in the ventral visual pathway destroying the lateral occipital area bilaterally resulting in form agnosia. D.F. patient was able to implicitly use information about objects features such as size and location to guide reaching and grasping actions towards the objects but was unable to explicitly discriminate these properties of the object. Based on these observations, the authors predicted that the ventral visual pathway is underlies the construction of representations of the visual world providing information to enable the identification of a target object whereas the dorsal visual pathway uses the visual information about the object (shape, size and location) to mediate the visual control of actions towards the same object. Within this framework, the two visual pathways are understood in terms of the outputs

systems that they serve rather than their visual input (A. Milner & Goodale, 2008). In this account, an additional distinction was proposed concerning the distinct frames of reference for perception and action. Hence, authors suggested that the information in the viewer-dependent (egocentric) coordinates is coded in the dorsal stream, whereas the ventral stream mainly operates in the viewer-independent (allocentric) coordinates (A. Milner & Goodale, 1995). In other words, the action towards a target object (with dorsal stream involvement) requires the computation of the size of the object and its orientation and location in relation to the observer (i.e. in an egocentric frame of reference) while the perceptual processing (with ventral stream involvement) entails the encoding of size, orientation and location of the objects in relation to other relevant objects of the context (i.e. in an allocentric frame of reference). Given aforementioned assumptions, the dissociation between egocentric and allocentric frames of reference allows the study of the dissociation between dorsal and ventral visual pathways in WS. These implications will be further detailed and explored in the Chapter 4 of this thesis.

Main paradigms to study visual stream function

The functional specialization of areas within both dorsal and ventral visual pathways has been investigated through different experimental paradigms. Particularly, to address motion processing, stimuli related to the perception of coherent 2D-patterns or 3D-structures derived from motion cues have been designed and are discussed below.

Global motion processing (coherent motion)

In the global motion paradigm, also named coherent motion, a proportion of visually presented dots move coherently in a given direction while the remaining dots (noise) move in random directions at the same speed, requiring the integration of motion signals over many dots. The smallest proportion of dots that have to move coherently for the observer to perceive coherent global flow gives the threshold for coherent motion detection (Braddick, Atkinson, & Wattam-Bell, 2003; Grinter, Maybery, & Badcock). In this type of stimuli, the perception of global motion emerges from cooperative processing between local motion detectors. There is evidence of efficient integration of local motion signals into global representations processing early in development, immediately after local motion processing mechanisms are consolidated in the developing brain (Banton, Bertenthal, &

Seaks, 1999). Moreover, global motion processing keeps developing during infancy with motion coherence thresholds reaching adult levels at approximately 6 years (Parrish, Giaschi, Boden, & Dougherty, 2005).

The neural correlates of visual coherent motion were found to encompass a set of extrastriate areas within the dorsal visual stream, namely, V5/MT and V3A (Heeger, Boynton, Demb, Seidemann, & Newsome, 1999; Salzman, Murasugi, Britten, & Newsome, 1992). However, the identified patterns of activity in V5/MT are not consistent since it was also described as being more activated by incoherent than coherent motion (McKeefry, Watson, Frackowiak, Fong, & Zeki, 1997). In addition, coherent motion elicited increased activations in other areas such as superior temporal sulcus (STS), intraparietal sulcus (IPS) and also sites on the posterior ventral surface of the occipital lobe including parts of the fusiform and lingual gyri. Interestingly, striate areas V1 and V2, besides failing to show responses to coherent motion (Braddick et al., 2001) were actually more active for incoherent patterns in a different study (McKeefry et al., 1997).

Structure-from-motion (SFM) processing

The standard stimuli in the structure-from-motion paradigm (also referred to as inducing kinetic depth effects) consist of physical motion on a screen that produces a vivid illusion of a three-dimensional (3D) object moving/rotating in depth (Wallach & O'Connell, 1953). A long debate has emerged in order to explain how the brain can compute the 3D structure from two-dimensional (2D) information and it is well established that local motion information cues are pivotal to the SFM extraction rather than the processing of local positional cues (Andersen & Bradley, 1998; Farivar, 2009). Thus, it is necessary to integrate the local motion cue over time to be able to extract the 3D shape. This computation depends on the detection of coherent motion (Braddick et al., 2003) and is processed in two stages: first, local motion cues are processed in area V1 and second, reconstruction occurs in MT in which direction opponency suppresses noise information (Andersen & Bradley, 1998). It has been suggested that the detection of SFM patterns starts developing earlier in the development in the 3-6 months old infants (Arterberry & Yonas, 2000) and reaches adult-like levels at the age of 7 (Parrish et al., 2005). However, fMRI evidence showed that neural activity in the dorsal stream of the occipital and parietal cortices recruited in adult SFM perception was not mature at the age of 6 (Klaver et al., 2008).

Since SFM perception requires motion and shape processing, it remains subject of debate to what extent do its neural correlates depend on the development of motion- and

shape-sensitivity areas or include areas beyond the above mentioned brain regions. Interestingly, although these stimuli may be mainly processed in areas along the dorsal visual stream, ventral stream contributions have been also reported. Additionally, given that the integration of local motion cues is required to construct a global coherent shape percept, the SFM stimulus is suitable for the study of dorsal and ventral visual streams in WS. This recruitment of both dorsal and ventral areas in SFM perception also suggests interconnectivity between both pathways which is currently a subject of widespread interest within this domain (Farivar, 2009; Farivar, Blanke, & Chaudhuri, 2009). In fact, even though the models advocating the dichotomotic organization of the visual system are widely accepted and triggered a vast series of studies to corroborate these assumptions, additional findings have emerged which suggest that the two pathways are not totally independent and the presence of interconnections between them is unavoidable (Schenk & McIntosh, 2010). Accordingly, anatomical cross-talk between the two pathways has been hypothesized to already occur in the striate cortex (V1-V2), as well as higher in the processing hierarchy. Furthermore, there is evidence that the bottom-up processing occurring from striate cortex to higher visual areas across both dorsal and ventral pathways does occur alongside with both transverse and top-down communications which are likely important to explain the “construction” of the whole visual percept. Dorsal-ventral pathways integration was also suggested by neuropsychological and functional neuroimaging studies which demonstrated that some aspects of object and face recognition (e.g. recognition of an objects spatial orientation) do not exclusively rely on the ventral pathway (for a review see Farivar, 2009). In line with this reasoning, studies using SFM experimental paradigms have also pointed out that this type of coherent perception does not exclusively rely on the dorsal visual stream and, in turn the ventral visual pathway participates in both the identification and learning of unfamiliar objects from SFM cues (Farivar, 2009). As an example, a striking case study reported a patient with ventral stream damage (prosopagnosia) and preserved dorsal stream function exhibited impaired identification of SFM unfamiliar faces, demonstrating that both visual pathways are necessary for the extraction of shape information from depth and motion cues (Farivar et al., 2009).

Dorsal stream vulnerability in neurodevelopment

There is strong evidence that the dorsal visual stream is more vulnerable than the ventral stream during development. Braddick et al (Braddick et al., 2003) provided a body of evidence suggesting that the ventral stream matures earlier than the dorsal visual stream. These authors conducted several studies comparing global motion and global form processing in healthy development and found distinct circuits of activated areas within dorsal and ventral streams for both tasks, with dorsal stream areas V5 and V3A showing linear increases with the degree of motion coherence and areas in the lingual/fusiform gyrus showing a linear response to form coherence (Braddick, O'Brien, Wattam-Bell, Atkinson, & Turner, 2000). They observed that form coherence reaches adult levels rather earlier than motion coherence and that at the age of 4 the perception of visual arrays into globally organized forms develops more securely than the equivalent perception from relative motion (Braddick et al., 2003). These findings led the authors to suggest the dorsal stream vulnerability hypothesis which states that the dorsal stream is more susceptible to dysfunction than the ventral stream and is present in multiple neurodevelopmental disorders. Given that the M cells (8-10%) are in smaller number compared to P cells (80%), the cell loss within the magnocellular pathway potentiates the detection of functional loss (Castelo-Branco et al., 2009; Grinter et al., 2010; Mendes et al., 2005).

Indeed, besides WS, dorsal stream dysfunction has been extensively reported in several neurodevelopmental disorders with different aetiologies and cognitive profiles, such as dyslexia (Skottun, 2000), hemiplegia (Braddick et al., 2003) and Fagile X (Kogan et al., 2004), although the affected stages of the dorsal pathway are distinct (Grinter et al., 2010). A striking example is the ASD which is associated with generalized deficits in global processing, impairments along higher-level dorsal stream were found, particularly higher motion coherence thresholds on global dot motion tasks. On the other hand, lower-level dorsal stream functioning was found to be preserved in this condition (Spencer et al., 2000). The suggestions of dorsal stream dysfunction in ASD places this disorder as an outstanding clinical model to compare with WS given that they share the same pattern of global processing deficits associated with dorsal stream dysfunction in contrast with distinctive social phenotypes.

Although there is the evidence that the dorsal stream is especially susceptible to damage in neurodevelopmental disorders, it is important to note that some abnormalities within the ventral stream were also found and in some cases the latter was not as extensively

investigated as the dorsal stream was. It remains unclear if the mentioned ventral stream impairments are derived from abnormal input received from the dorsal networks or if they are differentially affected instead. The interconnections between the two visual pathways should thus be taken into account in order to better clarify the extent of both dorsal and ventral streams' dysfunction in abnormal neurodevelopment.

General outline and aims of the thesis

As a neurobiological model of dissociation between dorsal and ventral visual pathways, WS bears an enormous potential for unveiling the neural mechanisms mediating the visuospatial processing. Furthermore, by unraveling and individuating the role of both visual pathways, the visual coherence deficits associated with visual integration frequently observed in atypical neurodevelopment can be explained. The present thesis is thus aimed at definitely establishing WS as a clinical model of impaired visual coherence and comprehensively investigating multiple levels of visual processing along the dorsal and ventral visual pathways in this condition.

Chapter 1 presents the current knowledge on the neurocognitive, neuroanatomical and neurophysiological functioning in WS. The main focus is on the WS neurocognitive features related to visuospatial dysfunction and its neural correlates. Moreover, the parallel organization of the visual system is described in order to better understand the functioning of both dorsal and ventral visual processing pathways in normal and abnormal development.

A brief overview of the main methodological modalities employed in this thesis is provided in *Chapter 2*, alongside with their fundamentals. These modalities encompass electroencephalography (EEG) and functional magnetic resonance imaging (fMRI) which due to their complementary temporal and spatial resolution are suited to the characterization of the visual pathways.

Chapters 3 to 6 present the body of results obtained from the experimental testing conducted to investigate the general dissociation between dorsal vs. ventral processing.

In the *Chapter 3* we investigate the nature of visual coherence deficits in WS by exploring global and local visual processing under different task conditions and using participants with other neurodevelopmental disorders, such as autism, as comparison model of putative loss of visual coherence. This framework for the study of impaired visual coherence provides a new insight into the neural mechanisms underlying these impairments.

Although previous studies have suggested dorsal stream vulnerability contrasting with ventral stream preservation in this disorder, ventral stream functioning has been barely investigated and the cross-talk between the two visual pathways has not been specifically explored. As a result, the following chapters are focused on the crucial assessment of the different levels of visual stream functioning, in addition to the response of these pathways to visual stimuli requiring dorsal-ventral integration.

Chapter 4 tests whether the hypothesis of a dorsal-ventral stream dissociation in WS is mirrored by the spatial reference frames (egocentric vs. allocentric dissociation) suggested by Milner & Goodale (1995), by employing a novel experimental paradigm. We expected, based on that framework, that an egocentric vs. allocentric dissociation should also be present.

Chapters 5 and 6 explicitly explore the dorsal-ventral integration in WS by investigating the neural underpinnings of 3D coherent perception of objects. *Chapter 5* focuses on the temporal dynamics of such interconnections, specifically by studying gamma-band oscillations. Since coherent perception has been associated to altered gamma-band oscillations, WS constitutes a privileged model to investigate the role of gamma-band in the construction of global coherent percept. *Chapter 6* examines the neural cortical organization in WS during the perception of both dynamic and static object stimuli. Given that these stimuli recruit category selective areas along both dorsal and ventral visual pathways, this chapter also provides a novel understanding on the nature and the extent of the dorsal stream deficits in WS and its implications on ventral stream (re)organization.

As a final point, the overall results are discussed in *Chapter 7* in order to provide an integrative view of the main findings of the present work and their integration in the current body of knowledge on dorsal and ventral visual pathways functioning and coherent categorical perception of visual objects in health and disease.

References

- Andersen, R., & Bradley, D. (1998). Perception of three-dimensional structure from motion. *Trends in Cognitive Sciences*, 2(6).
- Antonell, A., Del Campo, M., Flores, R., Campuzano, V., & Perez-Jurado, L. A. (2006). Williams syndrome: its clinical aspects and molecular bases. *Rev Neurol*, 42 Suppl 1, S69-75.
- Antonell, A., Del Campo, M., Magano, L. F., Kaufmann, L., de la Iglesia, J. M., Gallastegui, F., et al. (2010). Partial 7q11.23 deletions further implicate GTF2I and GTF2IRD1 as the main genes responsible for the Williams-Beuren syndrome neurocognitive profile. *J Med Genet*, 47(5), 312-320.
- Arterberry, M. E., & Yonas, A. (2000). Perception of three-dimensional shape specified by optic flow by 8-week-old infants. *Percept Psychophys*, 62(3), 550-556.
- Atkinson, J., Braddick, O., Rose, F. E., Searcy, Y. M., Wattam-Bell, J., & Bellugi, U. (2006). Dorsal-stream motion processing deficits persist into adulthood in Williams syndrome. *Neuropsychologia*, 44(5), 828-833.
- Atkinson, J., King, J., Braddick, O., Nokes, L., Anker, S., & Braddick, F. (1997). A specific deficit of dorsal stream function in Williams' syndrome. *Neuroreport*, 8(8), 1919-1922.
- Avery, S. N., Thornton-Wells, T. A., Anderson, A. W., & Blackford, J. U. (2012). White matter integrity deficits in prefrontal-amygdala pathways in Williams syndrome. *Neuroimage*, 59(2), 887-894.
- Banton, T., Bertenthal, B. I., & Seaks, J. (1999). Infants' sensitivity to statistical distributions of motion direction and speed. *Vision Res*, 39(20), 3417-3430.
- Bellugi, U., Bihrlé, A., Jernigan, T., Trauner, D., & Doherty, S. (1990). Neuropsychological, neurological, and neuroanatomical profile of Williams syndrome. *Am J Med Genet Suppl*, 6, 115-125.
- Bellugi, U., Lai, Z., & Wang, P. P. (1997). Language, communication, and neural systems in Williams syndrome. *Mental Retardation and Developmental Disabilities Research Reviews*, 3, 334-342.
- Bellugi, U., Lichtenberger, L., Jones, W., Lai, Z., & St George, M. (2000). I. The neurocognitive profile of Williams Syndrome: a complex pattern of strengths and weaknesses. *J Cogn Neurosci*, 12 Suppl 1, 7-29.
- Bellugi, U., Sabo, H., & Vaid, J. (1988). Dissociation between language and cognitive functions in Williams syndrome. In D. Bishop & K. Mogford (Eds.), *Language development in exceptional circumstances*. (pp. 177-189). London: Churchill-Livingstone.
- Beuren, A. J., Apitz, J., & Harmjan, D. (1962). Supravalvular aortic stenosis in association with mental retardation and a certain facial appearance. *Circulation*, 26, 1235-1240.
- Bihrlé, A. M., Bellugi, U., Delis, D., & Marks, S. (1989). Seeing either the forest or the trees: dissociation in visuospatial processing. *Brain Cogn*, 11(1), 37-49.
- Boddaert, N., Mochel, F., Meresse, I., Seidenwurm, D., Cachia, A., Brunelle, F., et al. (2006). Parieto-occipital grey matter abnormalities in children with Williams syndrome. *Neuroimage*, 30(3), 721-725.
- Braddick, O., Atkinson, J., & Wattam-Bell, J. (2003). Normal and anomalous development of visual motion processing: motion coherence and 'dorsal-stream vulnerability'. *Neuropsychologia*, 41(13), 1769-1784.
- Braddick, O., O'Brien, J. M., Wattam-Bell, J., Atkinson, J., Hartley, T., & Turner, R. (2001). Brain areas sensitive to coherent visual motion. *Perception*, 30(1), 61-72.
- Braddick, O., O'Brien, J. M., Wattam-Bell, J., Atkinson, J., & Turner, R. (2000). Form and motion coherence activate independent, but not dorsal/ventral segregated, networks in the human brain. *Curr Biol*, 10(12), 731-734.
- Brock, J. (2007). Language abilities in Williams syndrome: a critical review. *Dev Psychopathol*, 19(1), 97-127.
- Capitao, L., Sampaio, A., Sampaio, C., Vasconcelos, C., Fernandez, M., Garayzabal, E., et al. (2011). MRI amygdala volume in Williams Syndrome. *Res Dev Disabil*, 32(6), 2767-2772.
- Carandini, M., Movshon, J. A., & Ferster, D. (1998). Pattern adaptation and cross-orientation interactions in the primary visual cortex. *Neuropharmacology*, 37(4-5), 501-511.
- Carney, D. P., Brown, J. H., & Henry, L. A. (2013). Executive function in Williams and Down syndromes. *Res Dev Disabil*, 34(1), 46-55.

- Carrasco, X., Castillo, S., Aravena, T., Rothhammer, P., & Aboitiz, F. (2005). Williams syndrome: pediatric, neurologic, and cognitive development. *Pediatr Neurol*, *32*(3), 166-172.
- Castelo-Branco, M., Mendes, M., Silva, F., Massano, J., Januario, G., Januario, C., et al. (2009). Motion integration deficits are independent of magnocellular impairment in Parkinson's disease. *Neuropsychologia*, *47*(2), 314-320.
- Costanzo, F., Varuzza, C., Menghini, D., Addona, F., Giancesini, T., & Vicari, S. (2013). Executive functions in intellectual disabilities: A comparison between Williams syndrome and Down syndrome. *Res Dev Disabil*, *34*(5), 1770-1780.
- Csibra, G., Davis, G., Spratling, M. W., & Johnson, M. H. (2000). Gamma oscillations and object processing in the infant brain. *Science*, *290*(5496), 1582-1585.
- Cumming, B. G., & DeAngelis, G. C. (2001). The physiology of stereopsis. *Annu Rev Neurosci*, *24*, 203-238.
- Cusco, I., Corominas, R., Bayes, M., Flores, R., Rivera-Brugues, N., Campuzano, V., et al. (2008). Copy number variation at the 7q11.23 segmental duplications is a susceptibility factor for the Williams-Beuren syndrome deletion. *Genome Res*, *18*(5), 683-694.
- Damasio, A. R., Damasio, H., & Van Hoesen, G. W. (1982). Prosopagnosia: anatomic basis and behavioral mechanisms. *Neurology*, *32*(4), 331-341.
- Desimone, R., & Schein, S. J. (1987). Visual properties of neurons in area V4 of the macaque: sensitivity to stimulus form. *J Neurophysiol*, *57*(3), 835-868.
- Eckert, M. A., Galaburda, A. M., Karchemskiy, A., Liang, A., Thompson, P., Dutton, R. A., et al. (2006). Anomalous sylvian fissure morphology in Williams syndrome. *Neuroimage*, *33*(1), 39-45.
- Ewart, A. K., Morris, C. A., Atkinson, D., Jin, W., Sternes, K., Spallone, P., et al. (1993). Hemizyosity at the elastin locus in a developmental disorder, Williams syndrome. *Nat Genet*, *5*(1), 11-16.
- Fanconi, G., Girardet, P., Schlesinger, B., Butler, N., & Black, J. (1952). Chronic hypercalcemia, combined with osteosclerosis, hyperazotemia, nanism and congenital malformations. *Helv Paediatr Acta*, *7*(4), 314-349.
- Faria, A. V., Landau, B., O'Hearn, K. M., Li, X., Jiang, H., Oishi, K., et al. (2012). Quantitative analysis of gray and white matter in Williams syndrome. *Neuroreport*, *23*(5), 283-289.
- Farivar, R. (2009). Dorsal-ventral integration in object recognition. *Brain Res Rev*, *61*(2), 144-153.
- Farivar, R., Blanke, O., & Chaudhuri, A. (2009). Dorsal-ventral integration in the recognition of motion-defined unfamiliar faces. *J Neurosci*, *29*(16), 5336-5342.
- Farran, E. K., & Jarrold, C. (2003). Visuospatial cognition in Williams syndrome: reviewing and accounting for the strengths and weaknesses in performance. *Dev Neuropsychol*, *23*(1-2), 173-200.
- Frangiskakis, J. M., Ewart, A. K., Morris, C. A., Mervis, C. B., Bertrand, J., Robinson, B. F., et al. (1996). LIM-kinase1 hemizyosity implicated in impaired visuospatial constructive cognition. *Cell*, *86*(1), 59-69.
- Gagliardi, C., Bonaglia, M. C., Selicorni, A., Borgatti, R., & Giorda, R. (2003). Unusual cognitive and behavioural profile in a Williams syndrome patient with atypical 7q11.23 deletion. *J Med Genet*, *40*(7), 526-530.
- Gagliardi, C., Martelli, S., Burt, M. D., & Borgatti, R. (2007). Evolution of neurologic features in Williams syndrome. *Pediatr Neurol*, *36*(5), 301-306.
- Galaburda, A. M., & Bellugi, U. (2000). V. Multi-level analysis of cortical neuroanatomy in Williams syndrome. *J Cogn Neurosci*, *12 Suppl 1*, 74-88.
- Galaburda, A. M., Holinger, D. P., Bellugi, U., & Sherman, G. F. (2002). Williams syndrome: neuronal size and neuronal-packing density in primary visual cortex. *Arch Neurol*, *59*(9), 1461-1467.
- Gaser, C., Luders, E., Thompson, P. M., Lee, A. D., Dutton, R. A., Geaga, J. A., et al. (2006). Increased local gyrification mapped in Williams syndrome. *Neuroimage*, *33*(1), 46-54.
- Goebel, R., Muckli, L., & Kim, D. (2004). Visual System. In G. Paxinos & J. K. Mai (Eds.), *The human nervous system* (2nd ed.). Amsterdam ; Boston: Elsevier Academic Press.
- Golarai, G., Hong, S., Haas, B. W., Galaburda, A. M., Mills, D. L., Bellugi, U., et al. (2010). The fusiform face area is enlarged in Williams syndrome. *J Neurosci*, *30*(19), 6700-6712.
- Goodale, M. A., & Milner, A. (1992). Separate visual pathways for perception and action. *Trends Neurosci*, *15*(1), 20-25.

- Gothelf, D., Farber, N., Raveh, E., Apter, A., & Attias, J. (2006). Hyperacusis in Williams syndrome: characteristics and associated neuroaudiologic abnormalities. *Neurology*, *66*(3), 390-395.
- Green, T., Avda, S., Dotan, I., Zarchi, O., Basel-Vanagaite, L., Zalsman, G., et al. (2011). Phenotypic psychiatric characterization of children with Williams syndrome and response of those with ADHD to methylphenidate treatment. *Am J Med Genet B Neuropsychiatr Genet*, *159B*(1), 13-20.
- Grice, S. J., Haan, M. D., Halit, H., Johnson, M. H., Csibra, G., Grant, J., et al. (2003). ERP abnormalities of illusory contour perception in Williams syndrome. *Neuroreport*, *14*(14), 1773-1777.
- Grice, S. J., Spratling, M. W., Karmiloff-Smith, A., Halit, H., Csibra, G., de Haan, M., et al. (2001). Disordered visual processing and oscillatory brain activity in autism and Williams syndrome. *Neuroreport*, *12*(12), 2697-2700.
- Grinter, E. J., Maybery, M. T., & Badcock, D. R. (2010). Vision in developmental disorders: is there a dorsal stream deficit? *Brain Res Bull*, *82*(3-4), 147-160.
- Haas, B. W., Mills, D., Yam, A., Hoeft, F., Bellugi, U., & Reiss, A. (2009). Genetic influences on sociability: heightened amygdala reactivity and event-related responses to positive social stimuli in Williams syndrome. *J Neurosci*, *29*(4), 1132-1139.
- Heeger, D. J., Boynton, G. M., Demb, J. B., Seidemann, E., & Newsome, W. T. (1999). Motion opponency in visual cortex. *J Neurosci*, *19*(16), 7162-7174.
- Hoeft, F., Barnea-Goraly, N., Haas, B. W., Golarai, G., Ng, D., Mills, D., et al. (2007). More is not always better: increased fractional anisotropy of superior longitudinal fasciculus associated with poor visuospatial abilities in Williams syndrome. *J Neurosci*, *27*(44), 11960-11965.
- Hofer, S., Karaus, A., & Frahm, J. (2010). Reconstruction and dissection of the entire human visual pathway using diffusion tensor MRI. *Frontiers in Neuroanatomy*, *4*.
- Horwitz, G. D., & Hass, C. A. (2012). Nonlinear analysis of macaque V1 color tuning reveals cardinal directions for cortical color processing. *Nat Neurosci*, *15*(6), 913-919.
- Hubel, D. H., & Wiesel, T. N. (1968). Receptive fields and functional architecture of monkey striate cortex. *J Physiol*, *195*(1), 215-243.
- Jarrold, C., Baddeley, A. D., & Hewes, A. K. (1998). Verbal and nonverbal abilities in the Williams syndrome phenotype: evidence for diverging developmental trajectories. *J Child Psychol Psychiatry*, *39*(4), 511-523.
- Jernigan, T. L., & Bellugi, U. (1990). Anomalous brain morphology on magnetic resonance images in Williams syndrome and Down syndrome. *Arch Neurol*, *47*(5), 529-533.
- Kanwisher, N., McDermott, J., & Chun, M. M. (1997). The fusiform face area: a module in human extrastriate cortex specialized for face perception. *J Neurosci*, *17*(11), 4302-4311.
- Kaplan, E. (2004). The M, P, and K pathways of the primate visual system. In L. M. Chalupa & J. S. Werner (Eds.), *The visual neurosciences*. (Vol. 1, pp. 481-493). Cambridge, Massachusetts: The MIT Press.
- Karmiloff-Smith, A., Brown, J. H., Grice, S., & Paterson, S. (2003). Dethroning the myth: cognitive dissociations and innate modularity in Williams syndrome. *Dev Neuropsychol*, *23*(1-2), 227-242.
- Karmiloff-Smith, A., Thomas, M., Annaz, D., Humphreys, K., Ewing, S., Brace, N., et al. (2004). Exploring the Williams syndrome face-processing debate: the importance of building developmental trajectories. *J Child Psychol Psychiatry*, *45*(7), 1258-1274.
- Key, A. P., & Dykens, E. M. (2011). Electrophysiological study of local/global processing in Williams syndrome. *J Neurodev Disord*, *3*(1), 28-38.
- Klaver, P., Lichtensteiger, J., Bucher, K., Dietrich, T., Loenneker, T., & Martin, E. (2008). Dorsal stream development in motion and structure-from-motion perception. *Neuroimage*, *39*(4), 1815-1823.
- Kogan, C. S., Bertone, A., Cornish, K., Boutet, I., Der Kaloustian, V. M., Andermann, E., et al. (2004). Integrative cortical dysfunction and pervasive motion perception deficit in fragile X syndrome. *Neurology*, *63*(9), 1634-1639.
- Korenberg, J. R., Bellugi, U., Salandanan, L. S., Mills, D., & Reiss, A. L. (2003). Williams syndrome: a neurogenetic model of human behaviour. In D. Cooper (Ed.), *Encyclopedia of the Human Genome*(pp. 757-766). London: The Nature Publishing Group.
- Levitin, D. J., Menon, V., Schmitt, J. E., Eliez, S., White, C. D., Glover, G. H., et al. (2003). Neural correlates of auditory perception in Williams syndrome: an fMRI study. *Neuroimage*, *18*(1), 74-82.

- Leyfer, O. T., Woodruff-Borden, J., Klein-Tasman, B. P., Fricke, J. S., & Mervis, C. B. (2006). Prevalence of psychiatric disorders in 4 to 16-year-olds with Williams syndrome. *Am J Med Genet B Neuropsychiatr Genet*, *141B*(6), 615-622.
- Lowery, M. C., Morris, C. A., Ewart, A., Brothman, L. J., Zhu, X. L., Leonard, C. O., et al. (1995). Strong correlation of elastin deletions, detected by FISH, with Williams syndrome: evaluation of 235 patients. *Am J Hum Genet*, *57*(1), 49-53.
- Marenco, S., Siuta, M. A., Kippenhan, J. S., Grodofsky, S., Chang, W. L., Kohn, P., et al. (2007). Genetic contributions to white matter architecture revealed by diffusion tensor imaging in Williams syndrome. *Proc Natl Acad Sci U S A*, *104*(38), 15117-15122.
- Martens, M. A., Wilson, S. J., & Reutens, D. C. (2008). Research Review: Williams syndrome: a critical review of the cognitive, behavioral, and neuroanatomical phenotype. *J Child Psychol Psychiatry*, *49*(6), 576-608.
- McKeefry, D. J., Watson, J. D., Frackowiak, R. S., Fong, K., & Zeki, S. (1997). The activity in human areas V1/V2, V3, and V5 during the perception of coherent and incoherent motion. *Neuroimage*, *5*(1), 1-12.
- Mendes, M., Silva, F., Simoes, L., Jorge, M., Saraiva, J., & Castelo-Branco, M. (2005). Visual magnocellular and structure from motion perceptual deficits in a neurodevelopmental model of dorsal stream function. *Brain Res Cogn Brain Res*, *25*(3), 788-798.
- Meng, Y., Zhang, Y., Tregoubov, V., Janus, C., Cruz, L., Jackson, M., et al. (2002). Abnormal spine morphology and enhanced LTP in LIMK-1 knockout mice. *Neuron*, *35*(1), 121-133.
- Menghini, D., Di Paola, M., Federico, F., Vicari, S., Petrosini, L., Caltagirone, C., et al. (2011). Relationship between brain abnormalities and cognitive profile in Williams syndrome. *Behav Genet*, *41*(3), 394-402.
- Mervis, C. B. (2003). Williams syndrome: 15 years of psychological research. *Dev Neuropsychol*, *23*(1-2), 1-12.
- Mervis, C. B., & Klein-Tasman, B. P. (2000). Williams syndrome: cognition, personality, and adaptive behavior. *Ment Retard Dev Disabil Res Rev*, *6*(2), 148-158.
- Mervis, C. B., Robinson, B. F., Bertrand, J., Morris, C. A., Klein-Tasman, B. P., & Armstrong, S. C. (2000). The Williams syndrome cognitive profile. *Brain Cogn*, *44*(3), 604-628.
- Meyer-Lindenberg, A., Hariri, A. R., Munoz, K. E., Mervis, C. B., Mattay, V. S., Morris, C. A., et al. (2005). Neural correlates of genetically abnormal social cognition in Williams syndrome. *Nat Neurosci*, *8*(8), 991-993.
- Meyer-Lindenberg, A., Kohn, P., Mervis, C. B., Kippenhan, J. S., Olsen, R. K., Morris, C. A., et al. (2004). Neural basis of genetically determined visuospatial construction deficit in Williams syndrome. *Neuron*, *43*(5), 623-631.
- Mills, D., Llamas, T., St George, M., Doyle, T. F., Neville, H., & Korenberg, J. R. (2003). *Electrophysiological signatures of abnormal auditory language processing in infants, children and adults with Williams syndrome*. San Diego: Institute for Neural Computation, University of California.
- Mills, D. L., Alvarez, T. D., St George, M., Appelbaum, L. G., Bellugi, U., & Neville, H. (2000). III. Electrophysiological studies of face processing in Williams syndrome. *J Cogn Neurosci*, *12 Suppl 1*, 47-64.
- Milner, A., & Goodale, M. A. (1995). *The visual brain in action*. Oxford: Oxford University Press.
- Milner, A., & Goodale, M. A. (2008). Two visual systems re-viewed. *Neuropsychologia*, *46*(3), 774-785.
- Mimura, M., Hoefl, F., Kato, M., Kobayashi, N., Sheau, K., Piggot, J., et al. (2010). A preliminary study of orbitofrontal activation and hypersociability in Williams Syndrome. *J Neurodev Disord*, *2*(2), 93-98.
- Mobbs, D., Eckert, M. A., Menon, V., Mills, D., Korenberg, J., Galaburda, A. M., et al. (2007a). Reduced parietal and visual cortical activation during global processing in Williams syndrome. *Dev Med Child Neurol*, *49*(6), 433-438.
- Mobbs, D., Eckert, M. A., Mills, D., Korenberg, J., Bellugi, U., Galaburda, A. M., et al. (2007b). Frontostriatal dysfunction during response inhibition in Williams syndrome. *Biol Psychiatry*, *62*(3), 256-261.
- Mobbs, D., Garrett, A. S., Menon, V., Rose, F. E., Bellugi, U., & Reiss, A. L. (2004). Anomalous brain activation during face and gaze processing in Williams syndrome. *Neurology*, *62*(11), 2070-2076.

- Montfoort, I., Frens, M. A., Hooge, I. T., Haselen, G. C., & van der Geest, J. N. (2007). Visual search deficits in Williams-Beuren syndrome. *Neuropsychologia*, *45*(5), 931-938.
- Morris, C. A., Demsey, S. A., Leonard, C. O., Dilts, C., & Blackburn, B. L. (1988). Natural history of Williams syndrome: physical characteristics. *J Pediatr*, *113*(2), 318-326.
- Morris, C. A., Mervis, C. B., Hobart, H. H., Gregg, R. G., Bertrand, J., Ensing, G. J., et al. (2003). GTF2I hemizyosity implicated in mental retardation in Williams syndrome: genotype-phenotype analysis of five families with deletions in the Williams syndrome region. *Am J Med Genet A*, *123A*(1), 45-59.
- Morris, C. A., Thomas, I. T., & Greenberg, F. (1993). Williams syndrome: autosomal dominant inheritance. *Am J Med Genet*, *47*(4), 478-481.
- Munoz, K. E., Meyer-Lindenberg, A., Hariri, A. R., Mervis, C. B., Mattay, V. S., Morris, C. A., et al. (2010). Abnormalities in neural processing of emotional stimuli in Williams syndrome vary according to social vs. non-social content. *Neuroimage*, *50*(1), 340-346.
- Murphy, M. B., Greenberg, F., Wilson, G., Hughes, M., & DiLiberti, J. (1990). Williams syndrome in twins. *Am J Med Genet Suppl*, *6*, 97-99.
- Nakamura, M., Watanabe, S., Inagaki, M., Hirai, M., Miki, K., Honda, Y., et al. (2013). Electrophysiological study of face inversion effects in Williams syndrome. *Brain Dev*, *35*(4), 323-330.
- Navon, D. (1977). Forest before trees: The precedence of global features in visual perception. *Cognitive Psychology*, *9*(353-383).
- Neville, H., Mills, D., & Bellugi, U. (1994). Effects of altered auditory sensitivity and age of language acquisition on the development of language-relevant neural systems: Preliminary studies of Williams syndrome. In S. Broman & J. Grafman (Eds.), *Atypical cognitive deficits in developmental disorders: Implications for brain function*. (pp. 67-83). Hillsdale, NJ: Erlbaum.
- Nickerson, E., Greenberg, F., Keating, M. T., McCaskill, C., & Shaffer, L. G. (1995). Deletions of the elastin gene at 7q11.23 occur in approximately 90% of patients with Williams syndrome. *Am J Hum Genet*, *56*(5), 1156-1161.
- O'Hearn, K., Roth, J. K., Courtney, S. M., Luna, B., Street, W., Terwillinger, R., et al. (2011). Object recognition in Williams syndrome: uneven ventral stream activation. *Dev Sci*, *14*(3), 549-565.
- Olsen, R. K., Kippenhan, J. S., Japee, S., Kohn, P., Mervis, C. B., Saad, Z. S., et al. (2009). Retinotopically defined primary visual cortex in Williams syndrome. *Brain*, *132*(Pt 3), 635-644.
- Osborne, L. R. (2010). Animal models of Williams syndrome. *Am J Med Genet C Semin Med Genet*, *154C*(2), 209-219.
- Parrish, E. E., Giaschi, D. E., Boden, C., & Dougherty, R. (2005). The maturation of form and motion perception in school age children. *Vision Res*, *45*(7), 827-837.
- Paul, B. M., Snyder, A. Z., Haist, F., Raichle, M. E., Bellugi, U., & Stiles, J. (2009). Amygdala response to faces parallels social behavior in Williams syndrome. *Soc Cogn Affect Neurosci*, *4*(3), 278-285.
- Paul, B. M., Stiles, J., Passarotti, A., Bavar, N., & Bellugi, U. (2002). Face and place processing in Williams syndrome: evidence for a dorsal-ventral dissociation. *Neuroreport*, *13*(9), 1115-1119.
- Perez Jurado, L. A., Peoples, R., Kaplan, P., Hamel, B. C., & Francke, U. (1996). Molecular definition of the chromosome 7 deletion in Williams syndrome and parent-of-origin effects on growth. *Am J Hum Genet*, *59*(4), 781-792.
- Pinheiro, A. P., Galdo-Alvarez, S., Sampaio, A., Niznikiewicz, M., & Goncalves, O. F. (2010). Electrophysiological correlates of semantic processing in Williams syndrome. *Res Dev Disabil*, *31*(6), 1412-1425.
- Pober, B., & Dykens, E. M. (1996). Williams syndrome: An overview of medical, cognitive, and behavioral features. *Child and Adolescent Psychiatric Clinics of North America*, *5*, 929-943.
- Porter, M. A., Dobson-Stone, C., Kwok, J. B., Schofield, P. R., Beckett, W., & Tassabehji, M. (2012). A role for transcription factor GTF2IRD2 in executive function in Williams-Beuren syndrome. *PLoS One*, *7*(10), e47457.
- Reilly, J., Klima, E., & Bellugi, U. (1990). Once more with feeling: Affect and language in atypical populations. *Developmental Psychopathology*, *2*, 367-391.
- Reiss, A. L., Eckert, M. A., Rose, F. E., Karchemskiy, A., Kesler, S., Chang, M., et al. (2004). An experiment of nature: brain anatomy parallels cognition and behavior in Williams syndrome. *J Neurosci*, *24*(21), 5009-5015.

- Reiss, A. L., Eliez, S., Schmitt, J. E., Straus, E., Lai, Z., Jones, W., et al. (2000). IV. Neuroanatomy of Williams syndrome: a high-resolution MRI study. *J Cogn Neurosci*, *12 Suppl 1*, 65-73.
- Salzman, C. D., Murasugi, C. M., Britten, K. H., & Newsome, W. T. (1992). Microstimulation in visual area MT: effects on direction discrimination performance. *J Neurosci*, *12*(6), 2331-2355.
- Sampaio, A., Bouix, S., Sousa, N., Vasconcelos, C., Fernandez, M., Shenton, M. E., et al. (2012). Morphometry of corpus callosum in Williams syndrome: shape as an index of neural development. *Brain Struct Funct*, *218*(3), 711-720.
- Sampaio, A., Fernandez, M., Henriques, M., Carracedo, A., Sousa, N., & Goncalves, O. F. (2009). Cognitive functioning in Williams syndrome: a study in Portuguese and Spanish patients. *Eur J Paediatr Neurol*, *13*(4), 337-342.
- Sarpal, D., Buchsbaum, B. R., Kohn, P. D., Kippenhan, J. S., Mervis, C. B., Morris, C. A., et al. (2008). A genetic model for understanding higher order visual processing: functional interactions of the ventral visual stream in Williams syndrome. *Cereb Cortex*, *18*(10), 2402-2409.
- Schenk, T., & McIntosh, R. (2010). Do we have independent visual streams for perception and action? *Cognitive Neuroscience*, *1*(1), 52-62.
- Schmitt, J. E., Eliez, S., Bellugi, U., & Reiss, A. L. (2001). Analysis of cerebral shape in Williams syndrome. *Arch Neurol*, *58*(2), 283-287.
- Schmitt, J. E., Eliez, S., Warsofsky, I. S., Bellugi, U., & Reiss, A. L. (2001). Corpus callosum morphology of Williams syndrome: relation to genetics and behavior. *Dev Med Child Neurol*, *43*(3), 155-159.
- Schmitt, J. E., Watts, K., Eliez, S., Bellugi, U., Galaburda, A. M., & Reiss, A. L. (2002). Increased gyrification in Williams syndrome: evidence using 3D MRI methods. *Dev Med Child Neurol*, *44*(5), 292-295.
- Schubert, C. (2009). The genomic basis of the Williams-Beuren syndrome. *Cell Mol Life Sci*, *66*(7), 1178-1197.
- Searcy, Y. M., Lincoln, A. J., Rose, F. E., Klima, E. S., Bavar, N., & Korenberg, J. R. (2004). The relationship between age and IQ in adults with Williams syndrome. *Am J Ment Retard*, *109*(3), 231-236.
- Semel, E., & Rosner, S. (2003). *Understanding Williams syndrome: behavioral patterns and interventions*. London: Lawrence Erlbaum Associates, Inc.
- Skottun, B. C. (2000). The magnocellular deficit theory of dyslexia: the evidence from contrast sensitivity. *Vision Research*, *40*, 111-127.
- Smoot, L., Zhang, H., Klaiman, C., Schultz, R., & Pober, B. (2005). Medical overview and genetics of Williams-Beuren syndrome. *Progres in Pediatric Cardiology*, *20*(2), 195-205.
- Spencer, J., O'Brien, J., Riggs, K., Braddick, O., Atkinson, J., & Wattam-Bell, J. (2000). Motion processing in autism: evidence for a dorsal stream deficiency. *Neuroreport*, *11*(12), 2765-2767.
- St. George, M., Mills, D., & Bellugi, U. (2000). ERPs during auditory language comprehension in Williams syndrome. The effects of word frequency, imageability and length on word class. *Neuroimage*, *11*(5), 357.
- Stojanovik, V. (2006). Social interaction deficits and conversational inadequacy in Williams syndrome. *Journal of Neurolinguistics*, *19*(2), 157-173.
- Stromme, P., Bjornstad, P. G., & Ramstad, K. (2002). Prevalence estimation of Williams syndrome. *J Child Neurol*, *17*(4), 269-271.
- Thomson, A. M. (2010). Neocortical layer 6, a review. *Front Neuroanat*, *4*, 13.
- Thornton-Wells, T. A., Avery, S. N., & Blackford, J. U. (2011). Using novel control groups to dissect the amygdala's role in Williams syndrome. *Dev Cogn Neurosci*, *1*(3), 295-304.
- Thornton-Wells, T. A., Cannistraci, C. J., Anderson, A. W., Kim, C. Y., Eapen, M., Gore, J. C., et al. (2010). Auditory attraction: activation of visual cortex by music and sound in Williams syndrome. *Am J Intellect Dev Disabil*, *115*(2), 172-189.
- Tordjman, S., Anderson, G. M., Botbol, M., Toutain, A., Sarda, P., Carlier, M., et al. (2012). Autistic disorder in patients with Williams-Beuren syndrome: a reconsideration of the Williams-Beuren syndrome phenotype. *PLoS One*, *7*(3), e30778.
- Udwin, O., & Yule, W. (1991). A cognitive and behavioural phenotype in Williams syndrome. *J Clin Exp Neuropsychol*, *13*(2), 232-244.
- Ungerleider, L. G., & Haxby, J. V. (1994). 'What' and 'where' in the human brain. *Curr Opin Neurobiol*, *4*(2), 157-165.

- Ungerleider, L. G., & Mishkin, M. (1982). Two cortical visual systems. In D. J. Ingle, M. A. Goodale & R. J. W. Mansfield (Eds.), *Analysis of visual behavior*(pp. 549-586). Cambridge: MIT Press.
- Van Essen, D. C., Dierker, D., Snyder, A. Z., Raichle, M. E., Reiss, A. L., & Korenberg, J. (2006). Symmetry of cortical folding abnormalities in Williams syndrome revealed by surface-based analyses. *J Neurosci*, *26*(20), 5470-5483.
- Van Essen, D. C., Maunsell, J. H., & Bixby, J. L. (1981). The middle temporal visual area in the macaque: myeloarchitecture, connections, functional properties and topographic organization. *J Comp Neurol*, *199*(3), 293-326.
- van Hagen, J. M., van der Geest, J. N., van der Giessen, R. S., Lagers-van Haselen, G. C., Eussen, H. J., Gille, J. J., et al. (2007). Contribution of CYLN2 and GTF2IRD1 to neurological and cognitive symptoms in Williams Syndrome. *Neurobiol Dis*, *26*(1), 112-124.
- Van Hooser, S. D., & Nelson, S. (2005). Visual System. *Encyclopedia of Life Sciences* 1-8.
- Volterra, V., Longobardi, E., Pezzini, G., Vicari, S., & Antenore, C. (1999). Visuo-spatial and linguistic abilities in a twin with Williams syndrome. *J Intellect Disabil Res*, *43* (Pt 4), 294-305.
- von der Heydt, R., Peterhans, E., & Baumgartner, G. (1984). Illusory contours and cortical neuron responses. *Science*, *224*(4654), 1260-1262.
- Wallach, H., & O'Connell, D. N. (1953). The kinetic depth effect. *J Exp Psychol*, *45*(4), 205-217.
- Williams, J. C., Barratt-Boyes, B. G., & Lowe, J. B. (1961). Supravalvular aortic stenosis. *Circulation*, *24*, 1311-1318.
- Zihl, J., von Cramon, D., Mai, N., & Schmid, C. (1991). Disturbance of movement vision after bilateral posterior brain damage. Further evidence and follow up observations. *Brain*, *114* (Pt 5), 2235-2252.

METHODS

CHAPTER II

Neuroscientific tools for brain function investigation:

electroencephalography and functional
magnetic resonance imaging

The understanding of brain function in the last decades has taken a major leap forward due to the development and dissemination of advanced neuroimaging techniques. Electroencephalography (EEG) and functional magnetic resonance imaging (fMRI) constitute outstanding tools in cognitive neuroscience both in clinical and research applications as they provide unique contributions to the study of specific aspects of neural activity. These techniques are broadly applied to map the human brain and their complementary patterns of spatial and temporal resolution stimulates their complementary use. Both techniques are noninvasive and are extensively used in the diagnosis definition, treatment monitoring as well as in understanding mechanisms of brain disease. Having been the main tools used throughout this work, an overview into these two neuroscience techniques is provided in this chapter. As a note, in this work behavioural experimental paradigms and neuropsychological assessment procedures were implemented and they are described in the respective chapters.

Electroencephalography

The EEG technique allows the study of the electrical activity generated in the brain, by displaying and recording it through the use of scalp electrodes. The growing use of this technique is explained by its ease of set-up and application to a multitude of patient populations and contexts, with virtually no risk (non-invasive) and at a relatively inexpensive cost. However, its main advantage relies on the superior temporal resolution (in the order of the milliseconds), in contrast to its limited spatial resolution.

The origin of the EEG signal is as follows. Communicating neurons, or nerve cells, generate electrical signals (action potentials) that travel from cell body to the axon terminals and cause the release of chemical neurotransmitters at the synapses. In turn, these neurotransmitters activate receptors in the dendrite of the postsynaptic cells causing electrical currents named postsynaptic potentials. These electric potentials and ionic currents generated by single neurons are too small to be picked by EEG. Therefore, the detected EEG signals (in the range of microvolts) result from the summation of the synchronous activity of thousands of neurons acting as tiny dipole sources with spatial radial orientation to the scalp. In this manner, measureable activity on the scalp implies that a significant

cortical area is active and firing (see Figure 2.1). Given that the voltage fields fall off with the square of the distance, the recording of activity from deep sources (e.g. subcortical regions) becomes more difficult than those of cortical regions (Olejniczak, 2006).

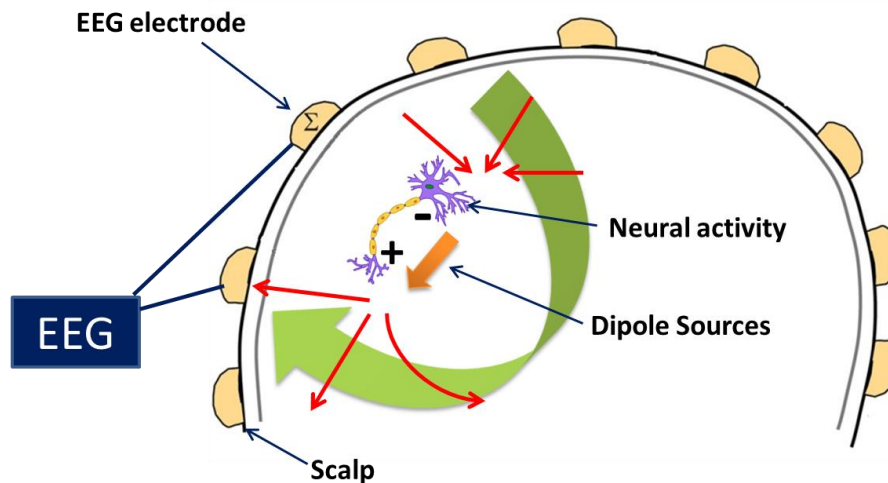


Figure 2.1. Schematic diagram of the EEG signal generation. EEG, through electrodes positioned on the scalp, measures the electrical potential differences that are generated by neural activity. Neurons transmitting neurological signals across their synapses act as dipole sources. (Adapted from Min, Marzelli, & Yoo, 2010)

EEG activity can be measured in the entire surface of the scalp by employing multi-channel arrays which usually comprise 64 or 128 electrodes montages. Importantly, the recording is performed with respect to a reference that is an arbitrarily chosen “zero level”. It should be noted that the voltage obtained does not reflect scalp activity at the active site but should be understood as a potential difference between the target site and the reference location (Davidson, Jackson, & Larson, 2000; Teplan, 2002). In the present work we used the vertex Cz reference, advantageous because it is located centrally among active electrodes of interest while keeping enough distance to ensures acceptable signal detection (see Figure 2.2).

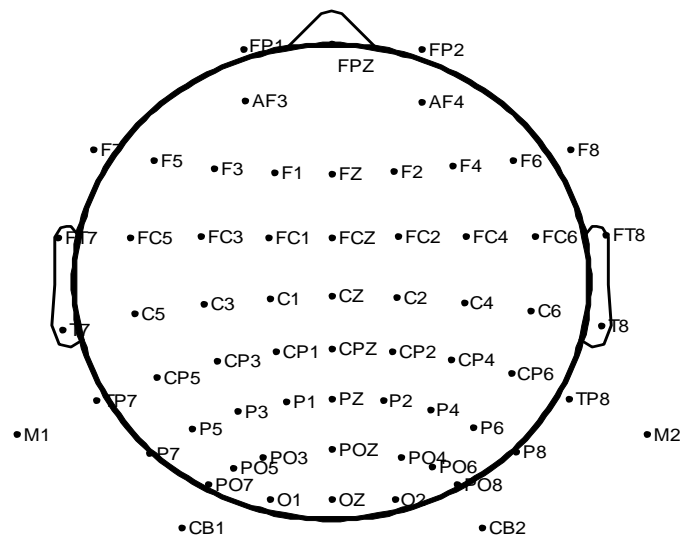


Figure 2.2. Multi-channel locations – 64 channel montage. Electrodes locations are projected from 3D to 2D and plotted according to the International 10/20 System of Electrode Placement adapted to this number of electrodes. The 10/20 system establishes standardized electrode locations allowing comparison between different studies. Electrodes display a specific nomenclature being labelled with letters which represent the lobe and numbers indicating the hemispheric location. (From EEGLAB, Delorme & Makeig, 2004)

Since the first human EEG recording in 1929 performed by Hans Berger, (Berger, 1929) many mathematical and technological breakthroughs have allowed the EEG to become a routine and important tool particularly in the clinical context (e.g. in epilepsy diagnosis). Such improvements in EEG data recording, processing and analysis are crucial, since the electrodes register all ongoing electrical activity, which not only includes the brain signals of interest but also other physiological and non-physiological electrical signals. Therefore, EEG signals are commonly contaminated by signal distortions called artifacts which can be participant- (body and eye movements, blinks, sweating) or technical-related (impedance fluctuation, cable movements, electric current 50/60Hz).

In this manner, there are a number of processing steps that are commonly employed to isolate and strengthen the signals of interest while minimizing the effect of unwanted noise, as described below.

Event-related potentials (ERP)

As mentioned, the EEG signal represents a combination of a wide range of sources of activity. Among these, the ones that respond in a time and phase-locked manner to a given

stimulus are called *event related potentials* (ERPs) (Luck, 2005). Accordingly, in an ERP experiment, a given stimulus is repeatedly shown to the participant, and assuming that the brain response is similar across the trials and the noise is constituted by random fluctuations, the averaging across a large number of trials allows the reduction of the noise level (the random fluctuations cancel each other) and the increased visibility of the brain response time-locked to the stimulus presentation. This procedure is commonly computed and presented separately for each electrode (see Figure 2.3A and 2.3B).

The grand average ERP waveforms are also frequently computed in ERP studies and are created by averaging together the average waveforms of the individual subjects (Luck, 2005). The resulting ERP waveforms reflect the flow of information through the brain and consist of a sequence of positive and negative voltage deflections (named peaks or components) that are identified by their time of occurrence and polarity (e.g. the face selective component N170, occurs as a negative wave that peaks at or near 170 ms after a stimulus onset) (see Figure 2.3B). The ERP procedure therefore allows the investigation of specific perceptual and cognitive processes which has led to the identification of various cognitive ERP components (e.g. P100, N170, P300).

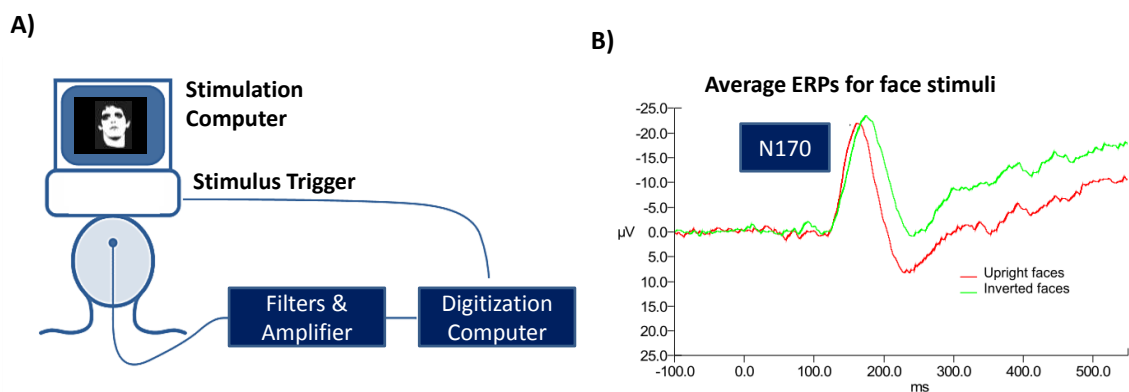


Figure 2.3. Example of an ERP experiment. A) The stimulus is repeatedly shown on a computer monitor while the EEG is recorded. The signal is filtered and amplified. B) The signal segments corresponding to the stimulus presentation are averaged resulting in an ERP waveform in which different components may be identified. (Adapted from Luck, 2005)

Independent Component Analysis (ICA)

ERP analysis is commonly performed by measuring amplitudes and latencies of the components identified in the average waveform. However, such measures are discrete

indexes of the sensory and cognitive event-related processes that do not take into account the distributional properties of the ensemble single-trial time series. Several alternative techniques have been proposed to tackle this issue, among which we highlight the *independent component analysis* (ICA).

In short, ICA is a procedure that separates a linear mixture of signals, thereby yielding their individual manifestation on the recording sensors, as well as the original individual time course of each source. Such technique has demonstrated great efficacy in identifying both temporally and functionally independent source signals in multi-channel EEG or other electrophysiological signals.

The example of the ‘cocktail party problem’ is typically used to illustrate the concurrence of mixed source signals to the final observed waveform. In this example, a range of microphones records mixtures of voices of several people talking at the same time in a party. Here, the recordings sound as indecipherable noise and it is difficult to capture the isolated voice of one speaker. Thus, the problem is how to combine the recorded signals in order to separate the speaker’s voice without having any prior information about the nature or properties of each individual source. The ICA creates spatial filters which cancel out the contributions of all but one distinct source signals that contribute to the scalp data. As a result, ICA constitutes a method of data information-driven spatial filtering that learns spatial filters which differentially focus on a distinct physical source of EEG signals, thereby separating out different brain generator processes as well as artifacts. A great value of this technique relies on the separation of the EEG signal from non-brain EEG artifacts such as eye blinks, eye movement potentials, electromyographic and electrocardiographic signals (Makeig & Onton, 2012; Vigario, Sarela, Jousmaki, Hamalainen, & Oja, 2000). Furthermore, the output of this technique can be used to assess if the same neural generators are present for the same paradigm in different populations, and to compare the timing and contribution of each generator to the recorded signals.

Time-frequency analysis

Even though time domain analysis has been consistently used in the ERP studies, the last two decades have witness a paradigm shifted towards the investigation of power, coherence and phase locking of oscillatory non-averaged signals (time-frequency analysis). *Time-frequency analysis* allows the investigation of the brain’s parallel functioning, with states that oscillations

at different frequencies reflect multiple neural processes occurring simultaneously. In such spectral decompositions, the amplitude and phase of the frequencies of interest are estimated for different time windows along the pre and post-stimulus period, yielding both time and frequency domain information (Roach & Mathalon, 2008). The time-frequency decomposition of the EEG data is usually performed through a sliding time window Fast Fourier transform (FFT) or the Wavelet transform (Bruns, 2004) which allows tracking of the temporal evolution of spectral values. Regardless of the decomposition approach employed, the resulting output shows the frequency components of the input signal for every point in time and for each frequency (see an example in Figure 2.4). In short, this technique reveals which frequencies have the most power at specific points in time in a spectro-temporal representation.

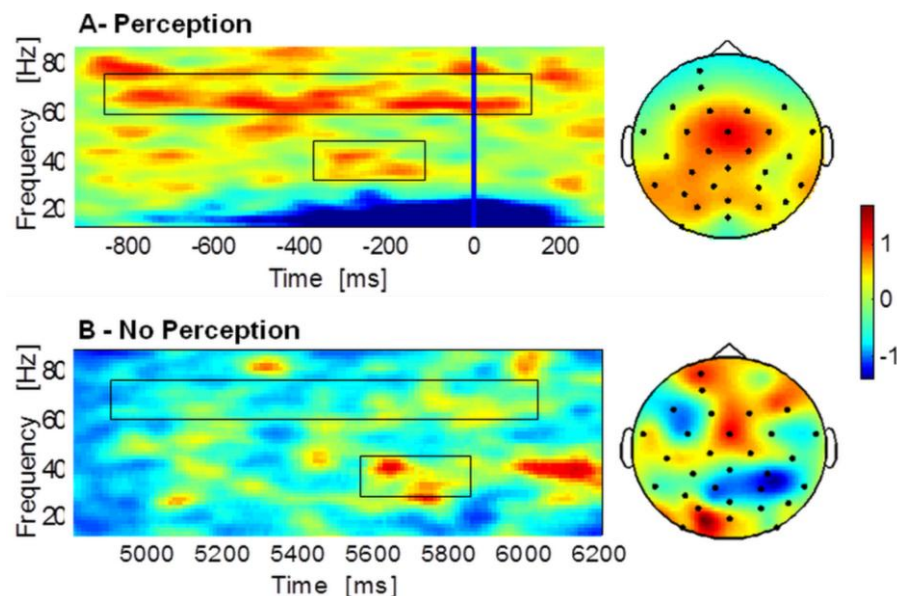


Figure 2.4. Example of time-frequency representations. The figure illustrates the spectral representation within the gamma-band frequencies for the A) perception and B) no perception conditions of an experimental task involving visual detection of Mooney faces. (From a study of our lab Castelhamo, Rebola, Leitao, Rodriguez, & Castelo-Branco, 2013)

The functional role of gamma-band frequency

The shift in the paradigm concerning the ERP analyses occurred mainly due to the gathered evidence of synchronized oscillatory pattern in neuronal spiking activity (Uhlhaas, Haenschel, Nikolic, & Singer, 2008). Neural networks were found to exhibit a strong

tendency to engage in oscillatory activity at multiple frequency bands defined on the basis of lower and upper frequency boundaries. The classic bands in which the rhythmic electroencephalographic activity can be decomposed include: delta (0-4Hz), theta (5-7Hz), alpha (8-12Hz), beta (13-30Hz) and gamma (30-200Hz) and exhibit distinctive involvement in a wide range of sensory and cognitive processes. The functional role of the main frequency bands is described in Table 2.1, except for delta band which has so far limited investigation regarding its anatomy and function.

Table 2.1. Neural Oscillations in Cortical networks

(Adapted from Uhlhaas et al., 2008)

	Theta (4-7 Hz)	Alpha (8-12Hz)	Beta (13-30Hz)	Gamma (30-200Hz)
Anatomy	Hippocampus, prefrontal cortex, sensory cortex	Thalamus, sensory cortex, motor cortex, hippocampus	All cortical structures, hippocampus, basal ganglia	All brain structures, retina, olfactory bulb
Function	Memory, synaptic plasticity, top-down control	Inhibition, attention, consciousness, top-down control	Sensory gating, attention, perception, motor control	Perception, attention, memory, consciousness, synaptic plasticity, motor control

The study of *gamma-band frequency* is particularly interesting in the context of the current work since they have been suggested to have a general computational role in the construction of coherent percepts. Oscillations within the gamma-band frequency range are thought to occur in all brain structures and play an important role in high-level brain functions such as perceptual organization, attention, working memory and consciousness. It has been shown that the gamma frequencies are involved in perceptual binding, a mechanism through which various features of a visual scene are integrated to construct a whole percept (Singer & Gray, 1995). Accordingly, EEG and magnetoencephalography (MEG) showed robust evidence of the role of gamma oscillations in perceptual grouping abilities which mediate the construction of coherent object representations (Tallon-Baudry & Bertrand, 1999). Gamma-

band activity has also been related to other cognitive phenomena such as working memory, language processing and motor coordination (for a review, see Uhlhaas & Singer, 2006). Interestingly, gamma oscillations cover a large range of frequencies from 30 to 200 Hz which suggests that different subclasses of rhythms may exist. Some evidence has been gathered in favour of this hypothesis with higher gamma-band oscillations being associated with perceptual grouping and lower gamma frequencies being mainly implicated in attentional processes (Vidal, Chaumon, O'Regan, & Tallon-Baudry, 2006). The aforementioned role of gamma-band oscillations in coherent perception place this frequency band as a privileged and potentially revealing subject of study in the WS group.

Source Localization (Inverse Problem)

So far we have highlighted the EEG excellence in separating, identifying and characterizing sensory or cognitive processes and components. However, caution should be taken when considering its capability to precisely determine where in the cortex are the sources that generate the activity (spatial resolution).

The problem of finding the neuronal generators responsible for the measured EEG phenomena is called *source localization* or *inverse problem*. Such type of problem is referred as an ill-posed problem because for all admissible output voltages, there are non-unique and unstable solutions (sensitive to the changes in noise data) (Grech et al., 2008). In other words, for the same recorded electrical signal there is an infinite combination of electrical sources which could have generated it. In the last decades, several algorithms have been proposed to avoid this problem by trying to estimate the current sources inside the brain that best fit the measured voltage potential at various locations on the scalp. Such unique estimation is made possible by incorporating a number of assumptions on the data, generally met by neurophysiological processes. Among the most popular solutions, this work uses the non-parametric sLORETA (standardized low resolution brain electromagnetic tomography), a widely used method that was found to exhibit the best performance in what concerns to the localization error and ghost sources (Grech et al., 2008).

Source localization techniques have been included in cognitive neuroscience studies to localize the sources of different frequency bands and to investigate the dynamics of several higher cognitive functions. However, the limited spatial resolution of these techniques still falls short of other imaging techniques capable of accurately determining the neural correlates underlying several cognitive functions. In this line, fMRI emerges as the most

adequate tool to complement the study of the location of the neural substrates of brain activity elicited by the experimental stimulation. This parallel use of EEG and fMRI thus maximizes the reliability of the reported findings on preserved and impaired brain function in WS.

Functional Magnetic Resonance Imaging

Functional magnetic resonance imaging (fMRI) is a modern, non-invasive imaging technique to measure and localize specific functions of the human brain (Bandettini, Wong, Hinks, Tikofsky, & Hyde, 1992; Kwong et al., 1992). In order to understand how fMRI creates images of neural activity it is important to go through some important physiological concepts (see Figure 2.5).

The brain is a highly active organ and the information processing activity of neurons consumes energy. As a consequence, neural activity triggers an increase of blood flow surrounding active areas, to supply the required glucose and oxygen. However, the total delivery of oxygen exceeds consumption demands. Thus, a surplus of oxygenated blood surrounds the active areas of the brain some seconds after its activation. This causes change in oxy and deoxyhaemoglobin status with increasing concentration of oxyhaemoglobin and decreasing concentration of deoxyhaemoglobin. Given that oxygenated and deoxygenated blood have different magnetic properties, they cause a different impact in the magnetic resonance (MR) signal. Oxyhaemoglobin (present in oxygenated blood) has diamagnetic properties (weak, negative susceptibility to magnetic fields) and therefore does not distort the surrounding magnetic field. In turn, deoxyhaemoglobin (present in deoxygenated blood) is paramagnetic (positive susceptibility to magnetic field and leads to magnetic field distortions and signal loss. This differential effect represents the basis of the blood-oxygen level dependent (BOLD) contrast used in fMRI (Ogawa, Lee, Kay, & Tank, 1990; Ogawa et al., 1993). It is important to note that BOLD fMRI consists of an indirect measure of brain activity and the debate into the neural mechanisms underlying BOLD signal still remains. However, BOLD constitutes the most common functional imaging method applied in neuroscience, and the chain of events leading to BOLD signal is summarized below.

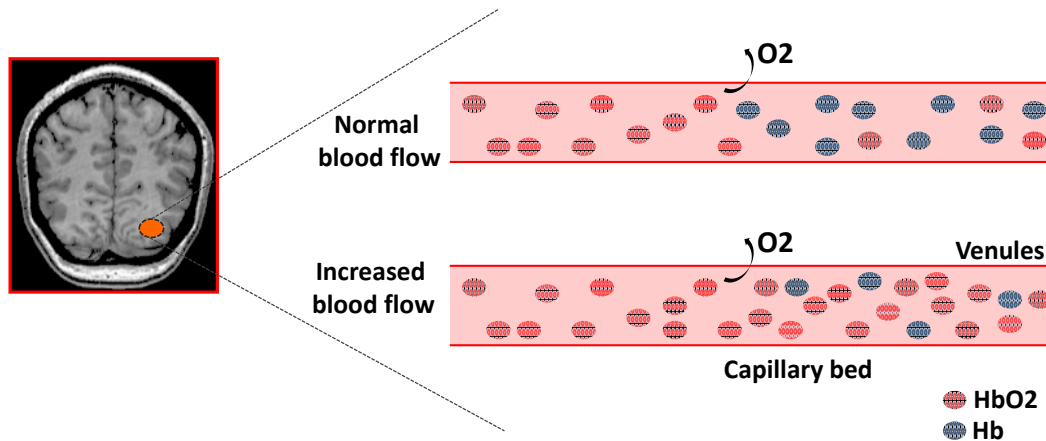


Figure 2.5. Illustration of the physiological changes leading to fMRI data. As a consequence of increased brain activity, there is an increase in blood flow, which transports oxygenated haemoglobin (HbO₂) to the capillary bed (Adapted from, Borsook, Becerra, & Hargreaves, 2006).

Hemodynamic BOLD response

The change in the MR signal caused by neural activity is named hemodynamic response (HDR) and comprises three known phases (see Figure 2.6):

1. **Initial dip:** consists of a short-term decrease in the MR signal immediately after the onset of neuronal activity, before the main component of the hemodynamic response and is caused by a brief increase in oxygen consumption that is not immediately accompanied by a change in the blood flow;
2. **Positive BOLD response:** corresponds to the maximal amplitude of the hemodynamic response, occurring typically about 4 to 6 sec following the stimuli presentation onset. If the neuronal activity is extended in time, the peak may be similarly extended into a plateau, typically with slightly lower amplitude than the peak.
3. **Undershoot:** occurs upon cessation of the stimulus before BOLD returns to the baseline level and has been suggested to occur due to biophysical and metabolic effects.

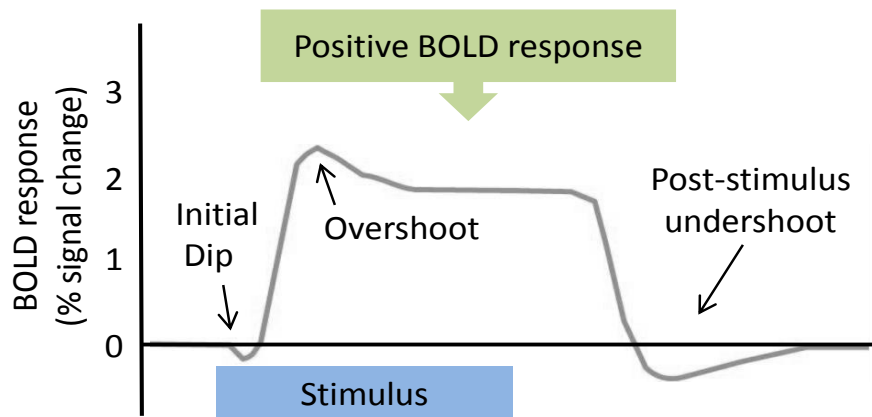


Figure 2.6. Schematic representation of the hemodynamic BOLD response. Representative waveform for the hemodynamic response to a block of multiple consecutive events: a small negative initial deep is followed by the robust positive BOLD response peaking at maximum level approximately 5 sec after stimulation which decreases upon the cessation of the stimulus returning to baseline (post-stimuli undershot). (Adapted from, Goebel, 2007)

fMRI experimental designs and issues

The major goal in fMRI is to assess and locate sensory, motor and cognitive function. To this end, careful paradigm choice and experimental design is crucial.

Paradigm choices relates to the problem of isolating the task or process for which a brain map is intended. This generally involves a comparison between the activity patterns elicited by at least two different experimental conditions: a condition of interest, and a control condition. For instance, if a researcher wants to isolate the neural correlates of object perception, subjects inside the MR scanner need to see images of objects but also simple images of meaningless textures or patterns, so that the activity elicited by simple image viewing (any image) can be subtracted. This comparison or subtraction is called a contrast and constitutes the basis of most fMRI studies. This reasoning and its accompanying brain maps are illustrated in Figure 2.7. (example from, Malach et al., 1995).

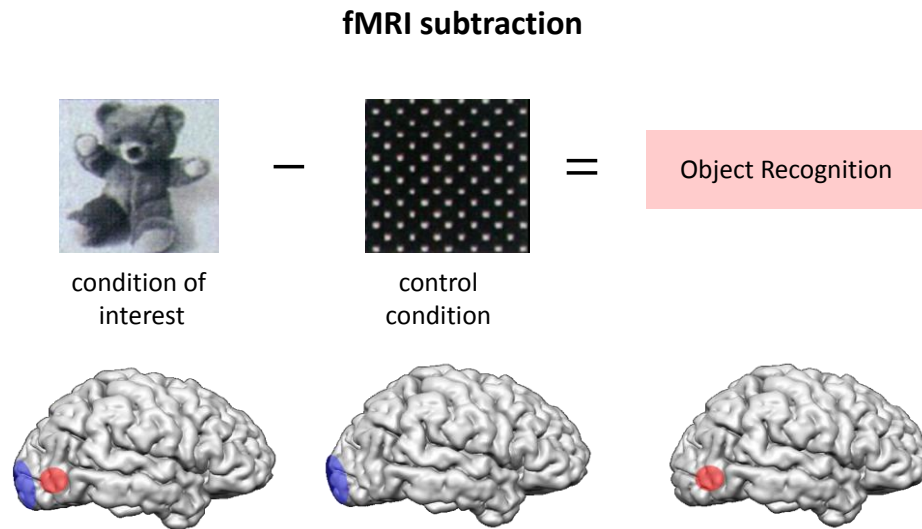


Figure 2.7. Schematic representation of fMRI subtraction. The figure illustrates one of the most important concepts in fMRI experiments, contrast. Contrast refers to a comparison between the activation levels evoked by two independent variables (or different levels of the same variable). In short, the main goal of fMRI analyses is to evaluate if a given experimental manipulation evoked a meaningful change in activation, that is, if a contrast between two conditions reach statistical significance. (Adapted from, Malach et al., 1995)

Regarding design, two main formats can be used in fMRI experiments: block-designs and event-related designs. In a *block design*, each condition is presented continuously for an extended period (one block lasting from 16 sec to a minute, on average) and blocks of different conditions are usually interchanged. The signal from one given condition is then contrasted with blocks of other conditions which, as mentioned above, typically differed only in the factor of interest. Alternatively, the signal from one condition can be compared against rest, as to reveal the whole network responsible for the execution of a given task.

In turn, in the *event-related designs* the stimuli are presented one at a time (trials) instead of being sequentially presented in a block. In this type of design, each event is separated from the subsequent event by a period named interstimulus interval (ISI). In contrast with what occurs in the block design, here the different conditions are usually randomly presented which avoids cognitive adaptation strategies of the subjects (Goebel, 2007). Event-related designs are generally better suited for estimation, and block design for detection. Estimation is the measurement of the time course within an active voxel in response to the experimental manipulation and does not require an *a priori* model. Such information is especially used when making inferences about the relative timing of neuronal activity, about processes occurring in different parts of the trial and about functional connectivity. Detection is the

determination of whether activity of a given voxel (or region) changes in response to the experimental manipulation (Huettel, Song, & McCarthy, 2009). Block designs thus exhibit superior detection power and are less sensitive to differences in the shape and timing of the hemodynamic models. In the current thesis both block and event-related designs were employed and a more detailed description is provided in Chapter 6.

To finalize this characterization of fMRI, some key concepts should be mentioned. Usually each volunteer participant undergoes a single experimental *session*. Each session includes collection of anatomical images and one or more functional runs. A *run* (4D volume composed information on space and time) consists of a set of functional images collected during the experimental task. Within each run, the functional data are acquired as a time series of *volumes* which consist of a single image of the brain made up of multiple slices. *Slices*, in turn, are acquired at a different point in time within the *repetition time* (TR – time interval between successive excitation pulses) and contain thousands of *voxels* (three-dimensional volume element) that together form an image of the brain (Huettel et al., 2009).

As occurs in the EEG, fMRI signal can be contaminated by artifacts and noise. In this manner, several pre-processing steps are generally carried out before proceeding with further analysis. These pre-processing steps typically include correction for subject motion, correction for differences in slice acquisition times, linear de-trending as well as spatial and temporal filtering.

After these pre-processing procedures statistical analyses are performed in order to investigate which regions exhibit increased or decrease activation in response to the experimental manipulation. The resulting differences are shown in statistical maps which allow visualization and further interpretation of the results

References

- Bandettini, P. A., Wong, E. C., Hinks, R. S., Tikofsky, R. S., & Hyde, J. S. (1992). Time course EPI of human brain function during task activation. *Magn Reson Med*, 25(2), 390-397.
- Berger, H. (1929). *Über das Electrenkephalogramm des Menschen*. Translated and reprinted in Pierre Gloor, Hans Berg (1969). *On the electroencephalogram of man. Electroencephalography and Clinical Neurophysiology*. Amsterdam: Elsevier.
- Borsook, D., Becerra, L., & Hargreaves, R. (2006). A role for fMRI in optimizing CNS drug development. *Nat Rev Drug Discov*, 5(5), 411-424.
- Bruns, A. (2004). Fourier-, Hilbert- and wavelet-based signal analysis: are they really different approaches? *J Neurosci Methods*, 137(2), 321-332.
- Castelhano, J., Rebola, J., Leitao, B., Rodriguez, E., & Castelo-Branco, M. (2013). To Perceive or Not Perceive: The Role of Gamma-band Activity in Signaling Object Percepts. *PLoS One*, 8(6), e66363.
- Davidson, R., Jackson, D., & Larson, C. (2000). Human electroencephalography. In J. Cacioppo, L. Tassinary & G. Bernston (Eds.), *Handbook of Psychophysiology*(pp. 27-56). Cambridge: Cambridge University Press.
- Delorme, A., & Makeig, S. (2004). EEGLAB: an open source toolbox for analysis of single-trial EEG dynamics including independent component analysis. *J Neurosci Methods*, 134(1), 9-21.
- Goebel, R. (2007). Localization of brain activity using functional magnetic resonance imaging *Clinical functional MRI: presurgical functional neuroimaging*: Springer.
- Grech, R., Cassar, T., Muscat, J., Camilleri, K. P., Fabri, S. G., Zervakis, M., et al. (2008). Review on solving the inverse problem in EEG source analysis. *J Neuroeng Rehabil*, 5, 25.
- Huettel, S. A., Song, A. W., & McCarthy, G. (2009). *Functional magnetic resonance imaging* (2nd ed.). Sunderland: Sinauer Associates, Inc Publishers.
- Kwong, K. K., Belliveau, J. W., Chesler, D. A., Goldberg, I. E., Weisskoff, R. M., Poncelet, B. P., et al. (1992). Dynamic magnetic resonance imaging of human brain activity during primary sensory stimulation. *Proc Natl Acad Sci U S A*, 89(12), 5675-5679.
- Luck, S. J. (2005). *An introduction to the event-related potential technique*. Cambridge MA: MIT Press.
- Makeig, S., & Onton, J. (2012). ERP features and EEG dynamics: an ICA perspective. In S. Luck & E. Kappenman (Eds.), *Oxford Handbook of Event-Related Potential Components*. New York: Oxford University Press.
- Malach, R., Reppas, J. B., Benson, R. R., Kwong, K. K., Jiang, H., Kennedy, W. A., et al. (1995). Object-related activity revealed by functional magnetic resonance imaging in human occipital cortex. *Proc Natl Acad Sci U S A*, 92(18), 8135-8139.
- Min, B. K., Marzelli, M. J., & Yoo, S. S. (2010). Neuroimaging-based approaches in the brain-computer interface. *Trends Biotechnol*, 28(11), 552-560.
- Ogawa, S., Lee, T. M., Kay, A. R., & Tank, D. W. (1990). Brain magnetic resonance imaging with contrast dependent on blood oxygenation. *Proc Natl Acad Sci U S A*, 87(24), 9868-9872.
- Ogawa, S., Menon, R. S., Tank, D. W., Kim, S. G., Merkle, H., Ellermann, J. M., et al. (1993). Functional brain mapping by blood oxygenation level-dependent contrast magnetic resonance imaging. A comparison of signal characteristics with a biophysical model. *Biophys J*, 64(3), 803-812.
- Olejniczak, P. (2006). Neurophysiologic basis of EEG. *J Clin Neurophysiol*, 23(3), 186-189.
- Roach, B. J., & Mathalon, D. H. (2008). Event-related EEG time-frequency analysis: an overview of measures and an analysis of early gamma band phase locking in schizophrenia. *Schizophr Bull*, 34(5), 907-926.
- Singer, W., & Gray, C. M. (1995). Visual feature integration and the temporal correlation hypothesis. *Annu Rev Neurosci*, 18, 555-586.
- Tallon-Baudry, C., & Bertrand, O. (1999). Oscillatory gamma activity in humans and its role in object representation. *Trends Cogn Sci*, 3(4), 151-162.
- Teplan, M. (2002). Fundamentals of EEG measurement. *Measurement Science Review*, 2(2), 1-11.
- Uhlhaas, P. J., Haenschel, C., Nikolic, D., & Singer, W. (2008). The role of oscillations and synchrony in cortical networks and their putative relevance for the pathophysiology of schizophrenia. *Schizophr Bull*, 34(5), 927-943.

- Uhlhaas, P. J., & Singer, W. (2006). Neural synchrony in brain disorders: relevance for cognitive dysfunctions and pathophysiology. *Neuron*, 52(1), 155-168.
- Vidal, J. R., Chaumon, M., O'Regan, J. K., & Tallon-Baudry, C. (2006). Visual grouping and the focusing of attention induce gamma-band oscillations at different frequencies in human magnetoencephalogram signals. *J Cogn Neurosci*, 18(11), 1850-1862.
- Vigario, R., Sarela, J., Jousmaki, V., Hamalainen, M., & Oja, E. (2000). Independent component approach to the analysis of EEG and MEG recordings. *IEEE Trans Biomed Eng*, 47(5), 589-593.

RESULTS

CHAPTER 3

Williams syndrome as a clinical model to study the neural correlates of visual coherence:

A direct comparison of local-global
visual integration in VWS and Autism

This chapter was based on: **Bernardino, I.**, Mougá, S., Almeida, J., van Asselen, M., Oliveira, G. & Castelo-Branco, M. (2012). A Direct Comparison of Local-Global Integration in Autism and other Developmental Disorders: Implications for the Central Coherence Hypothesis. *PLoS ONE* 7(6): e3935

Abstract

Visual coherence impairments have been reported in Williams syndrome (WS) as a putative consequence of a locally focused visual processing style. The same pattern of visual processing had been described in other clinical models that exhibit distinct and even opposed social and behaviour phenotypes, such as Autism Spectrum Disorders (ASD). This renders the direct comparison between these conditions as encouraging for the understanding of the mechanisms underlying impaired visual coherence in atypical neurodevelopment. In ASD, the weak central coherence (WCC) hypothesis was proposed as one of its explanatory models and several experimental paradigms based on hierarchical figures have been used to test this controversial account in both WS and ASD. Here, we comprehensively tested central coherence in these conditions (as well as in additional mental age-, chronological age- and intellectual disability-matched control groups). Subjects were required to perform local/global preference judgments using hierarchical figures under 6 different experimental settings (memory and perception tasks with 3 distinct geometries with and without local/global manipulations). We replicated these experiments under 4 additional conditions in which subjects had to report the correct local or global configurations (memory/perception*local/global conditions). Finally, we used a visuoconstructive task to measure local/global perceptual interference. As a prediction, we expected that central coherence should be most impaired in ASD for the weak central coherence account to hold true. An alternative account includes dorsal stream dysfunction which dominates in WS. We found that WS participants were the most impaired in central coherence. Surprisingly, ASD participants showed the expected pattern of coherence loss only in four task conditions favouring local analysis but this trend actually tended to disappear when matching for intellectual disability. We conclude that abnormal central coherence does not provide a comprehensive explanation of ASD deficits and is more prominent in populations, namely WS, characterized by strongly impaired dorsal stream functioning and other phenotypic traits that contrast with the autistic phenotype. Taken together these findings suggest that other mechanisms such as dorsal stream deficits (largest in WS) may underlie impaired central coherence.

Introduction

The Williams syndrome (WS) cognitive profile is characterized by predominant visuospatial impairments as was described in the Chapter 1 of this thesis (Bellugi et al., 2000; Castelo-Branco et al., 2007; Mendes et al., 2005; Mervis et al., 2000). These visuospatial deficits have been explored in terms of local-global visual processing in WS. Impaired visual coherence characterized by a local processing bias in WS is particularly evident in the visuoconstructive domain (E. K. Farran, Jarrold, & Gathercole, 2003; Rondan, Santos, Mancini, Livet, & Deruelle, 2008) and has been associated with dorsal stream dysfunction (Atkinson et al., 1997).

Impairments in visual coherence as a consequence of a detailed-focused cognitive style are not, however, believed to be a distinctive feature of WS. In fact, loss of central coherence has traditionally been thought to be stronger and central to the phenotype of other neurodevelopmental disorders, such as Autism Spectrum Disorders (ASD), which exhibit opposite behavioural features, in particular which concerns language and social communication. This leads to a question about the distinctiveness of the mechanisms underlying visual coherence impairments in WS and renders the direct comparison between the WS and ASD phenotypes important for the elucidation of the debate on the implications of loss of central coherence. This direct comparison is potentially fruitful since these neurodevelopmental disorders share, in one hand, visual and cognitive characteristics and in the other hand exhibit, as stated above, an opposite social behavioural profile. ASD represents a very interesting comparison model as is a condition with a relatively high prevalence in the population (Oliveira et al., 2007), in contrast with WS and has raised enormous interest in the cognitive neuroscience in the last decades. Many experimental groups all over the world devoted resources into the analysis of models that might explain its cognitive and social phenotype. One of these models is the Weak Central Coherence account (WCC). For this reason, the present study was aimed at characterizing the WS visual coherence impairments by taking advantage of the input provided by the direct comparison with other clinical models of impaired coherence.

ASD is characterized by a symptomatic triad including severely impaired social interaction, deficits in communication and restricted/stereotyped patterns of behaviour, interests and activities (American Psychiatric Association, 1994; Kanner, 1943). Superior visuospatial skills have been described in ASD, particularly in which concerns visual search (Joseph, Keehn, Connolly, Wolfe, & Horowitz, 2009; Keehn, Brenner, Palmer, Lincoln, &

Muller, 2008; Plaisted, O'Riordan, & Baron-Cohen, 1998) and puzzle assembly tasks (Happe, 1994; Shah & Frith, 1993). Nevertheless, there is some evidence of a distinctive visual perceptual style in this disorder that has been considered to account for high level deficits particularly in the face processing domain (Dakin & Frith, 2005; Deruelle, Rondan, Gepner, & Tardif, 2004; Deruelle, Rondan, Salle-Collemiche, Bastard-Rosset, & Da Fonseca, 2008). As mentioned above, an important cognitive theory - the WCC account (Uta Frith, 1989)- has been proposed to address cognitive weaknesses and strengths in ASD. The WCC account describes the perceptual and cognitive biases in ASD according to the claim that these patients perceive visual scenes as a sparse set of details rather than as a congruent and meaningful unit, failing in the extraction of the global configuration (Uta Frith, 1989; U. Frith & Happe, 1994). This hypothesis explains the cognitive phenotype of ASD in terms of dissociation between local and global information processing and has been mostly analyzed in the visual domain.

An extensive range of experimental paradigms have been used to measure WCC in WS and ASD, namely the block design subtest (Caron, Mottron, Berthiaume, & Dawson, 2006; Shah & Frith, 1993), the embedded-figure test (Mottron, Burack, Iarocci, Belleville, & Enns, 2003; Shah & Frith, 1983), the copying impossible-figure (Mottron, Belleville, & Menard, 1999) and visual illusion tasks (Happe, 1996; Ropar & Mitchell, 1999). However, the main paradigm in this domain has been the study of coherent visual processing using hierarchical figures, such as Navon stimuli (Mottron et al., 2003; Navon, 1977; Plaisted, Swettenham, & Rees, 1999; Rondan & Deruelle, 2007). This stimulus type provides an explicit separation of both local and global levels of visual processing.

The general pattern of findings has been inconsistent, suggesting the need for controlled experiments in multiple clinical populations directly testing the WCC hypothesis (Mottron, Belleville et al., 1999; Ozonoff, Strayer, McMahon, & Filloux, 1994; Porter & Coltheart, 2006; Rinehart, Bradshaw, Moss, Brereton, & Tonge, 2000; Rondan et al., 2008). The mixed findings particularly found in WS and ASD suggest that global processing in these disorders seems to be affected under some task conditions and spared under others. Therefore, it is crucial to test the central coherence abilities in WS (and other neurodevelopmental conditions) under the same task requirements in order to clarify the nature and impact of loss of coherence in visual processing. In this domain, there are some important methodological issues that should be addressed to better understand the pattern of visual perception of these developmental disorders. Accordingly, it is important to separate the ability to perceive global information from the detailed focused cognitive style

characterized by the preferential use of local approaches when analyzing a visual scene in the absence of overt instructions. Indeed, some studies focused on attention tasks giving direct instructions to attend to either local or global levels of information (E. K. Farran et al., 2003; Mottron, Belleville et al., 1999; Plaisted et al., 1999) while others only required free viewing to assess preference (Rondan & Deruelle, 2007; Rondan et al., 2008). So far, the crucial distinction of loss of coherence between different clinical populations and control groups, under the same task conditions, remains to be done, in the same study. Here, we aimed to address this issue and to explicitly separate perceptual bias and cognitive style from global processing impairment by using multiple measures of central coherence based on the classical Navon paradigm (Navon, 1977).

This study was therefore aimed at investigating the visual coherence deficits in WS by using classical paradigms of central coherence in clinical populations with clear categorical differences concerning intellectual disability and cognitive phenotype. This would allow us to understand if these conditions share the same underlying cognitive mechanisms of integration or if this perceptual feature can alternatively be considered specific to the pathophysiology of one of these conditions. The fact that WCC is a common denominator of both ASD and WS is at odds with their substantially distinct cognitive profile. Therefore, we predict that if central coherence deficits are distinctive in ASD as proposed by the WCC theory and underlie its pathophysiology, the coherence deficits should dominate in these patients. Although we believe that if such deficits only emerge under certain conditions (as was actually found in this study), this would also mean that they do not provide a full account of the phenotype and that mechanisms anchored on a specific neural basis, such as dorsal stream deficits, should also be considered.

The understanding of the neurobehavioural relevance of central coherence in WS and ASD requires addressing both perceptual bias and performance levels as well as the impact of intellectual disability in central coherence measures. As a result, in the current study, the intellectual disability was controlled for by selecting appropriate matched clinical and control groups. Participants were tested under three experimental tasks: a Preference task without a priori “correct” response to assess spontaneous visual processing preferences, a Correct Choice task to evaluate the accuracy in perceiving both global and local information and a Drawing task to explore visuoconstructive integrative abilities. We further explored the effect of the physical presence of the stimulus on the visual processing of hierarchical stimuli by introducing both perceptual and memory conditions. Furthermore, in the preference task,

we addressed the invariance of the processing bias to local and global rotation manipulations that were introduced to increase task sensitivity in the detection of mild perceptual bias.

Methods

Participants

Ninety-seven participants were included in this study: 18 WS patients, 19 ASD patients with intellectual disability (ASD_ID) (Intelligence Quotient (IQ) < 80), 20 ASD patients without intellectual disability (ASD_noID) (IQ ≥ 90), 20 typically developing participants matched for chronological age (C_TD) and 20 control participants with intellectual disability matched for IQ (C_ID). The characteristics of clinical and control groups are summarized in Table 3.1.

Table 3.1. Characteristics of clinical and control groups

	Chronological Age		Education		FSIQ (WISC-III or WAIS-III)		Gender (m:f)
	Mean (SE)	Range	Mean (SE)	Range	Mean (SE)	Range	
WS (n=18)	17.33 (1.81)	8-34	5.00 (1.00)	0-12	53.94 (2.01)	42-75	11:7
ASD_ID (n=19)	13.26 (0.58)	10-18	6.74 (0.43)	4-9	64.47 (1.76)	52-79	15:4
ASD_noID (n=20)	12.10 (0.46)	10-17	6.55 (0.48)	4-11	103.40 (2.41)	90-129	20:0
C_TD (n=20)	15.70 (1.81)	7-34	6.80 (0.79)	2-14	107.94 (1.73)	95-119	11:9
C_ID (n=20)	15.35 (0.96)	10-29	7.15 (0.46)	3-9	58.60 (1.95)	40-74	15:5

NOTE. WS = Williams Syndrome group; ASD_ID = Autism Spectrum Disorders group with intellectual disability; ASD_noID = Autism Spectrum Disorders group without intellectual disability; C_TD = typically developing control group; C_ID = control group with intellectual disability; FSIQ = Full-scale intellectual quotient; WISC-III = Wechsler Intelligence Scale for Children, 3rd. ed.; WAIS-III = Wechsler Adult Intelligence Scale, 3rd ed.; SE= Standard Error of the mean.

WS participants were recruited from a database used in previous studies (Castelo-Branco et al., 2007; Mendes et al., 2005). All patients were diagnosed based on clinical and genetic examinations confirmed by fluorescence *in situ* hybridization (FISH) analysis, which demonstrated the hemizygous Elastin deletion. Additional comprehensive genetic analysis was carried out for all WS participants except for two. Patients' DNA was extracted from peripheral blood using standard procedures. The DNA was sent to the Genetic Unity of the Pompeu Fabra University in Barcelona where the parental origin of the hemideletion and the precise location of the breakpoints were examined (CUSCO et al., 2008). All WS participants had similar deletion size (~1.55 Mb) and were hemizygous for GTF2IRD1 and GTF2I (Castelo-Branco et al., 2007). The genetic characterization of our WS patients is explained in Figure 3.1 and detailed in Table 3.2.

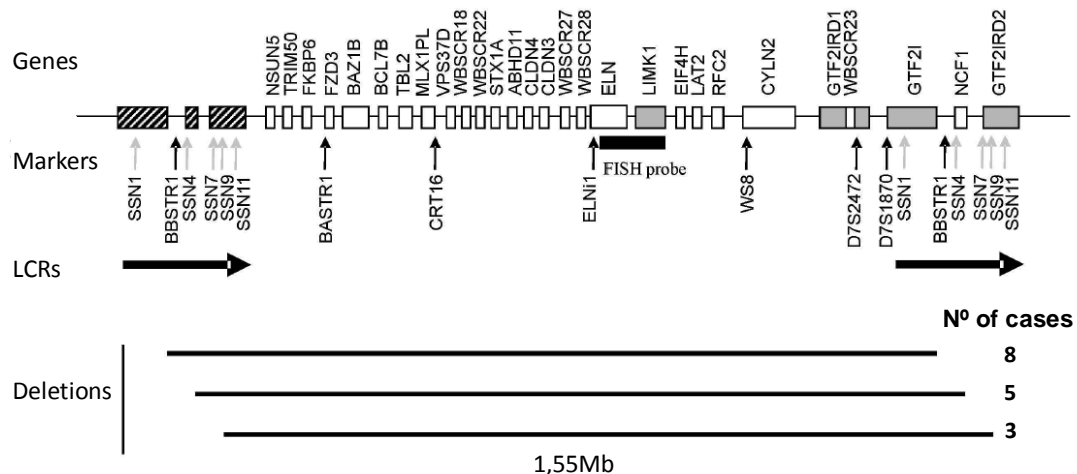


Figure 3.1. Schematic representation of the 7q11.23 region with its gene content. The location of the microsatellite markers (BBSTR1, BASTR1, CR16T, ELN1, WBS8, D7S2472, D7S180) and paralogous sequence variants (SSNs1, 4, 7, 9 & 11) used in this study is indicated by black and grey arrows, respectively. The blocks of segmental duplications or low copy repeats (LCRs) are represented by horizontal arrows. Hatched boxes on the centromeric LCR block represent pseudogene copies. The extent of each type of deletion found in the patients is shown. (Adapted from Castelo-Branco et al., 2007)

ASD participants were recruited from the Neurodevelopment and Autism Department from the Child Center of Pediatric Hospital of Coimbra. ASD diagnoses were assigned on the basis of gold standard instruments such as: parental or caregiver interview (Autism Diagnostic Interview– Revised, ADI-R (Lord, Rutter, & Le Couteur, 1994)), direct structured proband assessment (Autism Diagnostic Observation Schedule, ADOS (Lord,

Rutter, DiLavore, & Risis, 1999)), and clinical examination performed by an experienced neurodevelopmental Pediatrician, based on the diagnostic criteria for autistic disorder from Diagnostic and Statistical Manual of Mental Disorders IV, DSM-IV-TR (American Psychiatric Association, 1994). All ASD patients had positive results in the ADI-R and ADOS for autism or ASD, and met the criteria for autistic disorder from the DSM-IV-TR. Only idiopathic cases were included (negative karyotypic results in FISH ch 15 q11-13 - and FMR1 mutation). In this group, 7 patients were medicated with Risperidone and 2 were medicated with Methylphenidate. However, parents of these children were requested not to give their children the medication on the days of the testing.

Table 3.2. Detailed genetic characterization of WS patients

Subject	Deletion Size	Break Point
TCA	1.55 Mb	B-block, between NCF1 and GTF2IRD2
JAS	1.55 Mb	B-block before NCF1 starts
MPO	1.55 Mb	B-block – inside GTF21RD2
JMG	1.55 Mb	B-block before NCF1 starts
MFP	1.55 Mb	B-block, between NCF1 and GTF2IRD2
JAB	1.55 Mb	B-block – inside GTF2I between GTF2I and NCF1
SLT	1.55 Mb	B-block, between NCF1 and GTF21RD2
PSC	1.55 Mb	B-block before GTF2IRD2
JOP	1.55 Mb	B-block – inside GTF2I between GTF2I and NCF1
AMP	1.55 Mb	B-block – inside GTF2IRD2
ASA	1.55 Mb	B-block before NCF1 starts
RPB	1.55 Mb	B-block before NCF1 starts
MCD	1.55 Mb	B-block before GTF2IRD2
GMV	1.55 Mb	B-block – inside GTF21RD2
FTM	1.55 Mb	B-block – inside GTF2I between GTF2I and NCF1
JMS	1.55 Mb	B-block – inside GTF2I between GTF2I and NCF1
GPF	1.55Mb	Between blocks Bc and Bm

Control participants matched for IQ were recruited from the same department and from local special education institutes. None of these participants were taking selective serotonin reuptake inhibitor or neuroleptic medications. Co-morbid conditions were explicitly excluded (epilepsy, brain injury, sensory deficits, associated genetic syndromes, and motor deficits that could interfere with task response). Control participants matched for chronological age were healthy, with no history of psychiatric, neurologic and ophthalmologic illnesses and naïve concerning to the testing procedures. They were recruited from local schools and were individually tested at their own schools.

The parents of participants included in WS and C_ID groups completed the Social Communication Questionnaire to exclude co-morbidity with ASD (Rutter, Bailey, & Lord, 2003). The scores were below 15, which is the positive cut-off for ASD. All participants included in the study received the Portuguese adapted version of the Wechsler Intelligence Scale for Children – 3rd edition (WISC-III) (Wechsler, 2003) or the Wechsler Adult Intelligence Scale– 3rd edition (WAIS-III) (Wechsler, 2008), according to the participant's age. The ASD_ID group only includes subjects with IQ inferior to 80 while the ASD_noID group includes subjects with IQ superior or equal to 90, which is consistent with Wechsler definition of intellectual disability (Wechsler, 2003, 2008).

The three clinical groups (WS, ASD_ID and ASD_noID) were matched for chronological age and education level with both C_TD-matched (Mann-Whitney test, $p > 0.05$) and C_ID-matched (Mann-Whitney test, $p > 0.05$) control groups. Additionally, the clinical groups with intellectual disability (WS and ASD_ID) were matched for IQ (Mann-Whitney test, $p > 0.05$) with the C_ID-matched control group.

This study and all the procedures were reviewed and approved by the Ethics Commissions of the Faculty of Medicine of the University of Coimbra (Comissão de Ética da Faculdade de Medicina da Universidade de Coimbra) and of the Pediatric Hospital of Coimbra (Comissão de Ética do Hospital Pediátrico de Coimbra) and was conducted in accordance with the declaration of Helsinki. Written informed consent was obtained from participants older than 18 years of age and from the parents/guardians in the case of participants younger than 18 years of age. Children and adolescents younger than 18 years of age gave oral informed consent.

Materials and Procedure

We used Navon's hierarchical stimuli (Navon, 1977), which consisted of global geometrical figures made up of 18 smaller geometrical figures. In each hierarchical form, the shape of the local level differed from the shape of the global level. The stimuli were shown on a 33,8cm X 27,1cm computer screen (1280X1024 pixels) using the software package Presentation (Neurobehavioural systems). The size of the local shapes was 0.57° horizontally and 0.57° vertically and the distance between them was 0.57° . The horizontal and vertical sizes of the global shapes differed accordingly to the figure configuration. The colour of the stimuli was black and they were shown on a white background at high contrast (95%).

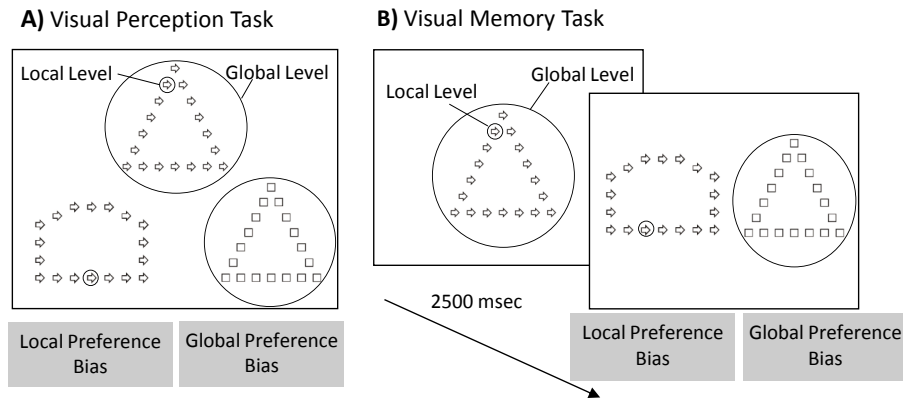
Participants were individually tested in a quiet and darkened room, seated at a distance of 50cm from the computer screen. They were asked to perform three experimental tasks: a Preference task, a Correct Choice task and, finally, a Drawing task.

Preference Tasks.

On each trial, participants performed a match to sample similarity task by comparing two figures with one target figure. This task was performed under different task conditions, in which task requirements (visual perception and visual memory tasks) and the geometric configuration of the stimuli (non-inversion, local-inversion, and global-inversion conditions) were manipulated. For the visual perception preference task, the participants viewed a display containing a target figure at the top of the screen and two comparison figures at the bottom (Figure 3.2A). One of the comparison figures shared only the global shape with the target figure and the other had the same local elements as the target but had different global configuration. That is, each comparison figure shared only one level (local or global) with the target figure and appeared randomly and equally often on the left and right positions. For the visual memory preference task, each trial comprehended a presentation phase, in which the target figure was shown during 2500ms, followed by the appearance, without delay, of the two comparison figures (Figure 3.2B). For both perceptual judgment and memory tasks, participants were asked to indicate which of the two bottom figures was more similar to the target, thereby reporting their visual processing preferences (bias). The instructions for the perceptual preference task were as follows (translated from Portuguese): "In this screen, you have three figures, one up here (pointing) and two below (pointing). You should look closely at all these pictures and indicate, in your opinion, which of the two figures down here (pointing), is more similar to the figure above". It is important to note

that, in this task, there is no correct response and the subjects' answers reflect only the preferred pattern of visual analysis when analyzing a hierarchical figure.

Perception & Visual Memory preference tasks



Instruction: 'Which of the two figures at the bottom is more similar to the target?'
 No 'a priori' correct responses— Focus on **Preference**

C) Assessing preference invariance to local and global rotation

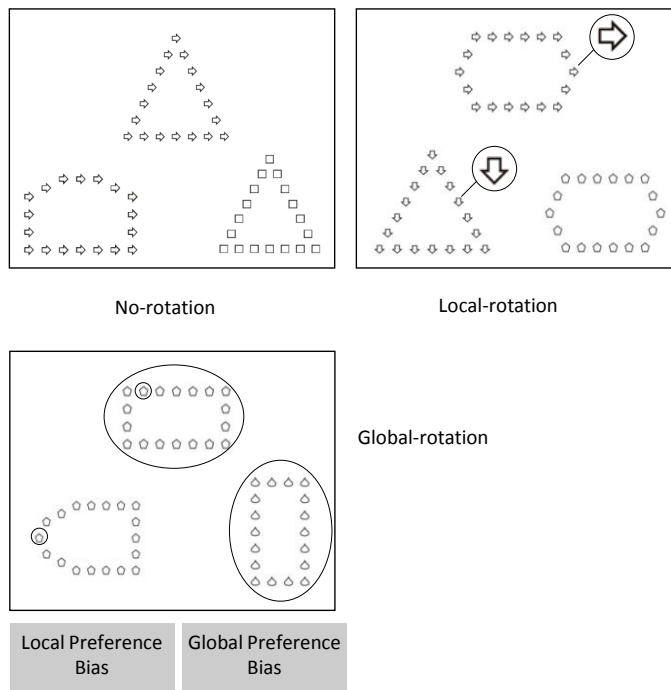


Figure 3.2. Illustration of the Visual Preference Tasks. Example of the configurations used in A) visual perception preference tasks and B) visual memory preference tasks. C) Illustration of the non-inversion, local-inversion and global-inversion conditions used on visual perception preference and visual memory preference tasks to assess preference invariance to global and local rotation.

NOTE. Figures are presented according to the real scale (not real size) and, therefore, visibility was higher in the experimental task.

In both perception and visual memory preference tasks, we included a no-rotation condition in which the local and global information of the comparison figures were presented in the same orientation of the target figure. Additionally, two control conditions (with different geometrical configurations) were also administered, namely local-rotation and global-rotation conditions, in which the orientation of either the local or global elements of the stimulus was manipulated to provide generalization and further, enhance the likelihood of detecting subtle forms of perceptual bias (Figure 3.2C). The local elements or the global shape were rotated 90 or 180 degrees to ensure that the figures exhibited different orientations of those presented in the target figure. In the local-rotation condition we rotated the local elements of the comparison figure matched for local level with the target figure. This approach favoured a change to a more global bias. In the global-rotation condition, we rotated the global shape of the comparison figure matched for global configuration with the target figure in order to explicitly increase the local similarity. This strategy favoured a change to a local bias.

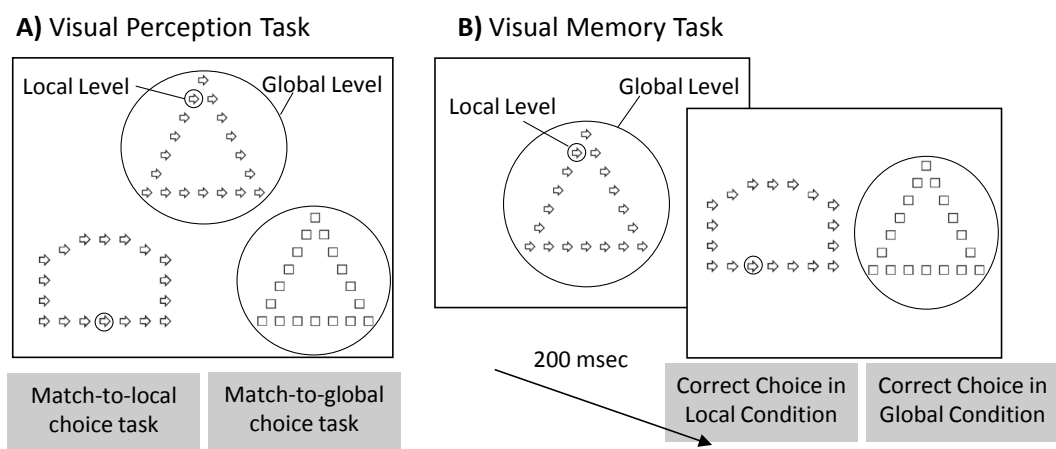
Participant underwent 20 test trials in each task condition performing a total of 60 test trials. Eight familiarization trials were administered for each task. The familiarization phase was repeated whenever the subjects did not understand the instructions or had difficulties coordinating the motor response. All participants included in the task understood the task instructions. The visual perception task was provided before the visual memory task for all participants

Correct Choice Tasks

Two different task conditions were included, namely a match-to-local choice task and a match-to-global choice task, differing only on the instruction given to the participants (but both requiring a correct response, unlike the Preference Tasks). In the match-to-local choice task, participants indicated which of the two comparison figures had the same local shapes as the target, while in the match-to-global choice task participants indicated which of the two comparison figures was matched with the target in terms of the global configuration. Additionally, as occurred in the Preference task, participants were performed visual judgments under visual perception and visual memory conditions. In the visual perception correct choice task, participants viewed a display containing one target figure and two comparison figures (Figure 3.3A). In the visual memory correct choice task, the target figure

was presented during 200 ms, followed by the appearance of two comparison figures (Figure 3.3B). For both experimental tasks, we presented six blocks of eight trials each, alternating between match-to-local and match-to-global conditions (three blocks for each condition). Participants performed a total of 48 trials for each perception and memory conditions. Five consecutive correct practice trials were administered for all conditions to ensure that all participants understood the task instructions.

Perception & Visual Memory correct choice tasks



Instruction: ‘Which of the two figures at the bottom show the same local elements (**Local Choice task**) or the global configuration (**Global Choice Task**) as the target?’
Focus on **Perceptual Performance**

Figure 3.3. Illustration of the Correct Choice Tasks. Example of the configuration used in A) visual perception correct choice tasks and B) visual memory correct choice tasks. Note. Figures are presented according to the real scale (not real size) and, therefore, visibility was higher in the experimental task. Note that questions posed to participants were in simple Portuguese.

Drawing Task

A Drawing (visuoconstructive) task was included, in which participants copied two hierarchical figures (a large triangle made of smaller arrows and a large ‘P’ made of smaller ‘A’s’) (Figure 3.4). Designs were shown in an A5 paper until participants finished the copy. There was no time limit for completion of the task. A rating scale, similar to that used by Porter & Coltheart (2006), was created to rate visuoconstructive integrative ability. Three scores were carried out for each drawing task, namely a local score, a global score and an

integration score. For local and global scores, ratings were between 0 (“totally absent”) and 3 (“perfect reproduction”). We computed the local and global scores for each participant by summing the score of the two drawings produced by each participant. In sum, local and global scores had a minimum score of zero and a maximum of six. For the integration score, ratings were 0 (if the local and global shapes were drawn independently) or 1 (if the local and global configurations were accurately integrated as a whole). Two WS participants were not able to draw the triangle and one refused to draw the hierarchical letter resulting in a total of 191 drawings produced by the clinical and control groups which were rated by two independent raters. The raters were not aware that the drawings had been produced by different groups. Inter-rater reliability scores were 0.912 for local score, 0.880 for global score and 0.878 for integration score (Spearman’s rho correlations, $p < 0.05$).

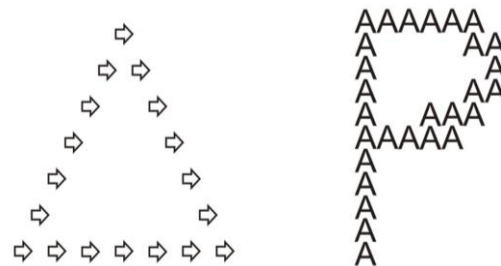


Figure 3.4. Stimuli used in the drawing task. A simple geometric figure and a letter used in the drawing task.

Statistical analysis

Nonparametric statistics (Mann-Whitney U tests, Fisher’s Exact Tests and Spearman’s Rho correlations) were carried out for all statistical analyses to avoid biases due to deviations from normality and variance heterogeneity. All statistical analyses were performed with the IBM SPSS Statistics 19.0 software package.

Results

Preference (bias) Tasks

Visual Perception Preference Task

Group analyses revealed a bimodal distribution in the WS group specifically for this task, with a subgroup showing a clear preference for local strategies (with more than 80% of local choices) while the other subgroup showed a clear global visual bias (with more than 80% of global choices). The WS subgroup who preferred local bias showed significantly more local choices than both C_TD and C_ID controls groups on all task conditions (Mann-Whitney U test, $p < 0.05$). Concerning the WS subgroup who preferred global choices, no significant differences were found when comparing with the C_ID control group for all task conditions (Mann-Whitney U test, $p > 0.05$), however, significant differences were found when comparing with the C_TD group but only for the local-rotation condition (Mann-Whitney U test, $p < 0.05$) and the global-rotation condition (Mann-Whitney U test, $p < 0.05$).

Conversely, both ASD clinical groups with or without intellectual disability (ASD_ID and ASD_noID) have a relative preference for global configurations in all no-rotation, local-rotation and global-rotation conditions. Surprisingly, their choice behaviour was similar to both C_TD and C_ID control groups. Thus, no significant differences were found between the ASD clinical groups and respective control groups in all task conditions (Mann-Whitney U test, $p > 0.05$, see Table 3.3 for details on exact p-values and specific comparisons).

Visual Memory Preference Task

Similar results were found for the visual memory preference task. In the WS group we replicated the bimodal pattern found in the perception preference task. Significant differences were found between the WS subgroup who preferred local choices and both C_TD and C_ID control groups for all task conditions (Mann-Whitney U test, $p < 0.05$), showing a clear preference for using local strategies when performing a match to sample similarity task with no a priori correct responses. Concerning the WS subgroup who preferred global choices, significant differences were found when comparing with the C_TD control group for all task conditions (Mann-Whitney U test, $p < 0.05$) but no significant differences were found when comparing with the C_ID control group for all task conditions (Mann-Whitney U test, $p > 0.05$).

In the ASD, group analyses revealed no significant differences between the ASD_ID group and the C_ID across no-rotation, local-rotation and global-rotation conditions (Mann-Whitney U test, $p > 0.05$, for details on exact p-values see Table 3.3). When comparing the ASD_ID group with the C_TD group no significant differences were found for no-rotation (Mann-Whitney U test, $p > 0.05$) and local-rotation (Mann-Whitney U test, $p > 0.05$) conditions but significant differences emerged for the global-rotation (Mann-Whitney U test, $p < 0.05$), as expected from the fact that global stimulus rotation induces a local bias. Likewise, no significant differences were found between the ASD_noID and the C_TD (Mann-Whitney U test, $p > 0.005$) group, both evidencing a preference for using global strategies when analyzing hierarchical geometric figures irrespective of the control manipulations introduced in the task. Results are summarized in Table 3.3 and Figure 3.5.

Table 3.3. Group comparison analyses for Preference Tasks

		Visual Perception Preference			Visual Memory Preference		
		No-rotation	Local-rotation	Global-rotation	No-rotation	Local-rotation	Global-rotation
ASD_ID	vs.	$p=0.080$	$p=0.623$	$p=0.715$	$p=0.112$	$p=0.122$	$p=0.013$
C_TD							
ASD_ID	vs.	$p=0.852$	$p=0.314$	$p=0.143$	$p=0.763$	$p=0.852$	$p=0.550$
C_ID							
ASD_noID	vs.	$p=0.585$	$p=0.988$	$p=0.322$	$p=0.483$	$p=0.797$	$p=0.560$
C_TD							
WS_local	vs.	$p=0.000$	$p=0.001$	$p=0.002$	$p=0.001$	$p=0.001$	$p=0.035$
C_TD							
WS_local	vs.	$p=0.002$	$p=0.003$	$p=0.002$	$p=0.000$	$p=0.003$	$p=0.090$
C_ID							
WS_global	vs.	$p=0.018$	$p=0.182$	$p=0.087$	$p=0.006$	$p=0.022$	$p=0.009$
C_TD							
WS_global	vs.	$p=0.541$	$p=0.915$	$p=0.884$	$p=0.149$	$p=0.586$	$p=0.487$
C_ID							

◀ All comparisons signaled at bold are significant and related to increased local bias. **NOTE.** WS_local = Williams Syndrome subgroup with local bias; WS_global = Williams Syndrome subgroup with global bias; ASD_ID = Autism Spectrum Disorders group with intellectual disability; ASD_noID = Autism Spectrum Disorders group without intellectual disability; C_TD = typically developing control group; C_ID = control group with intellectual disability;

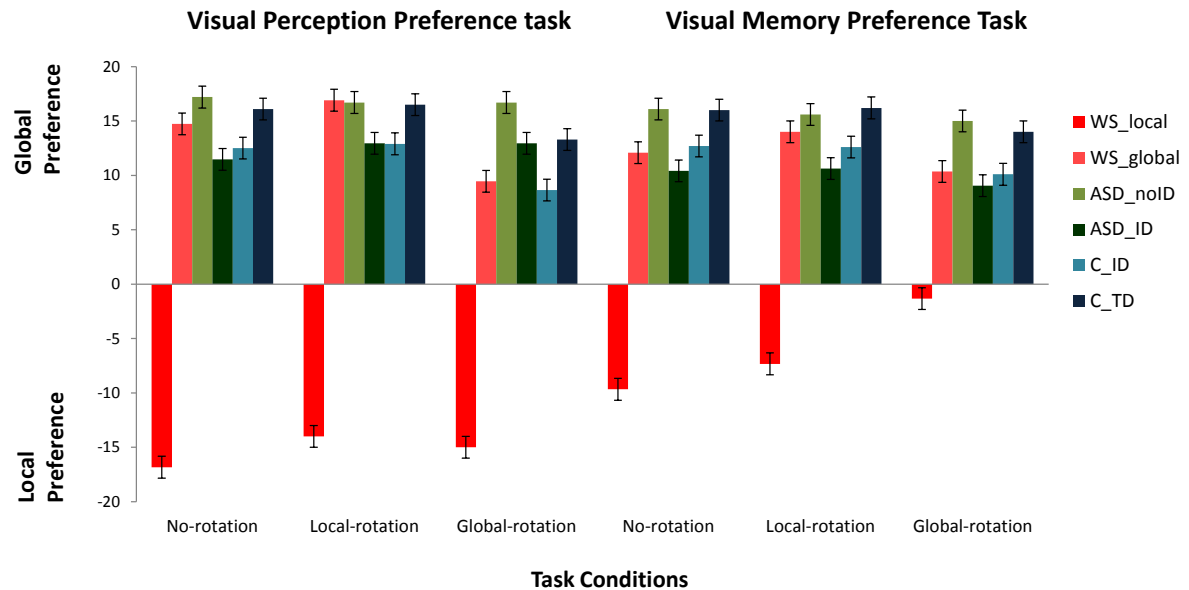


Figure 3.6. Mean percentage of global responses for all clinical and control groups for the visual perception preference task conditions and the visual memory preference task conditions. Given the bimodal pattern found in WS only for this task, and for sake of clarity we plot two WS subgroups, according to dominantly local or global preference (see text). Bar graphs show the percentage of global responses and error bars the SEM. **NOTE.** WS_local = Williams Syndrome subgroup with local bias; WS_global = Williams Syndrome subgroup with global bias; ASD_ID = Autism Spectrum Disorders group with intellectual disability; ASD_noID = Autism Spectrum Disorders group without intellectual disability; C_TD = typically developing control group; C_ID = control group with intellectual disability.

Correct choice (performance) Tasks

Visual perception correct choice task

Group analyses revealed significant differences when comparing WS group with the C_TD group in all conditions (Mann-Whitney U tests; $p < 0.05$), but when comparing with the C_ID group significant differences were specifically found for the local condition (Mann-Whitney U tests; $p < 0.05$).

No significant differences were found when comparing the ASD_ID group with the C_ID group in both match-to-local and match-to-global conditions (Mann-Whitney U tests; $p > 0.05$; see Table 3.4 for details on exact p-values and specific comparisons). However, when comparing the ASD_ID and the C_TD groups, results indicated that the clinical group made significantly more errors than the control group for the match-to-global condition (Mann-Whitney U test; $p < 0.05$), but not for the local-to-match condition (Mann-Whitney U test; $p > 0.05$). No significant differences were found when comparing ASD_noID group with the matched C_TD control group concerning the identification of local and global similarities (Mann-Whitney U tests; $p > 0.05$).

Visual memory correct choice task

Similar results were found as in the perception task. The WS group made significantly more errors than both C_TD and C_ID control groups in all conditions (Mann-Whitney U tests; $p < 0.05$). The ASD_ID group performed in a similar way as the C_ID group in all task conditions (Mann-Whitney U tests; $p > 0.05$; see Table 3.4 for further details), but made significantly more errors than the (non IQ-matched) C_TD group on both match-to-local (Mann-Whitney U test; $p < 0.05$) and match-to-global (Mann-Whitney U tests; $p < 0.05$) task conditions. Results are summarized in Table 3.4 and Figure 3.6.

Table 3.4. Group comparison analyses for Correct Choice Task

	Visual Perception Preference		Visual Memory Preference	
	Global condition	Local condition	Global condition	Local condition
ASD_ID vs. C_TD	$p = 0.012$	$p = 0.131$	$p = 0.020$	$p = 0.012$
ASD_ID vs. C_ID	$p = 0.479$	$p = 0.162$	$p = 0.282$	$p = 0.283$
ASD_noID vs. C_TD	$p = 0.223$	$p = 0.171$	$p = 0.452$	$p = 0.659$
WS vs. C_TD	$p = 0.000$	$p = 0.000$	$p = 0.000$	$p = 0.000$
WS vs. C_ID	$p = 0.158$	$p = 0.024$	$p = 0.001$	$p = 0.037$

Mann-Whitney U tests; all comparisons signaled at bold are significant and related to increased local bias. **NOTE.** WS = Williams Syndrome group; ASD_ID = Autism Spectrum Disorders group with intellectual disability; ASD_noID = Autism Spectrum Disorders group without intellectual disability; C_TD = typically developing control group; C_ID = control group with intellectual disability.

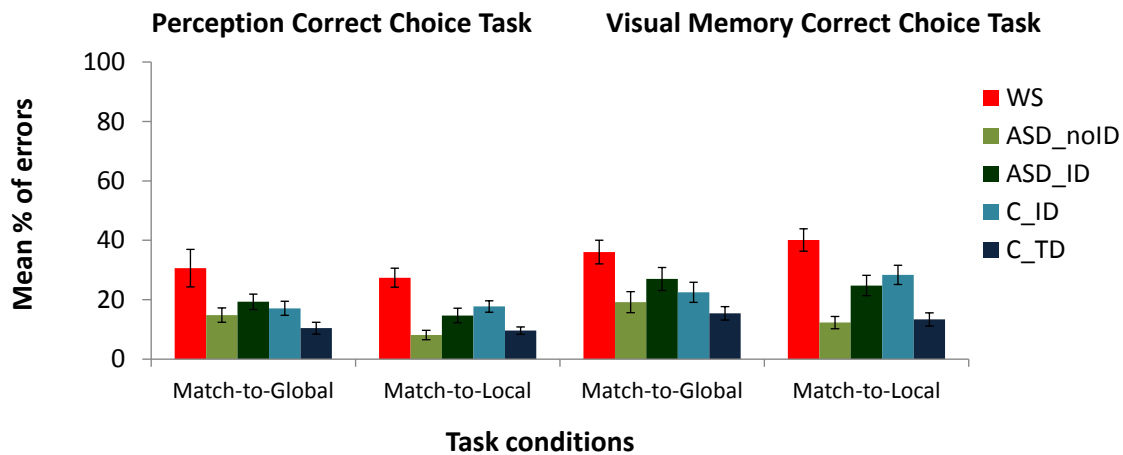


Figure 3.6. Loss of central coherence in matching forced choice tasks. Mean percentage of errors for all clinical and control groups for the visual perception and visual memory “correct choice” task conditions. Bar graphs show the percentage of errors and error bars the SEM. **NOTE.** WS = Williams Syndrome group; ASD_ID = Autism Spectrum Disorders group with intellectual disability; ASD_noID = Autism Spectrum Disorders group without intellectual disability; C_TD = typically developing control group; C_ID = control group with intellectual disability.

Visuoconstructive Task (Drawing)

For global and local scores, between-group comparisons revealed significant differences when comparing WS group with both control groups regarding local and global scores, which indicates that WS participants were worse at copying global and local shapes (Mann-Whitney U tests; $p < 0.001$).

Conversely, both ASD groups (ASD_ID and ASD_noID) did not differ significantly from the C_TD and the C_ID control groups on both local and global scores (Mann-Whitney U tests; $p > 0.05$; see Table 3.5 for details on exact p-values). Therefore, the ASD groups were able to draw the global and local configuration in a similar way when compared with control participants (see examples in Figure 3.7).

Table 3.5. Comparison of blinded Local and Global scores

	Drawing Task	
	Global Score	Local Score
ASD_IDvs.C_TD	$p=0.092$	$p=0.051$
ASD_IDvs. C_ID	$p=0.567$	$p=0.396$
ASD_noIDvs.C_TD	$p=0.721$	$p=0.222$
WS vs. C_TD	$p=0.000$	$p=0.000$
WS vs. C_ID	$p=0.000$	$p=0.000$

Mann-Whitney U tests; all comparisons marked in bold are significant and related to increased local bias. **NOTE.** WS = Williams Syndrome group; ASD_ID = Autism Spectrum Disorders group with intellectual disability; ASD_noID = Autism Spectrum Disorders group without intellectual disability; C_TD = typically developing control group; C_ID = control group with intellectual disability.

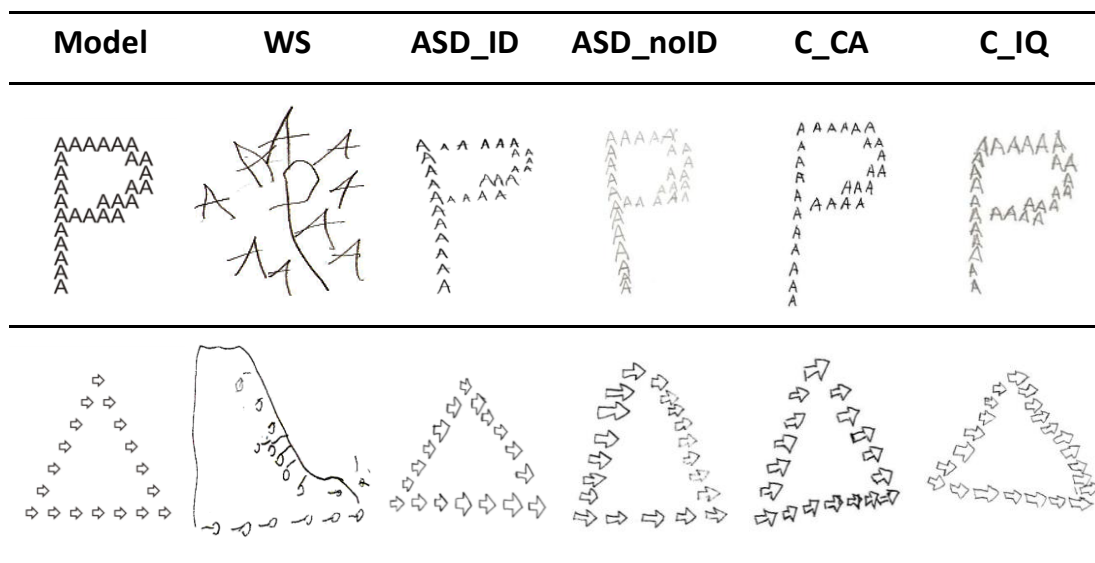


Figure 3.7. Examples of drawings produced by clinical and control groups.

NOTE. WS = Williams Syndrome group; ASD_ID = Autism Spectrum Disorders group with intellectual disability; ASD_noID = Autism Spectrum Disorders group without intellectual disability; C_TD = typically developing control group; C_ID = control group with intellectual disability.

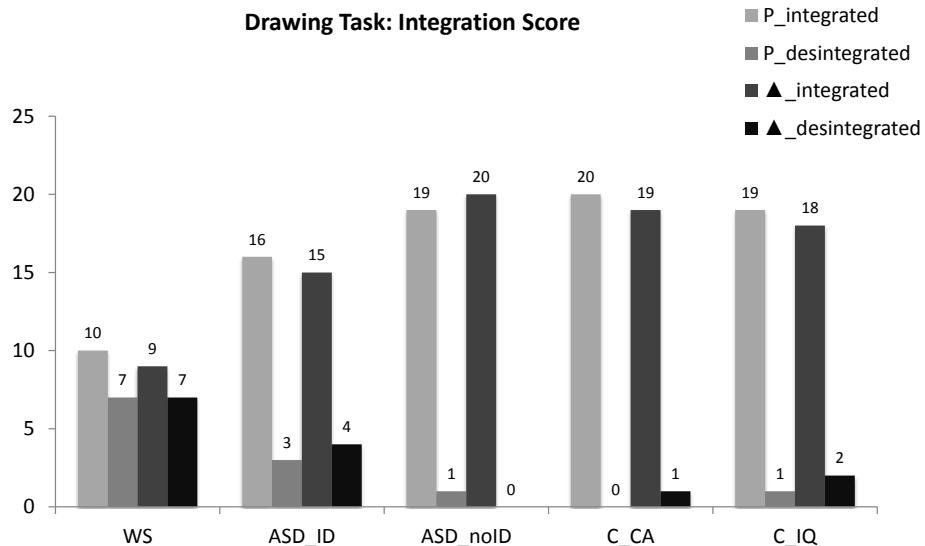
Concerning the integration score, results indicated that WS participants were significantly worse at integrating local and global levels of analysis when compared with C_TD and C_ID control groups (Fisher’s Exact Test; $p < 0.05$).

On the other hand, ASD participants, as well as their matched control groups, were able to integrate the local elements in order to correctly construct the global configuration. Thus, group comparison analyses revealed that the number of subjects who were able to integrate both triangle and ‘P’ drawing did not differ between the ASD groups and the control participants (Fisher’s Exact Test; $p > 0.05$; see Table 3.6 for details on exact p -values). Results are summarized in Figure 3.8.

Table 3.6. Comparison of blinded Integration score

Drawing Task: Integration Score		
	‘P’ Drawing	Triangle Drawing
ASD_ID vs. C_TD	$p=0.106$	$p=0.155$
ASD_ID vs. C_ID	$p=0.283$	$p=0.305$
ASD_noID vs. C_TD	$p=0.500$	$p=0.500$
WS vs. C_TD	$p=0.000$	$p=0.004$
WS vs. C_ID	$p=0.000$	$p=0.001$

Mann-Whitney U tests; all comparisons marked with bold are significant and related to increased local bias. **NOTE.** WS = Williams Syndrome group; ASD_ID = Autism Spectrum Disorders group with intellectual disability; ASD_noID = Autism Spectrum Disorders group without intellectual disability; C_TD = typically developing control group; C_ID = control group with intellectual disability.



◀ **Figure 3.8. Visuoconstructive integrative abilities.** Integration score for all groups indicating the number of subjects who were able to integrate the local elements in order to correctly reproduce the global configuration regarding the geometric hierarchical figure (Triangle) and the hierarchical letter ('P'). **NOTE.** WS = Williams Syndrome group; ASD_ID = Autism Spectrum Disorders group with intellectual disability; ASD_noID = Autism Spectrum Disorders group without intellectual disability; C_TD = typical developing control group; C_ID = control group with intellectual disability.

Discussion

In this study we investigated visual coherence in WS by performing a direct comparison with other neurodevelopmental disorder which has been classically associated with weak central coherence, ASD. In order to understand into which extent can these neurodevelopmental disorders represent clinical models of impaired visual coherence, we used classical markers of central coherence under distinct task constraints in clinical populations with categorical distinctions in intellectual disability and cognitive phenotype. Tasks were performed in the perceptual, memory and visuoconstructive domains, with explicit manipulations of levels of bias to better understand the distinction between cognitive style and performance.

We found that a significant bias towards local information processing was in general found in the WS group, regardless of IQ which is consistent with previous evidence of a local visual preference in this disorder (E. K. Farran & Jarrold, 2003; Porter & Coltheart, 2006). On the other hand, ASD participants showed a surprising global preference pattern that is at odds with previous claims (Uta Frith, 1989), although we also replicated local preference under particular conditions (see below). In other words, weakest central coherence was not found in the autistic group but rather in WS (with explicitly excluded autistic co-morbidity). Therefore, we found a gradient of central coherence impairment (WS>ASD>C_ID=C_TD) that is not consistent with the pattern derived from the WCC account (ASD>WS>C_ID=C_TD). Interestingly we could experimentally manipulate the preference level, in agreement with the task dependence and clinical heterogeneity found in previous studies (Porter & Coltheart, 2005).

Our study demonstrated that in WS the local bias co-exists with a deficit in correctly perceiving local and global visual information and with clear visuoconstructive integration impairment. Conversely, the global bias in ASD patients is accompanied by the presence of a global visual processing adequate to their intellectual level. It is important to note that ASD patients also showed tendency towards a local bias when experimental manipulations

emphasized local processing as occurred in the global-rotation condition in the preference task. In other words, we could replicate the local pattern found in other studies, showing that it can indeed emerge under particular conditions, but that it is not general.

Physical properties of the hierarchical stimulus used here have been described to influence the pattern of global-local processing (Navon, 2003). Although there is evidence that ASD patients are not vulnerable to changes in visual angle and exposure time (L. Wang, Mottron, Peng, Berthiaume, & Dawson, 2007), it is known that perceptual sensitivity of ASD patients can be modulated by the level of the perceptual task load (Remington, Swettenham, & Lavie, 2012). The manipulation of levels of stimulus rotation, in our task, may have contributed to the increase of local processing in ASD under these conditions. Moreover, ASD patients were, in general, able to process global information when the level of intellectual disability was controlled for, which agrees with previous claims (Caron et al., 2006; Mottron et al., 2003; Mottron, Burack, Stauder, & Robaey, 1999; Ozonoff et al., 1994).

Thus, ASD patients may oscillate between a local versus a global mode depending on task requirements and stimulus configuration. A different pattern was detected in WS with consistent local perceptual bias irrespective of task manipulations. Therefore, our findings provide a novel perspective on the WCC debate, without disputing previous findings.

The presence of a stronger detailed-focused perception as well as pronounced coherence deficits in WS may suggest a determinant link between impaired visual coherence and specific deficits within the dorsal visual stream. WS has been widely referred as involving deficits in tasks subserved by the visual dorsal stream (motion, 2D/3D object coherence and visuoconstructive ability), such as in perceiving 2D form-from-motion stimuli (J. E. Reiss, Hoffman, & Landau, 2005), discriminating 2D coherent motion (Atkinson et al., 2003) and visuomotor planning (Atkinson et al., 2006). Additionally, our group (Mendes et al., 2005) previously found a 3D coherence deficit, larger than the 2D deficit suggesting that dorsal stream coherence deficits build up in the processing hierarchy. Accordingly, WS patients exhibit a considerable visual coherence and visuoconstructive impairment in particular when they are required to integrate local and global information, which was confirmed by our results. These findings are consistent with identified anatomical abnormalities in the superior parietal sulcus (Jackowski et al., 2009), and functional neuroimaging data (Meyer-Lindenberg et al., 2004; Mobbs, Eckert, Menon et al., 2007).

Deficits along the dorsal visual stream have also been suggested in ASD, although the results indicate subtle (Bertone, Mottron, Jelenic, & Faubert, 2003; Spencer et al., 2000) or even inexistent (Koldewyn, Whitney, & Rivera, 2010, 2011) general dorsal stream

impairment. This led to the prediction that if central coherence is subserved by dorsal stream processing then it should be weaker in WS than ASD. Our results support this notion. In accordance with this prediction, recently, Poirel et al. (2011), studied the shift from local to global visual processing in 6 year-old children and found that the global visual processing is associated to the loss of grey matter in areas along the dorsal visual stream (occipital and parietal visuospatial areas).

In sum, we conclude that abnormal central coherence is present in WS and may be a marker of dorsal stream dysfunction. Accordingly, weak central coherence is not a unique and distinctive characteristic in ASD and was found to be most impaired in populations (WS) characterized by largest dorsal stream deficits and with phenotypic traits (such as hypersociability) that contrast with the autistic phenotype.

References

- American Psychiatric Association (1994). *Diagnostic and Statistical Manual of mental Disorders* (4th ed.). Washington DC: American Psychiatric Press.
- Atkinson, J., Braddick, O., Anker, S., Curran, W., Andrew, R., Wattam-Bell, J., et al. (2003). Neurobiological models of visuospatial cognition in children with Williams syndrome: measures of dorsal-stream and frontal function. *Dev Neuropsychol*, *23*(1-2), 139-172.
- Atkinson, J., Braddick, O., Rose, F. E., Searcy, Y. M., Wattam-Bell, J., & Bellugi, U. (2006). Dorsal-stream motion processing deficits persist into adulthood in Williams syndrome. *Neuropsychologia*, *44*(5), 828-833.
- Atkinson, J., King, J., Braddick, O., Nokes, L., Anker, S., & Braddick, F. (1997). A specific deficit of dorsal stream function in Williams' syndrome. *Neuroreport*, *8*(8), 1919-1922.
- Bellugi, U., Lichtenberger, L., Jones, W., Lai, Z., & St George, M. (2000). I. The neurocognitive profile of Williams Syndrome: a complex pattern of strengths and weaknesses. *J Cogn Neurosci*, *12 Suppl 1*, 7-29.
- Bertone, A., Mottron, L., Jelenic, P., & Faubert, J. (2003). Motion perception in autism: a "complex" issue. *J Cogn Neurosci*, *15*(2), 218-225.
- Caron, M. J., Mottron, L., Berthiaume, C., & Dawson, M. (2006). Cognitive mechanisms, specificity and neural underpinnings of visuospatial peaks in autism. *Brain*, *129*(Pt 7), 1789-1802.
- Castelo-Branco, M., Mendes, M., Sebastiao, A. R., Reis, A., Soares, M., Saraiva, J., et al. (2007). Visual phenotype in Williams-Beuren syndrome challenges magnocellular theories explaining human neurodevelopmental visual cortical disorders. *J Clin Invest*, *117*(12), 3720-3729.
- Cusco, I., Corominas, R., Bayes, M., Flores, R., Rivera-Brugues, N., Campuzano, V., et al. (2008). Copy number variation at the 7q11.23 segmental duplications is a susceptibility factor for the Williams-Beuren syndrome deletion. *Genome Res*, *18*(5), 683-694.
- Dakin, S., & Frith, U. (2005). Vagaries of visual perception in autism. *Neuron*, *48*(3), 497-507.
- Deruelle, C., Rondan, C., Gepner, B., & Tardif, C. (2004). Spatial frequency and face processing in children with autism and Asperger syndrome. *J Autism Dev Disord*, *34*(2), 199-210.
- Deruelle, C., Rondan, C., Salle-Collemiche, X., Bastard-Rosset, D., & Da Fonseca, D. (2008). Attention to low- and high-spatial frequencies in categorizing facial identities, emotions and gender in children with autism. *Brain Cogn*, *66*(2), 115-123.
- Farran, E. K., & Jarrold, C. (2003). Visuospatial cognition in Williams syndrome: reviewing and accounting for the strengths and weaknesses in performance. *Dev Neuropsychol*, *23*(1-2), 173-200.
- Farran, E. K., Jarrold, C., & Gathercole, S. E. (2003). Divided attention, selective attention and drawing: processing preferences in Williams syndrome are dependent on the task administered. *Neuropsychologia*, *41*(6), 676-687.
- Frith, U. (1989). *Autism : explaining the enigma*. Oxford, UK ; Cambridge, MA, USA: Basil Blackwell.
- Frith, U., & Happe, F. (1994). Autism: beyond "theory of mind". *Cognition*, *50*(1-3), 115-132.
- Happe, F. G. (1994). Wechsler IQ profile and theory of mind in autism: a research note. *J Child Psychol Psychiatry*, *35*(8), 1461-1471.
- Happe, F. G. (1996). Studying weak central coherence at low levels: children with autism do not succumb to visual illusions. A research note. *J Child Psychol Psychiatry*, *37*(7), 873-877.
- Jackowski, A. P., Rando, K., Maria de Araujo, C., Del Cole, C. G., Silva, I., & Tavares de Lacerda, A. L. (2009). Brain abnormalities in Williams syndrome: a review of structural and functional magnetic resonance imaging findings. *Eur J Paediatr Neurol*, *13*(4), 305-316.
- Joseph, R. M., Keehn, B., Connolly, C., Wolfe, J. M., & Horowitz, T. S. (2009). Why is visual search superior in autism spectrum disorder? *Dev Sci*, *12*(6), 1083-1096.
- Kanner, L. (1943). Autistic Disturbances of Affective Contact. *Nervous Child*, *2*, 217-250.
- Keehn, B., Brenner, L., Palmer, E., Lincoln, A. J., & Muller, R. A. (2008). Functional brain organization for visual search in ASD. *J Int Neuropsychol Soc*, *14*(6), 990-1003.
- Koldewyn, K., Whitney, D., & Rivera, S. M. (2010). The psychophysics of visual motion and global form processing in autism. *Brain*, *133*(Pt 2), 599-610.
- Koldewyn, K., Whitney, D., & Rivera, S. M. (2011). Neural correlates of coherent and biological motion perception in autism. *Dev Sci*, *14*(5), 1075-1088.
- Lord, C., Rutter, M., DiLavore, P., & Risis, S. (1999). *Autism Diagnostic Observation Schedule (ADOS)*. Los Angeles: Western Psychological Services.

- Lord, C., Rutter, M., & Le Couteur, A. (1994). Autism Diagnostic Interview-Revised: a revised version of a diagnostic interview for caregivers of individuals with possible pervasive developmental disorders. *J Autism Dev Disord*, *24*(5), 659-685.
- Mendes, M., Silva, F., Simoes, L., Jorge, M., Saraiva, J., & Castelo-Branco, M. (2005). Visual magnocellular and structure from motion perceptual deficits in a neurodevelopmental model of dorsal stream function. *Brain Res Cogn Brain Res*, *25*(3), 788-798.
- Mervis, C. B., Robinson, B. F., Bertrand, J., Morris, C. A., Klein-Tasman, B. P., & Armstrong, S. C. (2000). The Williams syndrome cognitive profile. *Brain Cogn*, *44*(3), 604-628.
- Meyer-Lindenberg, A., Kohn, P., Mervis, C. B., Kippenhan, J. S., Olsen, R. K., Morris, C. A., et al. (2004). Neural basis of genetically determined visuospatial construction deficit in Williams syndrome. *Neuron*, *43*(5), 623-631.
- Mobbs, D., Eckert, M. A., Menon, V., Mills, D., Korenberg, J., Galaburda, A. M., et al. (2007). Reduced parietal and visual cortical activation during global processing in Williams syndrome. *Dev Med Child Neurol*, *49*(6), 433-438.
- Mottron, L., Belleville, S., & Menard, E. (1999a). Local bias in autistic subjects as evidenced by graphic tasks: perceptual hierarchization or working memory deficit? *J Child Psychol Psychiatry*, *40*(5), 743-755.
- Mottron, L., Burack, J. A., Iarocci, G., Belleville, S., & Enns, J. T. (2003). Locally oriented perception with intact global processing among adolescents with high-functioning autism: evidence from multiple paradigms. *J Child Psychol Psychiatry*, *44*(6), 904-913.
- Mottron, L., Burack, J. A., Stauder, J. E., & Robaey, P. (1999b). Perceptual processing among high-functioning persons with autism. *J Child Psychol Psychiatry*, *40*(2), 203-211.
- Navon, D. (1977). Forest before trees: The precedence of global features in visual perception. *Cognitive Psychology*, *9*(353-383).
- Navon, D. (2003). What does a compound letter tell the psychologist's mind? *Acta Psychol (Amst)*, *114*(3), 273-309.
- Oliveira, G., Ataíde, A., Marques, C., Miguel, T. S., Coutinho, A. M., Mota-Vieira, L., et al. (2007). Epidemiology of autism spectrum disorder in Portugal: prevalence, clinical characterization, and medical conditions. *Dev Med Child Neurol*, *49*(10), 726-733.
- Ozonoff, S., Strayer, D. L., McMahon, W. M., & Filloux, F. (1994). Executive function abilities in autism and Tourette syndrome: an information processing approach. *J Child Psychol Psychiatry*, *35*(6), 1015-1032.
- Plaisted, K., O'Riordan, M., & Baron-Cohen, S. (1998). Enhanced visual search for a conjunctive target in autism: a research note. *J Child Psychol Psychiatry*, *39*(5), 777-783.
- Plaisted, K., Swettenham, J., & Rees, L. (1999). Children with autism show local precedence in a divided attention task and global precedence in a selective attention task. *J Child Psychol Psychiatry*, *40*(5), 733-742.
- Poirel, N., Simon, G., Cassotti, M., Leroux, G., Perchey, G., Lanoe, C., et al. (2011). The shift from local to global visual processing in 6-year-old children is associated with grey matter loss. *PLoS One*, *6*(6), e20879.
- Porter, M. A., & Coltheart, M. (2005). Cognitive heterogeneity in Williams syndrome. *Dev Neuropsychol*, *27*(2), 275-306.
- Porter, M. A., & Coltheart, M. (2006). Global and local processing in Williams syndrome, autism, and Down syndrome: perception, attention, and construction. *Dev Neuropsychol*, *30*(3), 771-789.
- Reiss, J. E., Hoffman, J. E., & Landau, B. (2005). Motion processing specialization in Williams syndrome. *Vision Res*, *45*(27), 3379-3390.
- Remington, A. M., Swettenham, J. G., & Lavie, N. (2012). Lightening the Load: Perceptual Load Impairs Visual Detection in Typical Adults but Not in Autism. *J Abnorm Psychol*.
- Rinehart, N. J., Bradshaw, J. L., Moss, S. A., Brereton, A. V., & Tonge, B. J. (2000). Atypical interference of local detail on global processing in high-functioning autism and Asperger's disorder. *J Child Psychol Psychiatry*, *41*(6), 769-778.
- Rondan, C., & Deruelle, C. (2007). Global and configural visual processing in adults with autism and Asperger syndrome. *Res Dev Disabil*, *28*(2), 197-206.
- Rondan, C., Santos, A., Mancini, J., Livet, M. O., & Deruelle, C. (2008). Global and local processing in Williams syndrome: drawing versus perceiving. *Child Neuropsychol*, *14*(3), 237-248.

- Ropar, D., & Mitchell, P. (1999). Are individuals with autism and Asperger's syndrome susceptible to visual illusions? *J Child Psychol Psychiatry*, *40*(8), 1283-1293.
- Rutter, M., Bailey, A., & Lord, C. (2003). *Social Communication Questionnaire*. Los Angeles: Western Psychological Services.
- Shah, A., & Frith, U. (1983). An islet of ability in autistic children: a research note. *J Child Psychol Psychiatry*, *24*(4), 613-620.
- Shah, A., & Frith, U. (1993). Why do autistic individuals show superior performance on the block design task? *J Child Psychol Psychiatry*, *34*(8), 1351-1364.
- Spencer, J., O'Brien, J., Riggs, K., Braddick, O., Atkinson, J., & Wattam-Bell, J. (2000). Motion processing in autism: evidence for a dorsal stream deficiency. *Neuroreport*, *11*(12), 2765-2767.
- Wang, L., Mottron, L., Peng, D., Berthiaume, C., & Dawson, M. (2007). Local bias and local-to-global interference without global deficit: a robust finding in autism under various conditions of attention, exposure time, and visual angle. *Cogn Neuropsychol*, *24*(5), 550-574.
- Wechsler, D. (2003). *Manual for the Intelligence Scale for Children*. Lisbon: Cegoc-Tea.
- Wechsler, D. (2008). *Manual for the Intelligence Scale for Adults*. Lisbon: Cegoc-Tea.

CHAPTER 4

Dorsal-ventral stream dissociation in Williams Syndrome:

a novel experimental paradigm exploring egocentric
and allocentric spatial representations

This chapter was based on: **Bernardino, I.**, Mouga, S., Castelo-Branco, M. & van Asselen, M. (2013). Egocentric and allocentric spatial representations in Williams syndrome. *Journal of the International Neuropsychological Society*, 19, 1-9.

Abstract

Williams syndrome (WS) is a neurodevelopmental disorder characterized by severe visuospatial deficits, particularly affecting spatial navigation and wayfinding. Creating egocentric (viewer- dependent) and allocentric (viewer- independent) representations of space is essential for the development of these abilities. However, it remains unclear whether egocentric and allocentric representations are impaired in WS. The study of how individuals with WS use these spatial reference frames provide a novel approach to the investigation on the dorsal-ventral dissociation in this condition. In this study, we investigate egocentric and allocentric frames of reference in WS. A WS group (n = 18), as well as a chronological age-matched control group (n =20), a non-verbal mental age-matched control group (n =20) and a control group with intellectual disability (n=17), was tested with a computerized and a 3D spatial judgment task. The results showed that WS participants are impaired when performing both egocentric and allocentric spatial judgments even when compared with mental age-matched control participants. This indicates that a substantial deficit affecting both spatial representations is present in WS. The egocentric impairment is in line with the dorsal visual pathway deficit previously reported in WS. Interestingly, the difficulties found in performing allocentric spatial judgments give important cues to better understand the ventral visual functioning in WS.

Introduction

Williams Syndrome (WS) is commonly associated with visuospatial dysfunction which have been widely reported particularly concerning the perception of two-dimensional (2D) form-from-motion stimuli (J. E. Reiss et al., 2005) and the discrimination of coherent motion and action planning (Atkinson et al., 2003). Furthermore, a decreased efficiency in visual search was reported and is characterized by a less structured scan-pattern. This involves an increase in fixation duration and number of fixations which results in more time required to process the visual scene (Montfoort et al., 2007). WS participants were also found to be impaired on visual working memory tasks requiring the recognition of the location of a previously presented object appearing in one of four quadrants (Vicari, Bellucci, & Carlesimo, 2005). These deficits regarding the processing of spatial information have been demonstrated in small-scale as well as in large-scale environments (E. Farran, Courbois, & Cruickshank, 2009). WS participants were found to be slightly impaired in learning a route in the real world (E. K. Farran, Blades, Boucher, & Tranter, 2010) and in correctly performing wayfinding tasks (Atkinson et al., 2001). The aforementioned weaknesses have important outcomes for the daily life of these patients which are evidenced by their parents' reports revealing difficulties in following directions and establishing their perceptual organization of space (Semel & Rosner, 2003).

The development of the spatial representation of the surrounded space under different frames of reference is pivotal for the acquisition of spatial navigation and wayfinding abilities. Nardini, Atkinson, Braddick and Burges (2008), defined developmental trajectories of different spatial frames of reference in WS by using a spatial memory paradigm including either array-, body- or environment-based frames of reference judgments. Results demonstrated that spatial memory coding in WS was slow and incomplete compared to controls, although it did not follow an anomalous developmental pattern. WS of all ages were severely impaired on this task, particularly when a local landmark was used as reference frame.

Two main classes of reference frames to represent spatial information can be distinguished, namely egocentric and allocentric representations. Egocentric coordinates represent positions of locations that are related to the position of the viewer (viewer-dependent). In contrast, allocentric information computes the positions of objects in relation to other objects in the environment, independent of the position of the viewer (viewer-independent). In line with what was referred in the Chapter 1, there is the evidence that the

dorsal visual stream is responsible for processing egocentric information while the ventral visual stream processes spatial information from an allocentric perspective (Goodale & Haffenden, 1998). Accordingly, neuroimaging studies, which have explored the neural basis of egocentric and allocentric reference frames, have confirmed different neural structures and pathways underlying these systems (Galati et al., 2000; Holdstock, Mayes, Cezayirli, Aggleton, & Roberts, 1999; Vallar et al., 1999).

Egocentric encoding of space has been shown to recruit a fronto-parietal network along the dorsal stream (Galati et al., 2000; Vallar et al., 1999) which plays an important role for spatial processing and mediates visual control of skilled actions directed at objects (A. Milner & Goodale, 2008). Patients with lesions along the dorsal visual pathway (parietal-lobe regions) were described to be less accurate in navigating through computer-simulated tunnels shown from a first person perspective than frontal lobe patients and age-matched control participants, supporting the role of the parietal lobe in processing egocentric information (Seubert, Humphreys, Muller, & Gramann, 2008). These findings are in line with neurophysiological approaches in the monkey in which neurons coding viewer-dependent spatial positions have been found in the posterior parietal and premotor cortices (Cohen & Andersen, 2002).

On the other hand, allocentric spatial processing is thought to recruit ventromedial temporal structures along the ventral visual stream (Holdstock et al., 1999) which is mainly responsible for the perception of object properties (A. Milner & Goodale, 2008). However, the cortical representation of the allocentric information seems to be more diffuse than that of the egocentric reference frame (Grimsen, Hildebrandt, & Fahle, 2008). Patients who underwent unilateral temporal lobectomy showed impairments in performing allocentric but not egocentric spatial memory tasks suggesting that the anterior temporal lobe, as well as the hippocampus play an important role in allocentric coordinates (Feigenbaum & Morris, 2004). Involvement of the hippocampal and parahippocampal regions was found exclusively in allocentric spatial memory processing (van Asselen et al., 2006). These findings are in line with the theory of O'Keefe and Nadel (1978) who stated that the hippocampus is pivotal in the processing of allocentric spatial information. In fact, the hippocampal formation has been described as crucial for the processing of spatial navigational information and was found to have an abnormal functioning in WS. Meyer-Lindenberg, Mervis and Berman (2005) reported abnormal function and metabolism of the anterior hippocampal formation despite preserved volume and subtle altered shape evidencing the neural basis for spatial navigation dysfunction in this disorder. Additionally, the dorsal visual stream, associated

with the processing of information from an egocentric perspective, has been described as impaired in WS. Indeed, the noticeable deficits in the visuospatial domain reported in WS have been explained by developmental impairments within the dorsal visual pathway (Jackowski et al., 2009; Meyer-Lindenberg et al., 2004). The ventral visual stream has been described to be relatively less affected in WS (Paul et al., 2002), resulting in fairly normal object recognition, colour processing and recognition of faces (Bellugi et al., 2000).

The goal of the present study was to explore the dissociation between dorsal and ventral visual function in WS by investigating how these patients use both egocentric and allocentric reference frames. Although several studies addressed spatial processing in WS, until now, no study has explicitly differentiated between the use of egocentric and allocentric reference frames in relation to dorsal and ventral stream functioning, respectively. Given the aforementioned neural correlates of egocentric and allocentric frames of reference, an experimental paradigm exploring these reference frames is suitable for the investigation of dorsal and ventral stream dissociation in this neurodevelopmental disorder. To achieve this goal, we used a computerized spatial judgment task as well as a 3D spatial judgment task. The 3D spatial judgment task was introduced to control for weaknesses in performing the task due to the difficulty in interacting with the computer. Thus, this 3D spatial task involves high ecological validity, in which the materials and setting approximate a real-life situation. This ecological approach is mainly important keeping in mind that this clinical group is characterized by mild to moderate retardation and these patients are not familiar with computerized environments.

Considering the importance of the posterior parietal cortex for processing spatial information from an egocentric perspective, we hypothesized that WS participants will be impaired on tasks involving viewer-dependent judgments. Furthermore, since processing information from an allocentric perspective is associated with areas along the ventral visual pathway and hippocampal formation, we expected that performance on viewer-independent tasks may also be affected in this disorder.

Methods

Participants

The same cohort of eighteen WS participants (11 males and 7 females) described in the previous chapter (Bernardino et al., 2012) was recruited for the current study (for further

information on demographic and genetic characterization, please see Chapter 3). None of the WS participants was diagnosed with Attention Deficit and Hyperactivity Disorder (ADHD) or was taking medication to control for attentional and behavioural problems.

Three control groups were created. A chronological age-matched control group (TD_CA), in which 20 typically developing participants were matched for chronological age ($t(36)=0.346, p=0.732$) and handedness (Fisher's exact test, $p=0.328$) with the WS group.

A non-verbal mental age matched control group (TD_NVMA), in which 20 typically developing participants were matched for non-verbal mental age ($t(36)=-1.442, p=0.158$) and handedness (Fisher's exact test, $p=0.328$) with the WS group. Non-verbal mental age was defined on the basis of the score on the Ravens Coloured Progressive Matrices (RCPM, Raven, 1974). The RCPM are recognised as a non-verbal measure of fluid intelligence and were previously described as being a useful tool to make an adequate match between WS and respective control groups (Van Herwegen, Farran, & Annaz, 2011). None of the control participants had a history of psychiatric, neurologic and ophthalmologic illness and all were naïve concerning the testing procedures. They were recruited from local schools and were individually tested at their own schools.

Finally, a control group with intellectual disability (ID) was included, in which 17 participants were matched for chronological age (Mann-Whitney test, $p=0.630$), full-scale intelligence quotient (FSIQ) ($t(33)=0.113, p=0.911$), education level ($t(33)=-1.494, p=0.145$) raven score ($t(33)=-0.641, p=0.526$) and handedness (Fisher's exact test, $p=0.443$) with the WS group. These participants were recruited from local special education institutes. None of these participants were taking selective serotonin reuptake inhibitor or neuroleptic medications. Participants with co-morbid conditions were excluded (epilepsy, brain injury, sensory deficits, associated genetic syndromes, and motor deficits that could interfere with task response).

The FSIQ score was obtained by using the Portuguese adapted version of the Wechsler Intelligence Scales, namely the Wechsler Intelligence Scale for Children – 3rd edition (WISC-III) or the Wechsler Adult Intelligence Scale – 3rd edition (WAIS-III), according to the participant's age (Wechsler, 2003, 2008). The assessment of handedness was performed based on the Edinburgh Handedness Inventory (Oldfield, 1971). The characteristics of the patient and control groups are summarized in Table 4.1. Informed consent was obtained from parents of participants or, when appropriate, the participants themselves. The study was approved by our local ethics committee and was conducted in accordance with the declaration of Helsinki.

Table 4.1. Characteristics of clinical and control groups

	WS		TD_CA		TD_NVMA		ID	
	(n=18)		(n=20)		(n=20)		(n=17)	
	Mean	Range	Mean	Range	Mean	Range	Mean	Range
	(SE)		(SE)		(SE)		(SE)	
CA (years)	17.33 (1.81)	8-34	17.25 (1.70)	9-34	6.00 (0.20)	4-9	19.53 (1.59)	9-35
Education (years)	5.00 (1.0)	0-12	7.95 (0.70)	4-14	0.90 (0.20)	0-4	7.00 (0.80)	0-9
FSIQ (WISC-III /WAIS-III)	53.94 (2.01)	42-75	110.71 (1.9)	95-120	106.14 (3.9)	89-119	53.59 (2.47)	40-77
RCPM score	18.56 (1.30)	9-30	33.56 (0.40)	30-36	21.10 (1.20)	13-30	19.71 (1.20)	12-28
Gender (m:f)	11:7		11:9		9:11		8:9	
Handedness (right:left)	15:3		19:1		19:1		12:5	

NOTE. WS = Williams Syndrome group; TD_CA = chronological age-matched typical developing control group; TD_NVMA = non-verbal mental age-matched typical developing control group; ID = control group with intellectual disability. FSIQ = Full-scale intellectual quotient; WISC-III = Wechsler Intelligence Scale for Children, 3rd. ed.; WAIS-III = Wechsler Adult Intelligence Scale, 3rd ed.; RCPM= Ravens Coloured Progressive Matrices; SE= Standard Error of the mean.

Materials and Procedure

Participants were asked to perform two experimental tasks: a computerized and a 3D spatial judgment task. Two different tasks were used in order to explore both egocentric and allocentric spatial frames of reference.

Computerized spatial judgment task

In the computerized spatial judgment task, participants were individually tested in a quiet and darkened room, seated in a comfortable chair. The room was totally darkened for the computerized spatial judgment task in order to prevent that participants use the borders of the monitor or other landmarks as reference frame when performing the task. Stimuli were

shown on a 33,8cm × 27,1cm computer screen using the software package Presentation (Neurobehavioral systems). After instructions were given, participants were asked to place their chin in a chin rest that was positioned at a distance of ≈ 50 cm from the computer screen. Two different experimental tasks were included: an egocentric task and an allocentric task.

In the egocentric task, an image of a tiger was shown during 300ms on a dark screen after which participants had to indicate whether the tiger appeared on their left or on their right, using their own body as a frame of reference (Figure 4.1A). No time limit was used to respond. All participants were able to differentiate between left and right directions. The distance between the tiger and the center of the screen was manipulated by defining eight different positions across the horizontal axis. The defined locations were 0.57°, 1.72°, 3.02° and 4.23° from the center of the screen on both left and right side, representing different levels of task difficulty. On each trial, the tiger was randomly presented on one of the eight locations. A total of 64 trials were included for the egocentric task. Eight practice trials were given and the practice phase was repeated whenever the subjects did not understand the instructions or had difficulties in coordinating the motor response.

In the allocentric task, participants were also required to judge the position of a tiger that appeared during 300ms. However, in this task, the judgments were performed in relation to two flowers that appeared on the screen (Figure 4.1B).

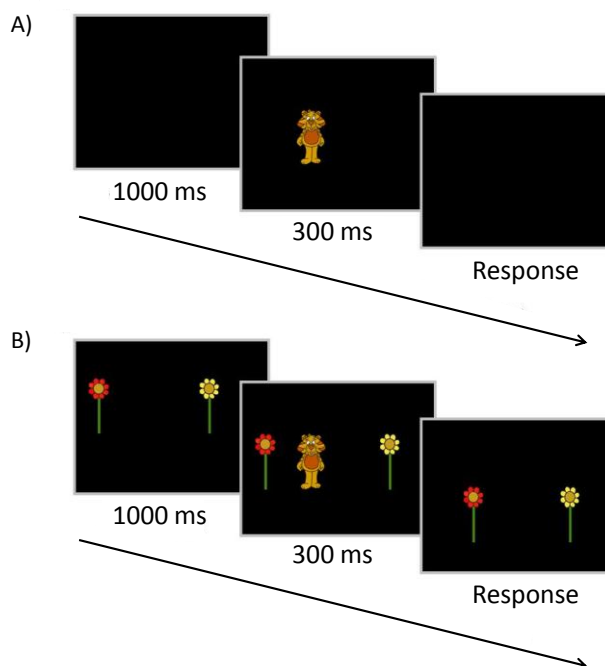


Figure 4.1. Example of the display used on A) egocentric and B) allocentric computer tasks.

Participants had to indicate whether the tiger was closer to the left or to the right flower. The distance between the two flowers was 22.90° . On each trial, the position of the flowers changed across the horizontal axis, although the distance between them remained constant, in order to avoid body-centered spatial judgments. The position of the tiger was never in the centre of the screen, but could be positioned in one of four locations on either left or right side of the centre (0.57° , 1.72° , 3.02° and 4.23°). A total of 64 trials was included as well as the eight practice trials.

3D spatial judgment task

In the 3D spatial judgment task participants were individually tested in a quiet and illuminated room, seated in a comfortable chair in front of a table where a white board was positioned. This task also included an egocentric and an allocentric task, as occurred in the previous task. For both tasks, three small toys were arranged on a white board of 42 cm x 29 cm. Ten trials were conducted and the position of the toys was manipulated on each trial. In the egocentric task, participants had to indicate which of the three toys was closer to their own body (Figure 4.2A). In the allocentric task, the procedure was the same as used in the egocentric task but including one additional toy (a white plane) (Figure 4.2B). No time limit was used for stimulus representation or response. Subjects were instructed to indicate which of the three toys was closer to the white plane. This task also included ten trials.

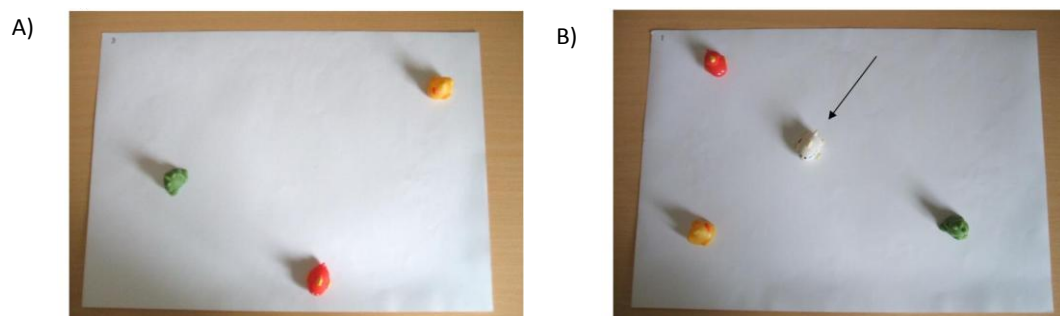


Figure 4.2. Example of the display used on A) egocentric and B) allocentric 3D tasks.

Results

Separate analyses were performed for the computerized and 3D spatial judgment tasks, using percentage of incorrect responses and reaction times in ms as dependent variables.

For the computerized spatial judgment task, a repeated measures ANOVA with Group (WS, TD_CA, TD_NVMA, ID) as between-subject factor and Task (egocentric, allocentric) and Condition (0.57°, 1.72°, 3.02°, 4.23°) as within-subject factor was conducted on the percentage of incorrect responses (Figure 4.3 A, B), including age as covariate. No significant effect was found for Task ($F(1, 71) = 1.30, p > .05, \eta^2 = 0.018$) nor an interaction effect for Task \times Group ($F(3, 71) = 0.190, p > .05, \eta^2 = 0.008$). These data suggest that, for the three groups, performance on both egocentric and allocentric tasks did not differ. Importantly, an overall effect of Group was found ($F(3, 71) = 31.19, p < .001, \eta^2 = 0.569$). Tukey's post-hoc testing showed that the WS group performed significantly worse than all control groups (TD_CA: $p < .001, d = 2.69$; TD_NVMA: $p < .001, d = 1.13$; ID: $p < .001, d = 1.43$). A main effect for Condition was found ($F(3, 71) = 232.732, p < .001, \eta^2 = 0.766$), indicating that the different conditions that were used really represent different levels of task difficulty. Furthermore, the interaction effect for Condition \times Group ($F(9, 71) = 4.398, p < .001, \eta^2 = 0.157$) suggest that the WS group made relatively more errors in the more difficult trials. Additionally, age did not show a significant contribution to explain the present findings ($p > 0.05$). Together, these results indicate that the WS group made significantly more errors than all control groups when asked to perform both egocentric and allocentric spatial judgments in this computer task.

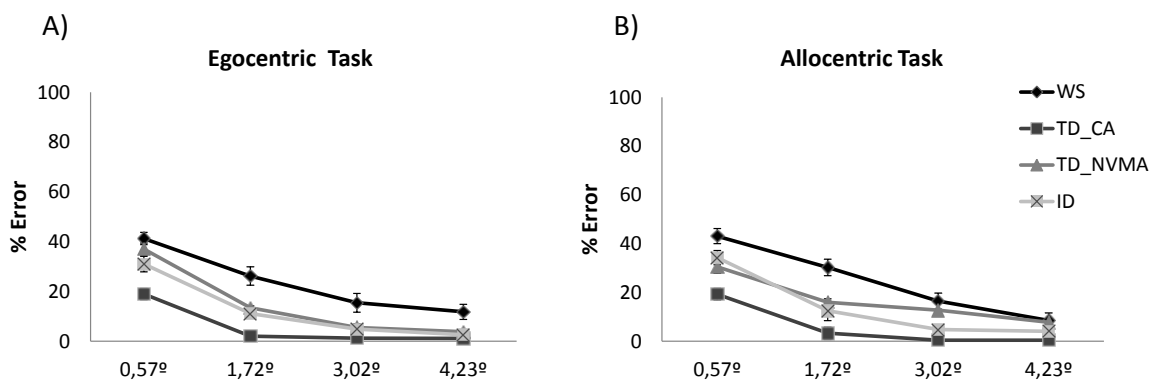


Figure 4.3. Computerized task: percentage of error and standard errors of the mean for WS, TD_CA, TD_NVMA and ID groups as a function of task difficulty (0.57°, 1.72°, 3.02° and 4.23°) on A) egocentric and B) allocentric tasks. **NOTE.** WS = Williams Syndrome group; TD_CA = chronological age-matched typical developing control group; TD_NVMA = non-verbal mental age-matched typical developing control group; ID = control group with intellectual disability. Error bars show the SEM (standard error of the mean)

In a complementary analysis, we fit a psychometric function to each subject's response in order to understand the effect of the different levels of difficulty introduced in the task on the subject's performance. As can be seen in Figure 4.4, the function that best fitted the pattern of performance in response to this task was the Gaussian function. Thus, the conditions that evoked more errors are those in which the tiger appeared near to the centre of the screen and the easiest conditions are those in which the tiger appeared in both extremes, both on left and right sides. The Gaussian fitting was performed by using the Curve Fitting Toolbox of the Matlab software (7.10.0 version). The function used to obtain the fitting was $a1 \cdot \exp(-((x-b1)/c1)^2)$, in which 'a' corresponds to the peak intensity, 'b' gives the peak position and 'c' represents the 'width' of the Gaussian curve. Additionally, we obtained the r-square (the correlation between the response values and the predicted response values) for each fitting, which measures how successful the fit is in explaining the variation of the data. The values of the r-square were between 0.85 and 1 for the egocentric task and between 0.88 and 1 for the allocentric task.

All these parameters were obtained for each subject in both egocentric and allocentric tasks. For the analyses including the parameters from the Egocentric task, a one-way ANOVA revealed a group effect for the 'width' of the curve measure ($F(3, 70) = 7.23, p < .05, \eta^2 = 0.237$), while no group effect was found for the peak intensity ($F(3, 70) = 2.63, p > .05, \eta^2 = 0.101$) and the peak position ($F(3, 70) = 1.30, p > .05, \eta^2 = 0.053$). Post-hoc analyses (Tukey's test) revealed that significant differences concerning the 'width' of the curve occurred between the WS group and all control groups (TD_CA: $p < .001, d = 1.08$; TD_NVMA: $p < .05, d = 0.93$; ID: $p < .05, d = 0.85$) (see Figure 4.4 A).

Regarding the analyses including the parameters from the Allocentric task, a one-way ANOVA did not show a group effect for the peak intensity ($F(3, 70) = 1.69, p > .05, \eta^2 = 0.069$), but revealed a group effect for the position of the peak ($F(3, 70) = 31.05, p < .001, \eta^2 = 0.578$) and for the 'width' of the curve ($F(3, 70) = 14.21, p > .05, \eta^2 = 0.385$). Post-hoc testing indicated that concerning the peak position, the WS group differed from the TD_NVMA ($p < .001, d = -1.93$) and the ID ($p < .001, d = -2.95$) control group, but not from the TD_CA ($p > .05, d = -1.13$) group. Concerning the 'width' of the curve, the WS group differed from the TD_CA ($p < .001, d = 2.57$) and the ID ($p < .001, d = 1.46$) group, but not from the TD_NVMA group ($p > .05, d = 0.63$) (see Figure 4.4 B).

Since we found a significant main effect for Group for the peak position in the allocentric task, we performed a One-Sample T-Test, for each group, comparing the value of the peak position with 0 (corresponding to the centre of the screen) in order to identify a

possible bias for one of the sides of the screen (left or right sides). Interestingly, significant differences were found for all control groups (TD_CA ($t(19) = 3.60, p < .05$), TD_NVMA ($t(19) = 5.764, p < .001$) and ID ($t(16) = 8.38, p < .001$)), but not for the WS group ($t(17) = -1.93, p > .05$). These results revealed that control participants showed a left visual hemifield advantage, whereas WS participants did not. The differences found concerning the ‘width’ of the curve revealed that WS participants made more errors in the intermediate and in the easiest conditions when compared with the controls, although in the allocentric task the performance was similar to the TD_NVMA controls. Additionally, the peak intensity results indicated that the difficulty of the task has the same impact on the performance of both WS and control group with all groups showing more errors on the more difficult conditions (0.57° left and right).

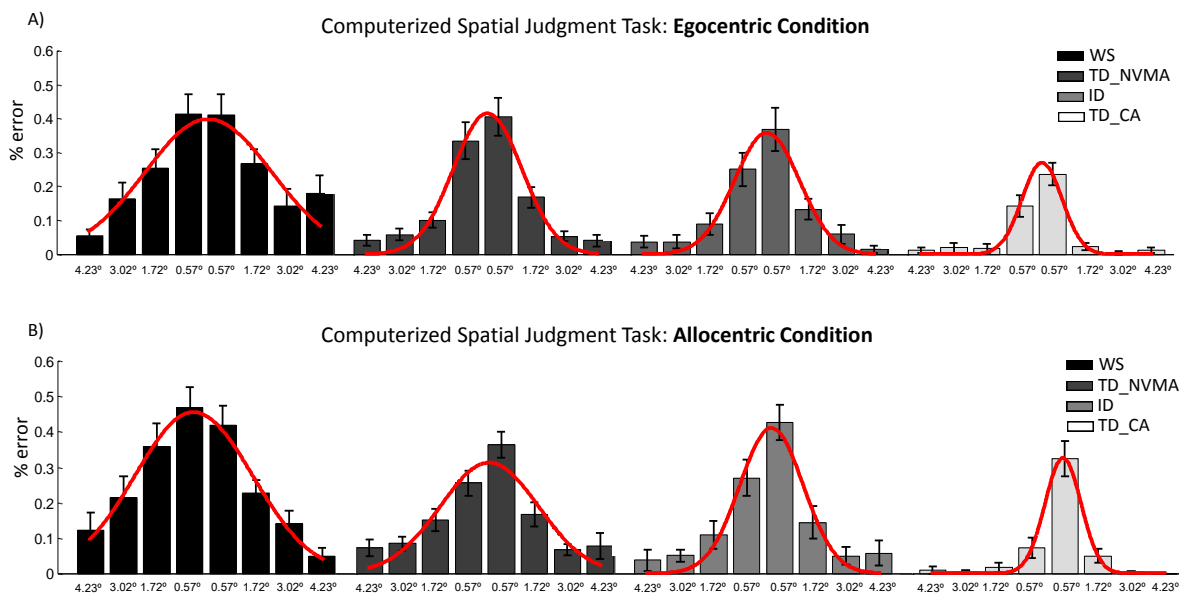


Figure 4.4. Gaussian fitting [$a1 \cdot \exp(-((x-b1)/c1)^2)$] to the error responses of the WS, TD_CA, TD_NVMA and ID groups for the A) egocentric and B) allocentric computerized tasks. **NOTE.** WS = Williams Syndrome group; TD_CA = chronological age-matched typical developing control group; TD_NVMA = non-verbal mental age-matched typical developing control group; ID = control group with intellectual disability. Error bars show the SEM

To analyse the reaction times of the computerized spatial judgment task, a repeated measures ANOVA with Group (WS, TD_CA, TD_NVMA, ID) as between-subject factor and Task (egocentric, allocentric) and Condition (0.57° , 1.72° , 3.02° , 4.23°) as within-subject factor was conducted (see Figure 4.5 A, B), including chronological age as covariate. Results

revealed no significant main effect for Task ($F(1, 71) = 0.06, p > .05, \eta^2 = 0.001$), nor a significant interaction effect for Task \times Groups ($F(3, 71) = 0.264, p > .05, \eta^2 = 0.011$). On the other hand, a significant main effect for Condition ($F(3, 71) = 27.594, p < .001, \eta^2 = 0.280$) was found as well as a significant interaction effect for Condition \times Group ($F(3, 71) = 2.486, p < .05, \eta^2 = 0.095$). Additionally, a significant effect of Group was also found ($F(3, 71) = 5.094, p > .05, \eta^2 = 0.177$). Tukey's post-hoc testing revealed that the WS group is significantly slower than the TD_CA group ($p < .05, d = 1.04$), but need the same time to respond as both the TD_NVMA ($p > .05, d = 0.32$) and the ID ($p > .05, d = 0.46$) control group. Again, age did not contribute to explain the results ($p > .05$).

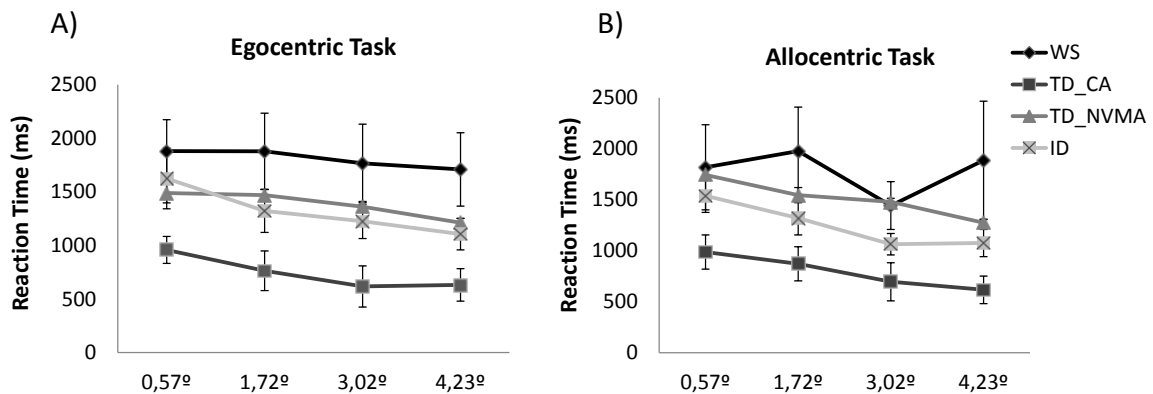


Figure 4.5. Computerized task: reaction times (ms) and standard errors of the mean for WS, TD_CA, TD_NVMA and ID groups as a function of task difficulty (0.57°, 1.72°, 3.02° and 4.23°) on A) egocentric and B) allocentric tasks. **NOTE.** WS = Williams Syndrome group; TD_CA = chronological age-matched typical developing control group; TD_NVMA = non-verbal mental age-matched typical developing control group; ID = control group with intellectual disability. Error bars show the SEM

For the 3D spatial judgment task, the pattern of results was similar to those obtained in the computerized spatial judgment task (Figure 4.6). A repeated measures ANOVA with Group (WS, TD_CA, TD_NVMA, ID) as between-subject factor and Task (egocentric vs. allocentric) as within-subject variable showed a significant effect for Task, ($F(1, 71) = 15.457, p < .001, \eta^2 = 0.179$). However, no significant interaction occurred for Task \times Group ($F(3, 71) = 0.15, p > .05, \eta^2 = 0.006$). Moreover, a significant effect of Group was found ($F(3, 71) = 6.53, p < .05, \eta^2 = 0.216$). Tukey's post-hoc tests indicated that WS

participants made significantly more errors than TD_CA ($p < .001$, $d=1.43$) but performed similarly as both TD_NVMA ($p > .05$, $d=0.53$) and ID ($p > .05$, $d=0.61$) control groups. Age did not contribute to explain the results ($p > .05$). The WS group exhibited deficits in perceiving egocentric as well as allocentric information when compared with chronological age-matched controls but achieved the level of performance exhibited by participants with intellectual disability and with matched non-verbal skills when tested in more ecological environments and without time-limits.

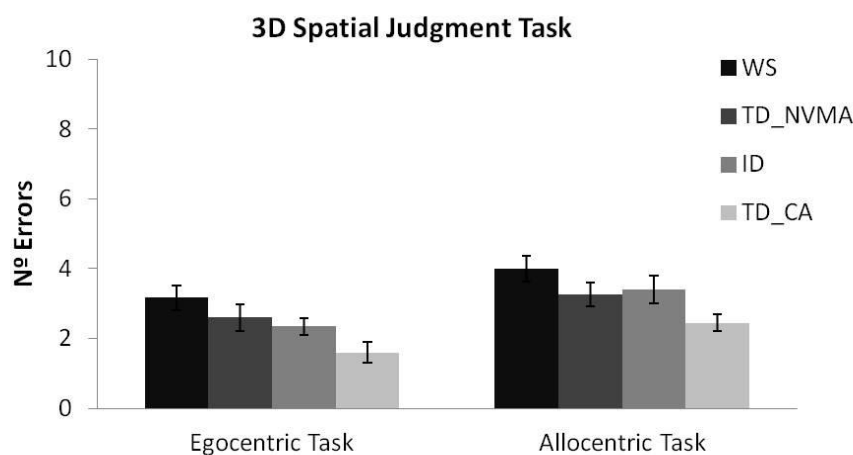


Figure 4.6. 3D Task: Number of errors and standard errors of the mean for WS, TD_NVMA, ID and TD_CA groups for the egocentric and allocentric tasks. **NOTE.** WS = Williams Syndrome group; TD_CA = chronological age-matched typical developing control group; TD_NVMA = non-verbal mental age-matched typical developing control group; ID = control group with intellectual disability. Error bars show the SEM

Discussion

The current study was aimed at investigating visual processing of egocentric and allocentric spatial relations between objects in WS as a measure of dorsal and ventral visual streams functioning, respectively. We conducted two experimental tasks requiring subjects to perform visual spatial judgments of the location of objects using their own-body or external objects as frames of reference.

In the first task, subjects needed to discriminate locations of objects that appeared on a computer screen using allocentric as well as egocentric frames of reference. The results of

this task indicate that the ability to make egocentric and allocentric spatial judgments is impaired in WS participants. Interestingly, no interaction effect emerged for Group and Task, indicating that the impairment exhibited by WS participants is equally serious for both egocentric and allocentric spatial judgments. WS participants performed significantly worse than all control participants on all levels of task difficulty for both reference frames. These results were found even when the groups were matched for non-verbal mental age and also for intellectual disability. Thus, WS participants were consistently impaired on all conditions. Importantly, the larger number of errors exhibited by WS group is not related to faster responses due to attentional problems and impulsive responses, as was demonstrated by reaction time analysis. Indeed, WS participants were slower than control participants matched for chronological age and needed the same time as both control participants matched on non-verbal mental age and intellectual disability. It remains, however, important to analyse the qualitative pattern of results especially taking into account the different levels of complexity introduced in the task. The fitting analysis demonstrated that the WS group show similar results as both control groups in the more difficult conditions (peak intensity measure), but committed more errors in the intermediate and in the easiest conditions ('width' of the curve measure). Additionally, for the allocentric task, the peak position analysis revealed a left visual hemifield advantage for all the control groups, but not for the WS participants. The left hemifield advantage found in control participants is in line with some studies suggesting that neurologically normal participants exhibit a phenomenon similar to that found in neglect patients called 'pseudoneglect' (Bowers & Heilman, 1980). In fact, this left visual hemifield advantage has been demonstrated in several tasks that involve visual attention (McCourt & Garlinghouse, 2000) and is thought to be the result of the dominant role of the right posterior parietal cortex in visuospatial attention.

It should be noted that the computerized spatial judgment task, particularly the egocentric task, required a well established knowledge of left and right directions which might introduce additional confounds for WS participants, even though they all were able to correctly discriminate between left and right.

In the second task, a more ecological approach was employed by using 3D small toys that were displayed on a board. Subjects were again asked to make either an egocentric or allocentric spatial judgment. The results of this task were similar to those found in the computer task confirming the egocentric and allocentric impairments in WS participants. Indeed, no interaction effect was found between the tasks and the groups, suggesting equal impairment for both egocentric and allocentric tasks. In this 3D spatial judgment task, WS

participants achieved similar results to those found in participants with the same level of intellectual disability and non-verbal mental age. This suggests performance improves when using more ecological approaches and by giving them unlimited viewing time.

These findings indicate that egocentric as well as allocentric perception is impaired in WS. These results are in line with the study of Nardini et al. (2008), who showed that both body- and landmark- spatial memory representations are impaired in this disorder. Our results indicate that the deficit found in WS participants regarding the spatial memory coding of egocentric and allocentric information might not only be a result of memory component requirements but it is present even when only perceptual judgments are involved.

The impairment in representing egocentric information is in agreement with existing literature suggesting a dorsal stream dysfunction in WS (Atkinson et al., 2003; Castelo-Branco et al., 2007; Meyer-Lindenberg et al., 2004). Moreover, the evidence of impaired processing concerning allocentric information suggests impaired ventral stream and hippocampal and parahippocampal functioning. That is, neural correlates of allocentric spatial representations are thought to include the ventral stream and hippocampal and parahippocampal regions (Holdstock et al., 2000). The latter regions have been found to be affected in WS participants (Meyer-Lindenberg, Mervis et al., 2005), although a ventral stream weakness is less documented. Although psychophysical and neuroimaging studies have provided important insights into the ventral functioning in WS (Paul et al., 2002), thus far most studies have focused on face perception and recognition skills of WS participants, who demonstrate an overall good performance on these tasks which seems to be comparable to typically-developing individuals, albeit conducted by differing mechanisms (Deruelle, Mancini, Livet, Casse-Perrot, & de Schonen, 1999; Karmiloff-Smith et al., 2004). Moreover, the involvement of both egocentric and allocentric spatial representations was found to be determinant for face processing. (Chang, Harris, & Troje, 2010). More research is still needed to understand the role of egocentric and allocentric frames of reference in face processing, thereby adding to our understanding of visual pathway functioning in WS.

It is interesting to note, however, that studies exploring the developmental trajectories for egocentric and allocentric representations as well as classical developmental literature (Piaget & Inhelder, 1948) suggest that the spontaneous use of allocentric representations develops during the school years, while the egocentric spatial coding emerges in early infancy. Bullens, Igóí, Berthoz, Postma and Rondi-Reig (2010) demonstrated that the correct use of allocentric representations arises between 7 and 10 years of age, reaching the ability to elaborate complex representations of the environment from 10 years onward. On the other

hand, the spontaneous use of egocentric spatial representations is established at 5 years of age (Bullens et al., 2010), although Nardini, Burgess, Breckenridge and Atkinson (2006) have proposed that the viewer-dependent spatial judgments are already present as early as 3 years. This suggests a progressive shift from body-centered perspectives to world-centered representations between 5 and 10 years of age. Accordingly, it was recently suggested by Zaehle et al. (2007) that the allocentric representations develop late in phylogenesis as well as in ontogenesis. The authors proposed that allocentric coding develops based on egocentric coding and partly shares the same neural sources (precuneus), although it recruits additional brain areas, namely right parietal areas, the bilateral ventral visual stream and the hippocampal formation. Therefore, although there are some studies claiming the parallel development of egocentric and allocentric spatial representations (Igloi, Zaoui, Berthoz, & Rondi-Reig, 2009), other studies argued that some dependencies occur between the two frames of reference and they interact to process complex representations of the environment (Burgess, 2006). Based on these findings, we could hypothesise that the egocentric deficits found in WS, as a result of dorsal visual stream impairment, might also be contributing to the difficulties evidenced in the allocentric spatial judgment tasks. Thus, the lack of body-centered spatial representations in WS participants could be an important factor for determining the incomplete development of external reference frames. In fact, the use of landmarks as a complement of the body-centered reference frame in wayfinding tasks has been consistently found to be impaired in this disorder (Atkinson et al., 2001).

Concluding, the current study demonstrated that perception of both egocentric and allocentric spatial relations is impaired in WS participants. The impairment concerning the processing of egocentric information confirms the dorsal visual pathway deficit extensively reported in WS. On the other hand, the difficulties found in performing allocentric spatial judgments are in line with the hippocampal dysfunction and may suggest impaired ventral visual stream function. However, further research is still needed to contribute for a better understanding of the ventral visual stream functioning in WS and its possible implications for the development of spatial representations in this disorder.

References

- Atkinson, J., Anker, S., Braddick, O., Nokes, L., Mason, A., & Braddick, F. (2001). Visual and visuospatial development in young children with Williams syndrome. *Dev Med Child Neurol*, *43*(5), 330-337.
- Atkinson, J., Braddick, O., Anker, S., Curran, W., Andrew, R., Wattam-Bell, J., et al. (2003). Neurobiological models of visuospatial cognition in children with Williams syndrome: measures of dorsal-stream and frontal function. *Dev Neuropsychol*, *23*(1-2), 139-172.
- Bellugi, U., Lichtenberger, L., Jones, W., Lai, Z., & St George, M. (2000). I. The neurocognitive profile of Williams Syndrome: a complex pattern of strengths and weaknesses. *J Cogn Neurosci*, *12 Suppl 1*, 7-29.
- Bernardino, I., Mouga, S., Almeida, J., van Asselen, M., Oliveira, G., & Castelo-Branco, M. (2012). A direct comparison of local-global integration in autism and other developmental disorders: implications for the central coherence hypothesis. *PLoS One*, *in press*.
- Bowers, D., & Heilman, K. M. (1980). Pseudoneglect: effects of hemispace on a tactile line bisection task. *Neuropsychologia*, *18*(4-5), 491-498.
- Bullens, J., Igloi, K., Berthoz, A., Postma, A., & Rondi-Reig, L. (2010). Developmental time course of the acquisition of sequential egocentric and allocentric navigation strategies. *J Exp Child Psychol*, *107*(3), 337-350.
- Burgess, N. (2006). Spatial memory: how egocentric and allocentric combine. *Trends Cogn Sci*, *10*(12), 551-557.
- Castelo-Branco, M., Mendes, M., Sebastiao, A. R., Reis, A., Soares, M., Saraiva, J., et al. (2007). Visual phenotype in Williams-Beuren syndrome challenges magnocellular theories explaining human neurodevelopmental visual cortical disorders. *J Clin Invest*, *117*(12), 3720-3729.
- Chang, D. H., Harris, L. R., & Troje, N. F. (2010). Frames of reference for biological motion and face perception. *J Vis*, *10*(6), 22.
- Cohen, Y. E., & Andersen, R. A. (2002). A common reference frame for movement plans in the posterior parietal cortex. *Nat Rev Neurosci*, *3*(7), 553-562.
- Deruelle, C., Mancini, J., Livet, M. O., Casse-Perrot, C., & de Schonen, S. (1999). Configural and local processing of faces in children with Williams syndrome. *Brain Cogn*, *41*(3), 276-298.
- Farran, E., Courbois, Y., & Cruickshank, A. (2009). Learning route in a virtual environment: the effects of differing cues on the performance of typical children and individuals with Williams syndrome. *Cognitive Processing*, *10*, 152-153.
- Farran, E. K., Blades, M., Boucher, J., & Tranter, L. J. (2010). How do individuals with Williams syndrome learn a route in a real-world environment? *Dev Sci*, *13*(3), 454-468.
- Feigenbaum, J. D., & Morris, R. G. (2004). Allocentric versus egocentric spatial memory after unilateral temporal lobectomy in humans. *Neuropsychology*, *18*(3), 462-472.
- Galati, G., Lobel, E., Vallar, G., Berthoz, A., Pizzamiglio, L., & Le Bihan, D. (2000). The neural basis of egocentric and allocentric coding of space in humans: a functional magnetic resonance study. *Exp Brain Res*, *133*(2), 156-164.
- Goodale, M. A., & Haffenden, A. (1998). Frames of reference for perception and action in the human visual system. *Neurosci Biobehav Rev*, *22*(2), 161-172.
- Grimsen, C., Hildebrandt, H., & Fahle, M. (2008). Dissociation of egocentric and allocentric coding of space in visual search after right middle cerebral artery stroke. *Neuropsychologia*, *46*(3), 902-914.
- Holdstock, J. S., Mayes, A. R., Cezayirli, E., Aggleton, J. P., & Roberts, N. (1999). A comparison of egocentric and allocentric spatial memory in medial temporal lobe and Korsakoff amnesics. *Cortex*, *35*(4), 479-501.
- Holdstock, J. S., Mayes, A. R., Cezayirli, E., Isaac, C. L., Aggleton, J. P., & Roberts, N. (2000). A comparison of egocentric and allocentric spatial memory in a patient with selective hippocampal damage. *Neuropsychologia*, *38*(4), 410-425.
- Igloi, K., Zaoui, M., Berthoz, A., & Rondi-Reig, L. (2009). Sequential egocentric strategy is acquired as early as allocentric strategy: Parallel acquisition of these two navigation strategies. *Hippocampus*, *19*(12), 1199-1211.
- Jackowski, A. P., Rando, K., Maria de Araujo, C., Del Cole, C. G., Silva, I., & Tavares de Lacerda, A. L. (2009). Brain abnormalities in Williams syndrome: a review of structural and functional magnetic resonance imaging findings. *Eur J Paediatr Neurol*, *13*(4), 305-316.

- Karmiloff-Smith, A., Thomas, M., Annaz, D., Humphreys, K., Ewing, S., Brace, N., et al. (2004). Exploring the Williams syndrome face-processing debate: the importance of building developmental trajectories. *J Child Psychol Psychiatry*, *45*(7), 1258-1274.
- McCourt, M. E., & Garlinghouse, M. (2000). Asymmetries of visuospatial attention are modulated by viewing distance and visual field elevation: pseudoneglect in peripersonal and extrapersonal space. *Cortex*, *36*(5), 715-731.
- Meyer-Lindenberg, A., Kohn, P., Mervis, C. B., Kippenhan, J. S., Olsen, R. K., Morris, C. A., et al. (2004). Neural basis of genetically determined visuospatial construction deficit in Williams syndrome. *Neuron*, *43*(5), 623-631.
- Meyer-Lindenberg, A., Mervis, C. B., Sarpal, D., Koch, P., Steele, S., Kohn, P., et al. (2005). Functional, structural, and metabolic abnormalities of the hippocampal formation in Williams syndrome. *J Clin Invest*, *115*(7), 1888-1895.
- Milner, A., & Goodale, M. A. (2008). Two visual systems re-viewed. *Neuropsychologia*, *46*(3), 774-785.
- Montfoort, I., Frens, M. A., Hooge, I. T., Haselen, G. C., & van der Geest, J. N. (2007). Visual search deficits in Williams-Beuren syndrome. *Neuropsychologia*, *45*(5), 931-938.
- Nardini, M., Atkinson, J., Braddick, O., & Burgess, N. (2008). Developmental trajectories for spatial frames of reference in Williams syndrome. *Dev Sci*, *11*(4), 583-595.
- Nardini, M., Burgess, N., Breckenridge, K., & Atkinson, J. (2006). Differential developmental trajectories for egocentric, environmental and intrinsic frames of reference in spatial memory. *Cognition*, *101*(1), 153-172.
- O'Keefe, J., & Nadel, L. (1978). *The hippocampus as a cognitive map*. Oxford: Clarendon.
- Oldfield, R. C. (1971). The assessment and analysis of handedness: the Edinburgh inventory. *Neuropsychologia*, *9*(1), 97-113.
- Paul, B. M., Stiles, J., Passarotti, A., Bavar, N., & Bellugi, U. (2002). Face and place processing in Williams syndrome: evidence for a dorsal-ventral dissociation. *Neuroreport*, *13*(9), 1115-1119.
- Piaget, J., & Inhelder, B. (1948). *The child's conception of space*. New York: Norton.
- Raven, J. C. (1974). *Coloured Progressive Matrices Sets A, Ab, B*. Oxford: Oxford Psychologists Press Ltd.
- Reiss, J. E., Hoffman, J. E., & Landau, B. (2005). Motion processing specialization in Williams syndrome. *Vision Res*, *45*(27), 3379-3390.
- Semel, E., & Rosner, S. (2003). *Understanding Williams syndrome: behavioral patterns and interventions*. London: Lawrence Erlbaum Associates, Inc.
- Seubert, J., Humphreys, G. W., Muller, H. J., & Gramann, K. (2008). Straight after the turn: the role of the parietal lobes in egocentric space processing. *Neurocase*, *14*(2), 204-219.
- Vallar, G., Lobel, E., Galati, G., Berthoz, A., Pizzamiglio, L., & Le Bihan, D. (1999). A fronto-parietal system for computing the egocentric spatial frame of reference in humans. *Exp Brain Res*, *124*(3), 281-286.
- van Asselen, M., Kessels, R. P., Kappelle, L. J., Neggers, S. F., Frijns, C. J., & Postma, A. (2006). Neural correlates of human wayfinding in stroke patients. *Brain Res*, *1067*(1), 229-238.
- Van Herwegen, J., Farran, E., & Annaz, D. (2011). Item and error analysis on Raven's Coloured Progressive Matrices in Williams Syndrome. *Res Dev Disabil*, *32*(1), 93-99.
- Vicari, S., Bellucci, S., & Carlesimo, G. A. (2005). Visual and spatial long-term memory: differential pattern of impairments in Williams and Down syndromes. *Dev Med Child Neurol*, *47*(5), 305-311.
- Wechsler, D. (2003). *Manual for the Intelligence Scale for Children*. Lisbon: Cegoc-Tea.
- Wechsler, D. (2008). *Manual for the Intelligence Scale for Adults*. Lisbon: Cegoc-Tea.
- Zaehle, T., Jordan, K., Wustenberg, T., Baudewig, J., Dechent, P., & Mast, F. W. (2007). The neural basis of the egocentric and allocentric spatial frame of reference. *Brain Res*, *1137*(1), 92-103.

CHAPTER 5

Reorganization of 3D visual processing in Williams syndrome:

an electrophysiological approach
of coherence perception

This chapter was based on: **Bernardino, I.,** Castelhana, J., Farivar, R. & Silva, E. & Castelo-Branco, M. (2013). Neural correlates of visual integration in Williams syndrome: gamma oscillation patterns in a model of impaired coherence. *Neuropsychologia*, 51, 1287-1295.

Abstract

Williams syndrome (WS) is a clinical model of dorsal stream vulnerability and impaired visual coherence. However, little is still known about the neurophysiological correlates of perceptual integration in this condition. We have used a 3D structure-from-motion (SFM) integrative task to characterize the neuronal underpinnings of 3D coherent perception in WS and to probe whether gamma oscillatory patterns reflect changed holistic perception. Coherent faces were parametrically modulated in 3D depth (three different depth levels) to vary levels of stimulus ambiguity. We have found that the electrophysiological (EEG/ERP) correlates of such holistic percepts were distinct across groups. Independent component analysis demonstrated the presence of a novel component with a late positivity around 200ms that was absent in controls. Source localization analysis of ERP signals showed a posterior occipital shift in WS and reduced parietal dorsal stream sources. Interestingly, low gamma-band oscillations (20Hz-40Hz) induced by this 3D perceptual integration task were significantly stronger and sustained during the stimulus presentation in WS whereas high gamma-band oscillations (60-90Hz) were reduced in this clinical model of impaired visual coherence, as compared to controls.

These observations suggest reorganization in the dorsal visual stream in WS when processing 3D SFM stimuli which may indicate that different cognitive strategies are employed by these patients to reach visual coherence. Importantly, we found evidence for the presence of different sub-bands (20-40Hz / 60-90Hz) within the gamma range which can be dissociated concerning the respective role on the coherent percept formation, both in typical and atypical development.

Introduction

Williams Syndrome (WS) is a clinical model of dorsal stream vulnerability and impaired visual integration, in line with what was demonstrated in the previous chapters. This rare genetic neurodevelopmental disorder involves a distinct cognitive profile of relative weaknesses and strengths and is an important model of impaired visual integration and coherence (Bellugi et al., 2000; P. P. Wang, Doherty, Rourke, & Bellugi, 1995). Accordingly, these patients exhibit a tendency to focus on parts or details of an image and consequently fail in integrating local and global levels of analysis such as in hierarchical figures (Bernardino et al., 2012, described in chapter 3). Moreover, the presence of visuospatial impairments along with motion coherence deficits has been described as the hallmark in this condition (Atkinson et al., 2006; Bellugi et al., 2000). A neural correlate for such developmental deficits has been corroborated by structural and functional imaging data showing dorsal visual pathway vulnerability (for further characterization of dorsal stream function, please see Chapter 1) (Eckert et al., 2006; Eckert et al., 2005; Jackowski et al., 2009; Meyer-Lindenberg et al., 2004; Meyer-Lindenberg, Mervis, & Berman, 2006; Mobbs, Eckert, Menon et al., 2007; A. L. Reiss et al., 2004; A.L. Reiss et al., 2000). As a whole, these evidences suggest WS as a representative model of impaired visual integration and coherence associated with dorsal visual stream dysfunction.

The magnitude of visual coherence deficits has been well documented in WS by behavioural studies focusing on 2D and 3D motion coherence, requiring the integration of local signals into object percepts (Atkinson et al., 2003; Atkinson et al., 2006; Castelo-Branco et al., 2007; Mendes et al., 2005). Our previous behavioural study (Mendes et al., 2005) demonstrated impairments in 3D structure-from-motion (SFM) perception in WS, into a higher extent than those found in 2D motion tasks.

The perception of 3D SFM objects requires local-global integration given that the 3D shape can only be extracted from dot moving patterns by integrating motion cues over time. The object is physically nonexistent when the dots are not moving. It is, therefore, important to integrate all local perceptual features and motion cues to achieve coherent holistic perception (a form of perceptual binding because the perception of an object based on dot motion requires correlation). Functional magnetic resonance imaging (fMRI) studies have shown that dorsal parietal regions are involved in the perception of 3D SFM objects (Kriegeskorte et al., 2003; Murray, Olshausen, & Woods, 2003). Our previous EEG and fMRI results do corroborate the notion that integration across dorsal and ventral pathways is

required for SFM perception (Graewe, De Weerd, Farivar, & Castelo-Branco, 2012; Graewe, Lemos et al., 2012). 3D SFM paradigms are, therefore, of particular interest in the study of dorsal stream vulnerability based on coherent holistic perception.

This paradigm is, for that reason, suitable for the study of neurophysiological correlates of 3D visual integration in WS. There are, to our knowledge, no prior EEG/ERP studies addressing this issue, in particular in which concerns general models for holistic perception. A previous ERP study on perception of flat static photographic faces in WS did not require coherence and showed behavioural differences in a one to back face matching task (D. L. Mills et al., 2000). These results are interesting because face processing involves mainly the ventral visual stream which has been described as relatively preserved in WS. By adding 3D coherence to the paradigm we are able to address how dorsal-ventral integration helps solving 3D visual coherence.

Visual coherence and a number of cognitive processes have been related to gamma-band activity which has been interpreted as reflecting feature binding by integrating the different visual features to produce a coherent object representation (Singer & Gray, 1995). Indeed, the neural mechanisms underlying this process have not been clearly defined and different sub-bands within the gamma-band range may have distinct functional significance (Castelo-Branco, Neuenschwander, & Singer, 1998).

Importantly, our paradigm may represent a useful model to elucidate whether patterns of gamma-band oscillations (20-90Hz) represent a neural correlate of perceptual coherence and binding, in particular, in which concerns percept formation and/or object representation (Singer, 2001; Singer & Gray, 1995). This may also provide a mechanism for clinically impaired visual coherence in neuropsychiatric disorders given the available evidence for perception related gamma-band abnormalities in pathologies of impaired coherent perception such as Autism, Attention Dysfunction Hyperactivity Disorder, Alzheimer's disease and Schizophrenia (Brown, Gruber, Boucher, Rippon, & Brock, 2005; Grice et al., 2001; Koenig et al., 2005; Lee, Williams, Breakspear, & Gordon, 2003; Uhlhaas & Singer, 2006; Yordanova, Banaschewski, Koley, Woerner, & Rothenberger, 2001). Gamma-band activity is often assumed to be associated with successful performance on perceptual coherence tasks and to be reduced in neurodevelopmental disorders but this view is not consensual and, in fact, previous studies reported both increases and decreases on gamma-band oscillations in neuropsychiatric conditions (Herrmann & Demiralp, 2005; Uhlhaas & Singer, 2006). This controversy may be explained by the fact that different sub-bands within the gamma-band range are frequently reported without a detailed analysis of

their respective role on the visual percept formation. Moreover, different task demands may lead to different findings which are not comparable across studies.

Here, we aimed at characterizing the neural underpinnings of 3D coherent perception in a representative model of impaired visual integration and coherence associated with dorsal stream dysfunction. For this purpose, we used a 3D SFM integrative task in which the depth level was parametrically modulated. Our investigation of electrophysiological neural correlates of coherent perception in this clinical model of dorsal stream dysfunction addressed the potentially distinct functional role of different sub-bands of gamma oscillations in the construction of coherent percepts.

Methods

Participants

The WS participants included in this study belong to a larger cohort from our previous studies (Bernardino et al., 2012; Bernardino, Mouga, Castelo-Branco, & van Asselen, 2013, described in chapters 3 and 4, respectively) and were selected based on age (≥ 15 years of age) and on the ability to cooperate in the EEG acquisition. We studied 9 patients with WS aged between 15 to 37 years (mean \pm SE = 21.44 ± 2.30) participated in this study. All patients were diagnosed based on clinical and genetic criteria (through fluorescence in situ hybridization analysis), as described in Chapter 3. The parents of the WS participants completed the Social Communication Questionnaire to exclude co-morbidity with Autism Spectrum Disorders (ASD) (Rutter et al., 2003). The scores were below 15, which is the positive cut-off for ASD. None of the WS participants was diagnosed with Attention Dysfunction Hyperactivity Disorder (ADHD) or was taking medication to control for attention and behavioural problems. All WS patients underwent a complete ophthalmologic examination performed by an experienced ophthalmologist (E.S.), including best-corrected visual acuity (Snellen optotypes), complete oculomotor examination, stereopsis evaluation using the Randot test, slit lamp examination of anterior chamber structures and fundus examination. No abnormalities that could affect vision were identified.

The control group included 8 control participants aged between 15 to 34 years (mean \pm SE = 21.89 ± 2.40) who were matched for chronological age (Mann-Whitney U test, $p > 0.05$), gender and handedness with the WS group. In each group there were two participants who demonstrated left-hand dominance. Healthy control participants had no history of

psychiatric and neurologic pathologies and were not taking medication for depression. They had normal or corrected-to-normal vision and were naïve regarding the testing procedures.

The participants included in the study received the Portuguese adapted version of the Wechsler Intelligence Scale for Children – 3rd edition (WISC-III) (Wechsler, 2003) or the Wechsler Adult Intelligence Scale– 3rd edition (WAIS-III) (Wechsler, 2008), according to the participant’s age. One control participant was unavailable to complete the IQ assessment. The assessment of handedness was performed based on the Edinburgh Handedness Inventory (Oldfield, 1971). The demographic characteristics of the patient and control groups are summarized in Table 5.1. Written informed consent was obtained from parents of participants or, when appropriate, the participants themselves. The study was conducted according to the declaration of Helsinki and was approved by the local Ethics Committees of the Faculty of Medicine of Coimbra.

Table 5.1. Characteristics of clinical and control groups

	WS (n=9)		Control (n=8)	
	Mean (SE)	Range	Mean (SE)	Range
Chronological Age (years)	21.44 (2.30)	15-37	21.89 (1.61)	15-34
FSIQ (WISC-III or WAIS-III)	53.94 (2.01)	42-75	118.57 (3.26)	106-129
Handedness (left: right)	2:7		2:6	
Gender (masculine: feminine)	4:5		4:4	

NOTE. WS = Williams Syndrome group; Control= control group; FSIQ = Full-scale intellectual quotient; WISC-III = Wechsler Intelligence Scale for Children, 3rd. ed.; WAIS-III = Wechsler Adult Intelligence Scale, 3rd ed; SE= Standard Error of the mean.

Materials and Procedure

During the experiment, participants were tested in a darkened, acoustically and electrically shielded cabin. Participants were seated in a comfortable chair and were positioned at a distance of ~ 120cm from the computer screen. The stimuli subtending ~13° horizontally and ~10° vertically were delivered using the software package Presentation (Neurobehavioral systems) and were presented in the centre of a CRT monitor screen (1024*768 with a refresh rate of 60Hz). The stimuli consisted of videos of SFM defined

faces with 980ms of duration (for further details, see Farivar et al., 2009). In the present study, depth manipulation was performed by showing videos of SFM defined faces at three different depth levels. The depth levels were parameterized in terms of anterior-posterior range in which full, intermediate and flat depth conditions had 10%, 60% and 90% less depth, respectively, using the posterior plane as a reference (see Figure 5.1A and C). The participants viewed a fixation cross followed by the SFM animation. The three depth level conditions were randomly presented and participants were required to indicate, with a button press, after stimulus offset, if they identified a face or not (see Figure 5.1B). This behavioural task also ensured that participants were able to maintain attention on the visual stimuli throughout the EEG recording session. Participant underwent 100 test trials for each task condition performing a total of 300 test trials which were divided in four blocks. Twelve learning trials were administered and the practice phase was repeated whenever necessary to ensure full understanding of the task.

In a control task within the same experiment, in which participants were required to discriminate face stimuli from non-face stimuli, we analyzed the average number of False Positives (Mean \pm SE= 0.12 \pm 0.05 for WS participants and Mean \pm SE= 0.05 \pm 0.04 for control participants) and False Negatives (Mean \pm SE= 0.17 \pm 0.07 for WS participants and Mean \pm SE= 0.01 \pm 0.007 for control participants) of both groups. We can therefore conclude that participants had very low error rates in catch trials.

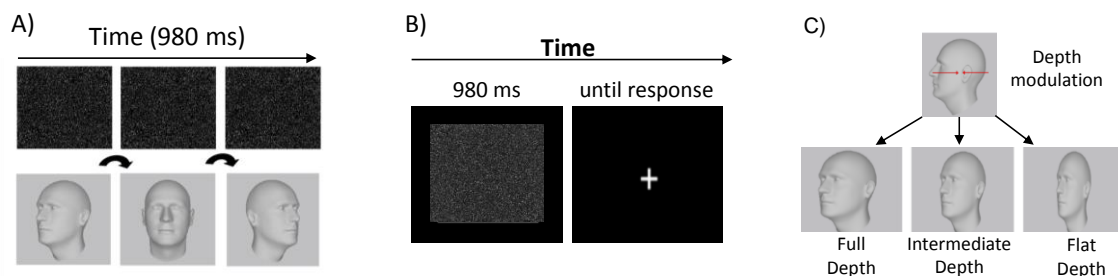


Figure 5.1. Stimuli and paradigm (adapted from Graewe, Lemos et al., 2012). A) SFM faces rotated from left to right in one cycle and were shown during 980 msec. B) Stimuli were presented randomly at one of the 3 depth levels separated by a fixation period during which the participants had unlimited time for response; C) The depth modulation resulted in SFM stimulus conditions with 3 different depth levels (full, intermediate and flat depth) parameterized in terms of anterior-posterior range. **NOTE.** The images of the heads included in the figure just illustrate the structure in the SFM stimuli and do not represent (because they are physically absent and not visible in static images) the exact percept during the movies' presentation.

Electrophysiological Recording

Continuous EEG data were recorded using the NeuroScan SynAmps 2 system (64 channel Quick-Cap). The recording was digitized at a 2kHz sampling rate with an active input range of ± 200 mV per bit and on-line low-pass filter of 500 Hz. The electrooculogram (EOG) was monitored via electrodes positioned above and below the left eye (in line with the pupil) (VEOG) and electrodes placed at the outer canthus (HEOG) in both left and right eyes, in order to reject artefacts due to blinking and eye movements. No notch filters were used and impedances of each electrode were kept below 10 k Ω (electrodes with higher impedances were marked as 'bad'). Recordings were made with all electrodes referenced to one reference electrode located close of CZ and data for each run were saved and processed offline.

Data processing and analysis

The recorded data were processed using the Scan 4.5 Edit Software (Neuroscan). The continuous data files were digitally low- and highpass filtered (at 30Hz, 24dB/oct and 1Hz, 12dB/oct, respectively). All the filtering was performed using the Zero Phase Shift option available in the Scan 4.5 Edit Software. The artefact rejection were performed and epochs with amplitudes exceeding ± 75 μ V (with $>80\%$ of the trials accepted for further processing) were removed in all the electrodes used for the analysis. The recorded files were then segmented into epochs (-100 to 500 ms) locked to stimulus onset. The epochs were baseline corrected based on the time interval (-100 to 0 ms) before stimulus onset. The epochs of each stimulus type were averaged and Event Related Potentials (ERP) were obtained for each depth level.

For the analysis, four different clusters of electrodes were defined adapted from (Graewe, De Weerd et al., 2012) namely: Occipital, Occipito-Temporal, Occipito-Parietal and Parietal, as is illustrated in Figure 5.2. The Occipital cluster included the O1, OZ and O2 electrodes, the Occipito-Temporal cluster is constituted by the TP7, CP5, P7, P5, PO7, TP8, CP6, P6, P8 and PO8 electrodes, the Occipito-Parietal cluster comprised the PO5, PO3, POZ, PO4 and PO6 electrodes, and, finally, the Parietal cluster included the CP3, CP1, P3, P1, CP2, CP4, P2 and P4 electrodes. We segmented the experimental timeline (from 80ms to 280ms) in 20ms windows. For each time window, the mean amplitude value was extracted. This procedure was performed for each subject (WS and Controls) and depth condition.

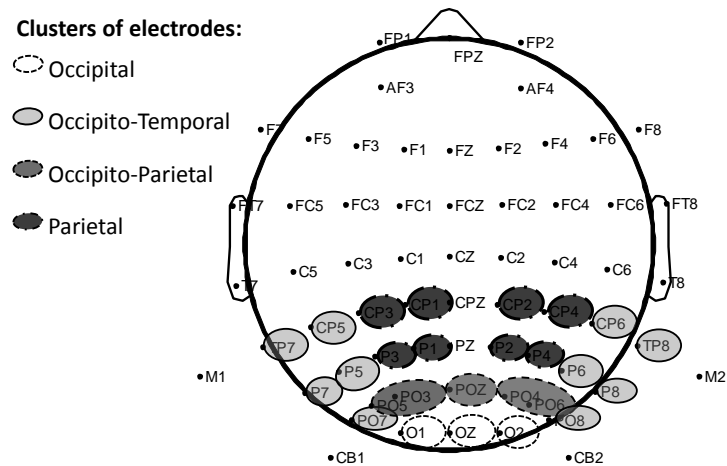


Figure 5.2. Clusters of electrodes. Illustration of the regional clusters of electrodes defined for the analysis: Occipital cluster (O1, OZ, O2), Occipito-Temporal cluster (TP7, CP5, P7, P5, PO7, TP8, CP6, P6, P8, PO8), Occipito-Parietal cluster (PO5, PO3, POZ, PO4, PO6) and Parietal cluster (CP3, CP1, P3, P1, CP2, CP4, P2, P4).

Source Localization

Source localization analysis was performed by Curry V5.0 software (Neuroscan) on a realistic head model. Current source density (CSD) computes a local current pattern on the cortex that explains the recorded EEG at a certain time point. Group average ERP data of each condition was co-registered with anatomical MR data using landmarks and applying standard xyz coordinates of the electrode positions and was then used for source reconstruction. For the source estimation, standard anatomical MR data were used to create the boundary element model (BEM). The CSD source localization was applied on 50 to 300ms data window based in sLORETA (standardized low resolution brain electromagnetic tomography) method (Pascual-Marqui, Michel, & Lehmann, 1994). Current density maps were constructed making no assumption regarding the number or location of active sources (for statistical details, see below).

Independent Component Analysis

After pre-processing the EEG data, an independent component analysis (ICA) was applied for each condition dataset. ICA was performed in Curry V5.0 software (Neuroscan). The main components were visually inspected and the components corresponding to P100, N170 and P200 were considered for final analysis. The projected power accounted for (ppaf) by each component was calculated (for additional statistics, see below).

Time-frequency Analysis

For time-frequency analysis, the continuous data files were digitally high-pass filtered at 1 Hz, 12dB/oct and low-pass filter at 100 Hz, 24dB/oct to focus the modulations of activity in the gamma-band range using a finite impulse response filter. In order to perform signal “correction” of eye movement related artefacts we computed independent component analysis (ICA) based on all electrodes (including 4 EOG channels) as performed in Keren, Yuval-Greenberg & Deouell (2010). We identified blinks and other ocular artefact components based on amplitude criteria of $\pm 75 \mu\text{V}$ and its relation to EOG channels peaks. The ocular component for saccade potentials attenuation was identified based on the scalp topography of the ICA components (higher activity around the orbits) (Keren et al., 2010).

Data (average referenced) were segmented into epochs (-1000 to 2000ms) locked to the beginning of the stimuli and automatic epoch rejection from EEGLab (version 10.2.5.6) was then applied with an amplitude criteria of $\pm 75 \mu\text{V}$ followed by visual inspection. On average $77.7 \pm 14.8\%$ for controls and $77.4 \pm 9.6\%$ for WS of the epochs remained for further analysis.

Time-frequency analysis was performed as in Uhlhaas, et al. (2006) and was carried out in Matlab® across the distinct defined electrode clusters (Occipital, Occipito-Temporal, Occipito-Parietal and Parietal) for frequencies ranging from 1Hz to 90Hz in steps of 1Hz either for induced or evoked activity (with EOG correction as described above and in Keren, et al. (2010).

Statistical Analysis

For the statistical analysis, nonparametric statistics (Mann-Whitney U tests, Wilcoxon rank sum test) were carried out to avoid biases due to deviations from normality and variance heterogeneity. The Bonferroni-Holms correction for multiple comparisons which strongly controls the family-wise error rate at level alpha was applied when appropriate (Holm, 1979). We performed ICA analysis to obtain an independent data driven statistical decomposition. To assess the significance of the main ICA components for each group, we performed a Generalized linear model regression (GLMfit function from Matlab® Statistics Toolbox, v. R2010a) with ICA component as predictors of the group average ERPs. This enables to find components that explained ERP data from one group and not the other.

Concerning the statistics of source localization, we applied the sLORETA method which yields a statistical value (F-distribution) from which the maximum current densities can be extracted.

All statistical analyses were performed with the IBM SPSS Statistics 19.0 software package and Matlab®.

Results

Behavioural Data

Both WS and control groups showed high detection rates that were matched across depth levels (Full: 88.1%, 97.0%; Intermediate: 77.8%, 89.4% and Flat: 65.0%, 68.6% for WS and controls respectively). Accordingly, although the WS group shows a small tendency for lower detection rates than controls, no significant performance differences were found between the two groups for full, intermediate and flat depth levels (Mann-Whitney tests, $p > 0.05$) on the percentage of identified faces. Therefore, results indicated that the participants were successful in recognizing the SFM defined faces and were matched for stimulus difficulty (see Figure 5.3). A within group depth effect was found both for controls (Friedman test, $p < 0.05$) and patients (Friedman test, $p < 0.05$) indicating that the depth manipulation resulted in significant within group effects in both cases.

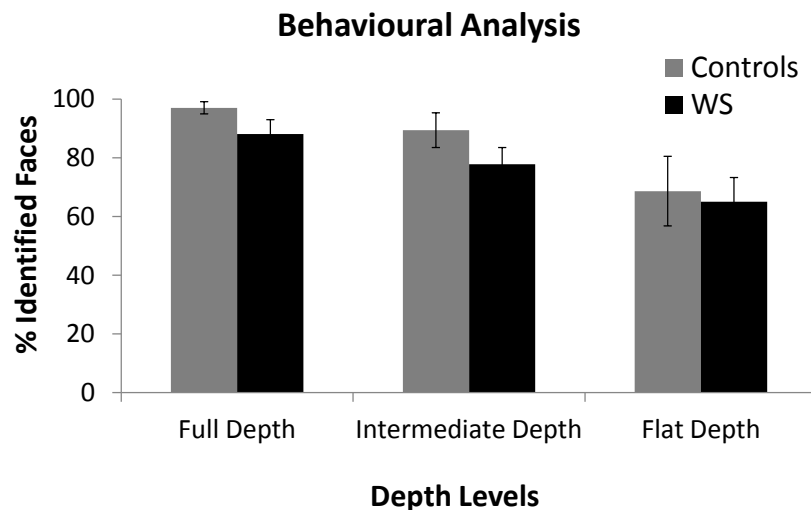


Figure 5.3. Performance across 3D depth levels. Percentage of identified faces for the three depth level conditions in WS and typical controls. The groups did not show significant behavioural differences and both show a within group perceptual depth effect (Friedman test, $p < 0.05$). Bar graphs show the percentage of identified faces and error bars the SEM. **NOTE.** WS = Williams Syndrome group; Controls = chronological age-matched typical developing control group.

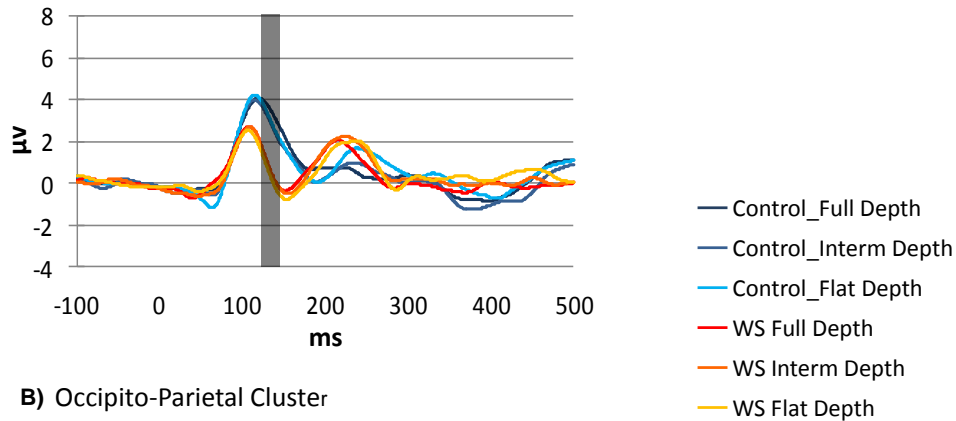
ERP Results

EEG data were analyzed offline for the different trials locked to the beginning of the stimulus. Figure 5.4 illustrates the grand average waveforms for WS and typical controls for all depth conditions. Our results show, in controls, the expected positive P100 early visual component, followed by a negative peak - N170 – the putative face component. Notably, all WS subjects showed lower P100 amplitude than control participants followed by an earlier N150 component and showed a novel component, a positive peak at 200ms - P200- that was virtually absent in controls (for independent validation of this novel component, and statistical testing see below).

We performed statistical analyses (Mann-Whitney tests with Bonferroni-Holms correction to control for the family-wise error rate) on every 20ms time window from 80 to 280ms, for all clusters (Occipital, Occipito-Temporal, Occipito-Parietal and Parietal regions) and depth conditions (Full, Intermediate and Flat). WS and control participants' neural responses differed mostly just before the emergence of the N170 standard face component, for all depth levels (see gray bars in Figure 5.4 A and B). Significant differences between the two groups (Mann-Whitney tests, $p < .05$) were identified for the 120-140ms time window, on full, intermediate and flat depth levels for both Occipito-Temporal and Occipito-Parietal clusters. Additionally, in the 140-160ms time window, groups differed on full, intermediate and flat depth levels only in the Occipito-Parietal electrodes. For all the other defined time windows, we did not find significant group differences.

Source localization analysis is shown in Figure 5.4C for the time windows in which the groups demonstrated different main components (150 and 200 ms). The highest sLORETA F statistical scores are shown. We found dominant parietal sources in controls contrasting with dominant posterior occipital sources in WS consistent across all depth levels.

A) Occipito-Temporal Cluster



B) Occipito-Parietal Cluster

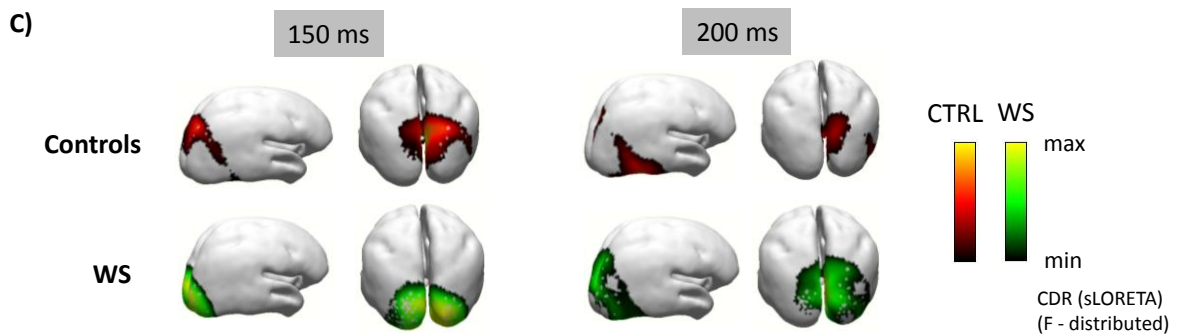
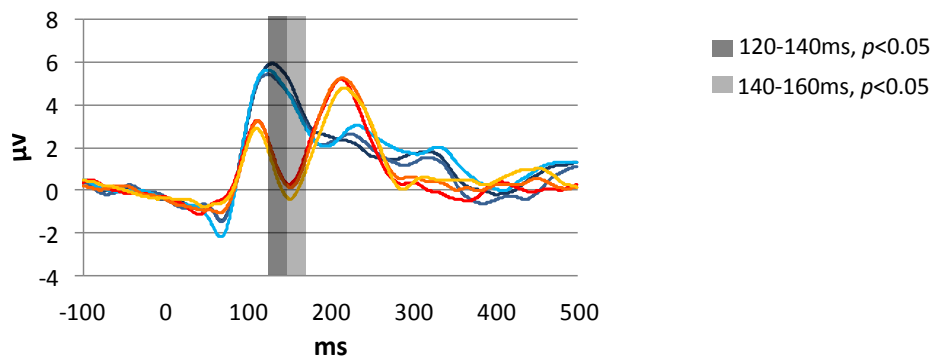


Figure 5.4. Electrophysiological analysis and source localization: WS patients use a distinct neural network to maintain matched performance. Electrophysiological responses for the different depth levels in A) Occipito-Temporal Cluster and B) Occipito-Parietal Cluster. WS and control subject's neural responses differ mostly around the timing before the emergence of the N170 standard face component; C) Source localization for the full depth level in the 150ms and 200ms after the onset of the stimulus. Controls (red scale) show dominant parietal sources around the timing of the emergence of the N170 standard face component whereas WS participants (green scale) show more posterior early level sources. The computed SLR method yields a statistical F score of the current density (colour scale in the figure, plot values above 50% of the maximum current density).

ICA analysis (for details see Methods) allowed us to separate the independent components in the ERP waveforms and to better understand the distinct ERP waveforms found between the groups. ICA analysis revealed distinct main components for each group (see Figure 5.5 data shown for full depth conditions). The first component in the control group accounts for 25.8% of statistically explained signal variance and the first component in the WS group accounts for 30.1% of the variance. This component is almost in antiphase with the main control component and explains the novel ERP late positivity observed in WS. Significance of the main ICA components for each group was determined using General linear model regression with ICA component as predictors of the group average ERPs. We found that the main group components fit their respective average ERPs signal ($p=0.000$) as would be expected since ICA is a decomposition of the ERP signal. Moreover, we found that the first component of the WS group did not significantly fit the first component of the control group ($p=0.323$).

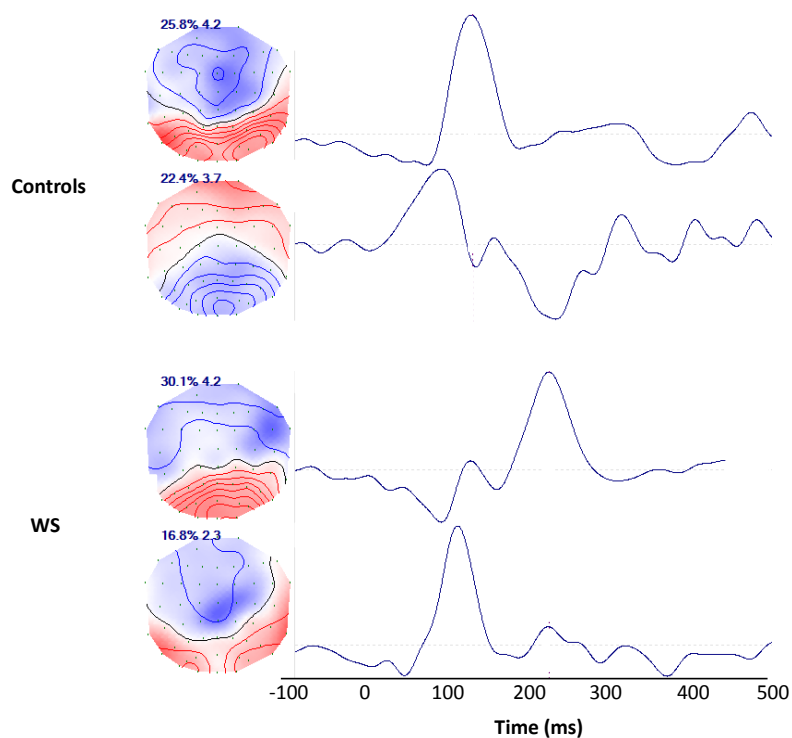


Figure 5.5. Independent component analysis shows distinct main components for WS and controls. Left: 2D maps, scalp distribution of components and statistically explained variance. Right: time courses. The two main ERP components are shown for the full depth level for each group. For additional statistical analyses see Methods and text.

Time-frequency Data Analysis

Regarding the analysis of the time-frequency patterns, we computed pseudo Wigner-Ville (Mecklenbrauker, 1993) time-frequency transforms of single epochs and averaged it across all trials. Therefore, we focused on the so-called ‘induced’ gamma activity which is not phase-locked to stimulus onset (Pantev, 1995).

We found distinct patterns of activity at low and high gamma sub-bands for each group. WS group showed increased activity in the low gamma-band range (20Hz-40Hz), as compared to controls (see Figure 5.6). This effect was observed at all depth levels. Note the slight smearing of time frequency data due to the sliding window aspect of the analysis (Debener et al., 2005).

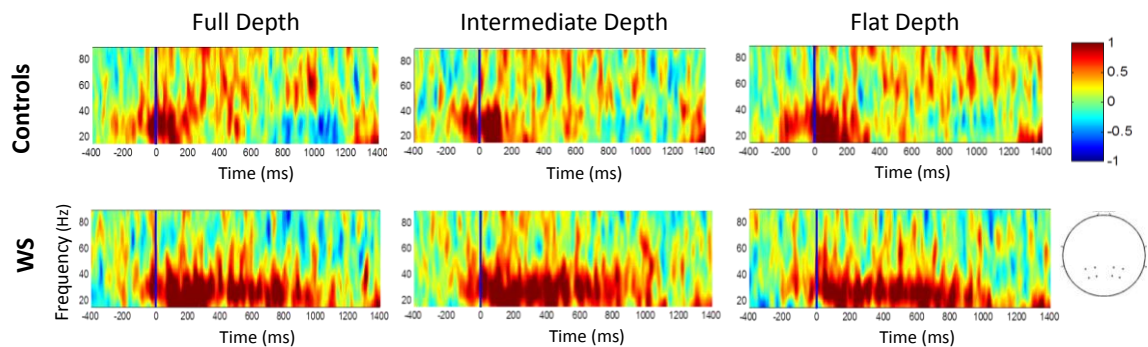


Figure 5.6. Time-frequency analysis during the 3D perceptual integration task. Upper panels: time frequency plots for the three depth levels for the control group; Lower panels: time frequency analysis for the WS group. 0 corresponds to the timing of stimulus appearance. The blue line represents the stimulus onset. Colour codes indicate normalized scores. The analysis depicted here corresponds to the parietal cluster (CP3, CP1, P3, P1, CP2, CP4, P2 and P4 electrodes). Stimulus driven low-gamma oscillations dominate in WS. For further statistical analysis of time frequency maps, see figure 5.7 (lower panel).

This higher modulation in WS for this particular sub-band is relatively sustained across the duration of stimulus presentation particularly in the parietal cluster whereas in the control group is present during the first 200ms of the stimulus presentation. Interestingly, the opposite pattern emerges in the high gamma-band range (60Hz-90Hz) in which WS exhibit decreased gamma-band oscillations, as compared to controls, a pattern that is particularly salient in the occipito-parietal cluster.

In order to confirm these findings we performed statistical comparisons between groups for all depth levels combined with Wilcoxon rank-sum test for each time and frequency points and for the different electrode clusters. Significant group differences were indeed dominant in the two sub-bands of gamma frequencies (20Hz-40Hz / 60Hz-90Hz) in the occipito-parietal and parietal clusters of electrodes (for statistics see figure 5.7 and legend, lower panels, left and right).

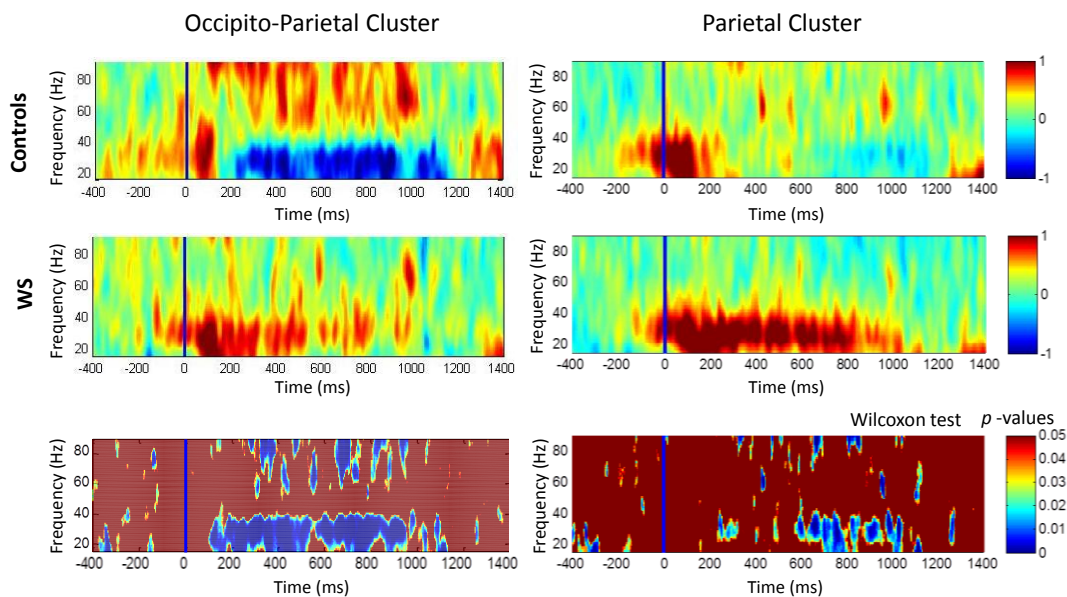


Figure 5.7. Time-frequency analysis shows differential oscillatory pattern across groups. Upper panels: time frequency plots for all pooled depth levels for control and WS groups. The blue line represents the stimulus onset. Colour codes indicate normalized scores. Lower panels: statistical maps of significant group differences across time and frequency in two spatial clusters (occipitoparietal and parietal); colour codes indicate range of p values. The analysis was performed for the parietal (CP3, CP1, P3, P1, CP2, CP4, P2 and P4) and occipitoparietal clusters (PO5, PO3, POZ, PO4 and PO6 electrodes)

Discussion

In the present study, we aimed at characterizing the neurophysiological correlates of coherent perception associated with 3D holistic integration in WS. This is a clinical model of dorsal stream dysfunction and impaired perceptual coherence (Bernardino et al., 2012) which may be helpful to elucidate the role of distinct subtypes of gamma-band activity patterns in the emergence of coherent percepts. Using a 3D coherence task requiring the

perception of 3D SFM defined faces with parametric modulation of depth, we found distinct neural correlates uncovered by ERP data in WS which suggest differential strategies to solve this 3D integration task. Distinctive oscillatory patterning across low and high sub-bands of the gamma range also emerged in the WS group corroborating the presence of different mechanisms underlying the construction of coherent percepts in this clinical model of dorsal stream dysfunction.

These results are relevant for the elucidation of the neural underpinnings of holistic coherent perception since we have recently shown that central coherence was shown to be dominantly impaired in WS at a level even higher than autistic spectrum disorder, irrespective of chronological and mental age (Bernardino et al., 2012). Deficits in holistic integration in WS have been extensively reported (Bellugi et al., 2000; P. P. Wang et al., 1995) and are associated to dorsal visual stream vulnerability (Atkinson et al., 2003; Atkinson et al., 2006; Meyer-Lindenberg et al., 2004).

Our electrophysiological data revealed distinct neural responses to 3D faces in WS. Group differences were particularly evident just before the emergence of the N170 standard face component. Moreover, the WS group showed a novel component peaking positive around 200ms which was further supported by ICA and GLM analysis. These results extend previous evidence of an abnormal electrophysiological pattern of response to static faces in WS (D. L. Mills et al., 2000). Moreover, although face perception ability has been found to be behaviourally preserved in this disorder (Deruelle, Rondan, Mancini, & Livet, 2006; Isaac & Lincoln, 2011), evidence for distinct underlying brain activity patterns have been identified in fMRI studies (Golarai et al., 2010; Mobbs et al., 2004).

Interestingly, neural responses to SFM faces in WS are accompanied by distinct source locations suggesting reorganization within the dorsal stream in this condition. The pattern found for the typically developing control participants is consistent with our previous EEG and fMRI results showing parietal correlates of 3D SFM perception (Graewe, De Weerd et al., 2012; Graewe, Lemos et al., 2012). On the other hand, our results provide further evidence for distinct dorsal stream processing in WS. Indeed, this is in line with the previous literature indicating dorsal visual stream deficits in this disorder (Atkinson et al., 2003; Atkinson et al., 2006; Mendes et al., 2005). The fact that an abnormally distinct electrophysiological pattern was found in a clinical model of dorsal stream dysfunction emphasizes the involvement of this visual pathway in 3D coherent perception and its relation to ventral stream networks more directly associated to face processing (Farivar et al., 2009).

We found a distinctive oscillatory pattern in WS characterized by an increase in low-frequency gamma (20Hz-40Hz) oscillations alongside with a decrease in high-frequency gamma (60Hz-90Hz) oscillations. Taking into account that WS is a representative model of impaired coherent perception, this may help clarifying the role of gamma-band in constructive perception processes. Our results may seem at first glance surprising given the evidence of reduced gamma-band activity in neuropsychiatric disorders, such as Autism and Schizophrenia, under specific task demands (Brown et al., 2005; Grice et al., 2001; Lee et al., 2003). Moreover, electrophysiological studies have provided evidence for gamma-band bursts of neural activity during successful object perception (Herrmann, Frund, & Lenz, 2010; Keil, Muller, Ray, Gruber, & Elbert, 1999; Tallon-Baudry, 2003). However this apparent discrepancy is reconciled by the observations that distinct gamma sub-bands may have different patterning. Our data also provide a novel framework for the interpretation of the previous study of Grice et al. (2001), where authors proposed abnormal gamma-band patterning of visual responses in WS.

Gamma-band activity has been described as playing an important role in a wide variety of processes from basic aspects of sensory processing to higher cognitive and executive functions, such as perceptual integration, attention, working memory and motor-planning (Fries, 2009; Herrmann et al., 2010; Tallon-Baudry & Bertrand, 1999). Nevertheless, the role of gamma-band activity is not yet well established and the wide range of task demands employed and frequency bands analysed does not allow direct comparison across the studies (Fries, 2009; Herrmann et al., 2010; Tallon-Baudry & Bertrand, 1999).

Our results further suggest that distinct frequency components of the gamma-band response may support distinct cognitive functions (Buschman & Miller, 2007; Vidal et al., 2006). This frequency specialization suggests that gamma-band activity reflects multiple mechanisms and that distinct sub-bands may contribute to distinct cognitive processes (Vidal et al., 2006). This evidence was previously reported in studies trying to separate different components of visual perception. Low-frequency gamma activity was associated with visual awareness and attention while high-frequency gamma activity was shown to be modulated in grouping and spatial attention tasks (Vidal et al., 2006; Wyart & Tallon-Baudry, 2008). Accordingly, in the present study, we found modulation of the high-frequency (60-90Hz) gamma-band activity in healthy participants in a 3D integration task. In contrast, WS patients exhibit higher oscillatory activity within the low-frequency gamma range. These findings suggest that WS patients exhibit differential strategies to solve a holistic integration which is further corroborated by the distinct neural correlates uncovered by ERP data

and fMRI evidences of dorsal stream dysfunction in this condition (Jackowski et al., 2009; Meyer-Lindenberg et al., 2004).

Given that some of the genes deleted in WS have been implicated in cortical circuit specification with a direct impact on the phenotype (Castelo-Branco et al., 2007) it is relevant here to consider the molecular mechanisms underlying abnormal oscillatory patterning. Changed gamma-band oscillatory activity has been associated with changes in the γ -aminobutyric acid (GABA) interneuron activity in some neuropsychiatric disorders (Traub, Jefferys, & Whittington, 1999). That is, gamma activity is generated through the interaction of glutamatergic pyramidal cells and GABAergic interneurons. The close link between gamma activity and both dopamine and GABA levels have been proposed to contribute to the positive symptoms of Schizophrenia, epileptic seizures and ADHD (Herrmann & Demiralp, 2005). In addition, gamma oscillation frequency was found to be positively correlated with GABA concentration in primary visual cortex suggesting that interindividual performance on a simple visual task is linked to neurotransmitter concentration (Edden, Muthukumaraswamy, Freeman, & Singh, 2009). To our knowledge, no previous studies investigated GABA levels in WS despite the suggestion of an impairment of dopaminergic pathways as an explanation for the accelerated ageing process found in this condition (Gagliardi et al., 2007). Future studies should further explore mechanisms underlying abnormal patterning of gamma-band activity in WS, given the evidence that GABA levels are altered in other pathologies with visuospatial impairment associated with dorsal stream dysfunction, such as Neurofibromatosis Type I (Violante et al., 2013) and Autism (Coghlan et al., 2012).

In sum, we found evidence for distinct spatiotemporal neural correlates underlying the perception of 3D coherent stimuli in WS. This finding corroborates the involvement of areas along the dorsal visual pathway on the perception of 3D coherent objects and supports the notion of dorsal stream functional redistribution in WS. Importantly, we identified differential patterning of gamma-band oscillatory activity across distinct gamma sub-bands in WS. The lower-frequencies (20-40Hz) were increased whereas the higher-frequencies (60-90Hz) were decreased, suggesting the existence of different cognitive strategies to reach visual coherence in WS. In sum, patterning of different sub-bands within the gamma range can be dissociated during coherent percept formation, in typical and atypical development.

References

- Atkinson, J., Braddick, O., Anker, S., Curran, W., Andrew, R., Wattam-Bell, J., et al. (2003). Neurobiological models of visuospatial cognition in children with Williams syndrome: measures of dorsal-stream and frontal function. *Dev Neuropsychol*, *23*(1-2), 139-172.
- Atkinson, J., Braddick, O., Rose, F. E., Searcy, Y. M., Wattam-Bell, J., & Bellugi, U. (2006). Dorsal-stream motion processing deficits persist into adulthood in Williams syndrome. *Neuropsychologia*, *44*(5), 828-833.
- Bellugi, U., Lichtenberger, L., Jones, W., Lai, Z., & St George, M. (2000). I. The neurocognitive profile of Williams Syndrome: a complex pattern of strengths and weaknesses. *J Cogn Neurosci*, *12 Suppl 1*, 7-29.
- Bernardino, I., Mouga, S., Almeida, J., van Asselen, M., Oliveira, G., & Castelo-Branco, M. (2012). A direct comparison of local-global integration in autism and other developmental disorders: implications for the central coherence hypothesis. *PLoS One*, *in press*.
- Bernardino, I., Mouga, S., Castelo-Branco, M., & van Asselen, M. (2013). Egocentric and allocentric spatial representations in Williams syndrome. *J Int Neuropsychol Soc*, *19*(1), 54-62.
- Brown, C., Gruber, T., Boucher, J., Rippon, G., & Brock, J. (2005). Gamma abnormalities during perception of illusory figures in autism. *Cortex*, *41*(3), 364-376.
- Buschman, T. J., & Miller, E. K. (2007). Top-down versus bottom-up control of attention in the prefrontal and posterior parietal cortices. *Science*, *315*(5820), 1860-1862.
- Castelo-Branco, M., Mendes, M., Sebastiao, A. R., Reis, A., Soares, M., Saraiva, J., et al. (2007). Visual phenotype in Williams-Beuren syndrome challenges magnocellular theories explaining human neurodevelopmental visual cortical disorders. *J Clin Invest*, *117*(12), 3720-3729.
- Castelo-Branco, M., Neuenschwander, S., & Singer, W. (1998). Synchronization of visual responses between the cortex, lateral geniculate nucleus, and retina in the anesthetized cat. *J Neurosci*, *18*(16), 6395-6410.
- Coghlan, S., Horder, J., Inkster, B., Mendez, M. A., Murphy, D. G., & Nutt, D. J. (2012). GABA system dysfunction in autism and related disorders: from synapse to symptoms. *Neurosci Biobehav Rev*, *36*(9), 2044-2055.
- Debener, S., Ullsperger, M., Siegel, M., Fiehler, K., von Cramon, D. Y., & Engel, A. K. (2005). Trial-by-trial coupling of concurrent electroencephalogram and functional magnetic resonance imaging identifies the dynamics of performance monitoring. *J Neurosci*, *25*(50), 11730-11737.
- Deruelle, C., Rondan, C., Mancini, J., & Livet, M. O. (2006). Do children with Williams syndrome fail to process visual configurational information? *Res Dev Disabil*, *27*(3), 243-253.
- Eckert, M. A., Galaburda, A. M., Karchemskiy, A., Liang, A., Thompson, P., Dutton, R. A., et al. (2006). Anomalous sylvian fissure morphology in Williams syndrome. *Neuroimage*, *33*(1), 39-45.
- Eckert, M. A., Hu, D., Eliez, S., Bellugi, U., Galaburda, A., Korenberg, J., et al. (2005). Evidence for superior parietal impairment in Williams syndrome. *Neurology*, *64*(1), 152-153.
- Edden, R. A., Muthukumaraswamy, S. D., Freeman, T. C., & Singh, K. D. (2009). Orientation discrimination performance is predicted by GABA concentration and gamma oscillation frequency in human primary visual cortex. *J Neurosci*, *29*(50), 15721-15726.
- Farivar, R., Blanke, O., & Chaudhuri, A. (2009). Dorsal-ventral integration in the recognition of motion-defined unfamiliar faces. *J Neurosci*, *29*(16), 5336-5342.
- Fries, P. (2009). Neuronal gamma-band synchronization as a fundamental process in cortical computation. *Annu Rev Neurosci*, *32*, 209-224.
- Gagliardi, C., Martelli, S., Burt, M. D., & Borgatti, R. (2007). Evolution of neurologic features in Williams syndrome. *Pediatr Neurol*, *36*(5), 301-306.
- Golarai, G., Hong, S., Haas, B. W., Galaburda, A. M., Mills, D. L., Bellugi, U., et al. (2010). The fusiform face area is enlarged in Williams syndrome. *J Neurosci*, *30*(19), 6700-6712.
- Graewe, B., De Weerd, P., Farivar, R., & Castelo-Branco, M. (2012a). Stimulus dependency of object-evoked responses in human visual cortex: an inverse problem for category specificity. *PLoS One*, *7*(2), e30727.
- Graewe, B., Lemos, R., Ferreira, C., Santana, I., Farivar, R., De Weerd, P., et al. (2012b). Impaired Processing of 3D Motion-Defined Faces in Mild Cognitive Impairment and Healthy Aging: An fMRI Study. *Cereb Cortex*.

- Grice, S. J., Spratling, M. W., Karmiloff-Smith, A., Halit, H., Csibra, G., de Haan, M., et al. (2001). Disordered visual processing and oscillatory brain activity in autism and Williams syndrome. *Neuroreport*, *12*(12), 2697-2700.
- Herrmann, C. S., & Demiralp, T. (2005). Human EEG gamma oscillations in neuropsychiatric disorders. *Clin Neurophysiol*, *116*(12), 2719-2733.
- Herrmann, C. S., Frund, I., & Lenz, D. (2010). Human gamma-band activity: a review on cognitive and behavioral correlates and network models. *Neurosci Biobehav Rev*, *34*(7), 981-992.
- Holm, S. (1979). A simple sequentially rejective multiple test procedure. *Scand J Statist*(6), 65-70.
- Isaac, L., & Lincoln, A. (2011). Featural versus configural face processing in a rare genetic disorder: Williams syndrome. *J Intellect Disabil Res*, *55*(11), 1034-1042.
- Jackowski, A. P., Rando, K., Maria de Araujo, C., Del Cole, C. G., Silva, I., & Tavares de Lacerda, A. L. (2009). Brain abnormalities in Williams syndrome: a review of structural and functional magnetic resonance imaging findings. *Eur J Paediatr Neurol*, *13*(4), 305-316.
- Keil, A., Muller, M. M., Ray, W. J., Gruber, T., & Elbert, T. (1999). Human gamma band activity and perception of a gestalt. *J Neurosci*, *19*(16), 7152-7161.
- Keren, A. S., Yuval-Greenberg, S., & Deouell, L. Y. (2010). Saccadic spike potentials in gamma-band EEG: characterization, detection and suppression. *Neuroimage*, *49*(3), 2248-2263.
- Koenig, T., Prichep, L., Dierks, T., Hubl, D., Wahlund, L. O., John, E. R., et al. (2005). Decreased EEG synchronization in Alzheimer's disease and mild cognitive impairment. *Neurobiol Aging*, *26*(2), 165-171.
- Kriegeskorte, N., Sorger, B., Naumer, M., Schwarzbach, J., van den Boogert, E., Hussy, W., et al. (2003). Human cortical object recognition from a visual motion flowfield. *J Neurosci*, *23*(4), 1451-1463.
- Lee, K. H., Williams, L. M., Breakspear, M., & Gordon, E. (2003). Synchronous gamma activity: a review and contribution to an integrative neuroscience model of schizophrenia. *Brain Res Brain Res Rev*, *41*(1), 57-78.
- Mecklenbrauker, W. F. G. (1993). *The Wigner Distribution - Theory and applications in signal Processing*. Amsterdam: Elsevier.
- Mendes, M., Silva, F., Simoes, L., Jorge, M., Saraiva, J., & Castelo-Branco, M. (2005). Visual magnocellular and structure from motion perceptual deficits in a neurodevelopmental model of dorsal stream function. *Brain Res Cogn Brain Res*, *25*(3), 788-798.
- Meyer-Lindenberg, A., Kohn, P., Mervis, C. B., Kippenhan, J. S., Olsen, R. K., Morris, C. A., et al. (2004). Neural basis of genetically determined visuospatial construction deficit in Williams syndrome. *Neuron*, *43*(5), 623-631.
- Meyer-Lindenberg, A., Mervis, C. B., & Berman, K. F. (2006). Neural mechanisms in Williams syndrome: a unique window to genetic influences on cognition and behaviour. *Nat Rev Neurosci*, *7*(5), 380-393.
- Mills, D. L., Alvarez, T. D., St George, M., Appelbaum, L. G., Bellugi, U., & Neville, H. (2000). III. Electrophysiological studies of face processing in Williams syndrome. *J Cogn Neurosci*, *12 Suppl 1*, 47-64.
- Mobbs, D., Eckert, M. A., Menon, V., Mills, D., Korenberg, J., Galaburda, A. M., et al. (2007). Reduced parietal and visual cortical activation during global processing in Williams syndrome. *Dev Med Child Neurol*, *49*(6), 433-438.
- Mobbs, D., Garrett, A. S., Menon, V., Rose, F. E., Bellugi, U., & Reiss, A. L. (2004). Anomalous brain activation during face and gaze processing in Williams syndrome. *Neurology*, *62*(11), 2070-2076.
- Murray, S. O., Olshausen, B. A., & Woods, D. L. (2003). Processing shape, motion and three-dimensional shape-from-motion in the human cortex. *Cereb Cortex*, *13*(5), 508-516.
- Oldfield, R. C. (1971). The assessment and analysis of handedness: the Edinburgh inventory. *Neuropsychologia*, *9*(1), 97-113.
- Pantev, C. (1995). Evoked and induced gamma-band activity of the human cortex. *Brain Topogr*, *7*(4), 321-330.
- Pascual-Marqui, R. D., Michel, C. M., & Lehmann, D. (1994). Low resolution electromagnetic tomography: a new method for localizing electrical activity in the brain. *Int J Psychophysiol*, *18*(1), 49-65.

- Reiss, A. L., Eckert, M. A., Rose, F. E., Karchemskiy, A., Kesler, S., Chang, M., et al. (2004). An experiment of nature: brain anatomy parallels cognition and behavior in Williams syndrome. *J Neurosci*, *24*(21), 5009-5015.
- Reiss, A. L., Eliez, S., Schmitt, J. E., Straus, E., Lai, Z., Jones, W., et al. (2000). IV. Neuroanatomy of Williams syndrome: a high-resolution MRI study. *J Cogn Neurosci*, *12 Suppl 1*, 65-73.
- Rutter, M., Bailey, A., & Lord, C. (2003). *Social Communication Questionnaire*. Los Angeles: Western Psychological Services.
- Singer, W. (2001). Consciousness and the binding problem. *Ann N Y Acad Sci*, *929*, 123-146.
- Singer, W., & Gray, C. M. (1995). Visual feature integration and the temporal correlation hypothesis. *Annu Rev Neurosci*, *18*, 555-586.
- Tallon-Baudry, C. (2003). Oscillatory synchrony and human visual cognition. *J Physiol Paris*, *97*(2-3), 355-363.
- Tallon-Baudry, C., & Bertrand, O. (1999). Oscillatory gamma activity in humans and its role in object representation. *Trends Cogn Sci*, *3*(4), 151-162.
- Traub, R. D., Jefferys, J. G., & Whittington, M. A. (1999). *Fast oscillations in cortical circuits*. Cambridge: MIT press.
- Uhlhaas, P. J., Linden, D. E., Singer, W., Haenschel, C., Lindner, M., Maurer, K., et al. (2006). Dysfunctional long-range coordination of neural activity during Gestalt perception in schizophrenia. *J Neurosci*, *26*(31), 8168-8175.
- Uhlhaas, P. J., & Singer, W. (2006). Neural synchrony in brain disorders: relevance for cognitive dysfunctions and pathophysiology. *Neuron*, *52*(1), 155-168.
- Vidal, J. R., Chaumon, M., O'Regan, J. K., & Tallon-Baudry, C. (2006). Visual grouping and the focusing of attention induce gamma-band oscillations at different frequencies in human magnetoencephalogram signals. *J Cogn Neurosci*, *18*(11), 1850-1862.
- Violante, I. R., Ribeiro, M. J., Edden, R. A., Guimaraes, P., Bernardino, I., Rebola, J., et al. (2013). GABA deficit in the visual cortex of patients with neurofibromatosis type 1: genotype-phenotype correlations and functional impact. *Brain*.
- Wang, P. P., Doherty, S., Rourke, S. B., & Bellugi, U. (1995). Unique profile of visuo-perceptual skills in a genetic syndrome. *Brain Cogn*, *29*(1), 54-65.
- Wechsler, D. (2003). *Manual for the Intelligence Scale for Children*. Lisbon: Cegoc-Tea.
- Wechsler, D. (2008). *Manual for the Intelligence Scale for Adults*. Lisbon: Cegoc-Tea.
- Wyart, V., & Tallon-Baudry, C. (2008). Neural dissociation between visual awareness and spatial attention. *J Neurosci*, *28*(10), 2667-2679.
- Yordanova, J., Banaschewski, T., Kolev, V., Woerner, W., & Rothenberger, A. (2001). Abnormal early stages of task stimulus processing in children with attention-deficit hyperactivity disorder--evidence from event-related gamma oscillations. *Clin Neurophysiol*, *112*(6), 1096-1108.

CHAPTER 6

Functional reorganization of the visual dorsal stream in Williams syndrome as probed by 3D visual coherence:

an fMRI approach

Bernardino, I., Rebola, J., Farivar, R., Silva, E. & Castelo-Branco, M. Functional reorganization of the visual dorsal stream in Williams syndrome as probed by 3D visual coherence (in preparation).

Abstract

Object and depth perception from motion cues involve the visual dorsal stream and are known to be impaired in WS. The behavioural performance in three-dimensional (3D) structure-from-motion (SFM) tasks was shown to be disrupted and electrophysiological neural substrates of such deficits were demonstrated to be distinctive in this condition, providing evidence for functional reorganization. In SFM perception, motion and depth need to be first extracted in the dorsal stream to allow object categorization which is mediated by the ventral stream. Such interplay justifies the use of SFM paradigms to understand dorsal-ventral integration of visual information. WS represents a privileged model to investigate these matters because of the well known dissociation in dorsal (impaired) vs. ventral visual stream (relatively preserved) function. In the current fMRI study, we assessed dorsal and ventral visual stream function by using a performance matched 3D SFM object categorization task. We found evidence for substantial reorganization of the visual dorsal stream in WS with relatively spared ventral stream patterns, as assessed by whole brain ANOVA Random Effects Analysis (ANOVA RFX). Individuals with WS recruited more medial regions (cuneus, precuneus and retrosplenial cortex) as compared to controls, who showed the expected dorsolateral pattern (caudal intraparietal sulcus and lateral occipital cortex/hMT+). Interestingly, this altered pattern of activation found in WS can already be identified in response to both low-level visual stimuli (static and 2D coherent dots) and images of visual object categories (static faces, places, objects and scrambled). In sum, we found a substantial reorganization of dorsal stream regions in WS in response to 3D SFM, shape and motion perception, with a less affected ventral stream. Our results suggest the existence of a medial dorsal pathway allowing for information rerouting and reorganization in WS. This interpretation is consistent with recent findings suggesting the parallel flow of information in medial (in cuneus) and lateral parts (including hMT+) of the dorsal stream.

Introduction

The detection of motion is one of the most ubiquitous features of visual processing and has been shown to have an important adaptive role in a wide range of species, namely in primates (Hubel & Wiesel, 1968; Newsome & Pare, 1988). Motion detection is particularly important for one of the earliest forms of depth perception, namely the perception of depth from motion cues (Wallach & O'Connell, 1953).

In Williams syndrome (WS), a rare genetic neurodevelopmental disorder characterized by predominant visuospatial impairments, motion detection was found to be disrupted (J. E. Reiss et al., 2005). These impairments have been particularly demonstrated in tasks requiring two-dimensional (2D) and three-dimensional (3D) motion coherence processing (Atkinson et al., 2003; Atkinson et al., 2006). Moreover, object and depth perception from motion cues was also reported as being affected in this condition (Castelo-Branco et al., 2007; Mendes et al., 2005) as assessed through experimental paradigms using 3D structure-from-motion (SFM) stimuli (Wallach & O'Connell, 1953). In this type of stimulus, a large set of dots is coherently moving in such a way that it enables the formation of 3D shape percepts (typically an object or face shape) (Wallach & O'Connell, 1953). Importantly, shape extraction can only be achieved when the dots are moving otherwise it remains invisible. It is therefore essential to integrate motion cues over time to be able to extract 3D shape information. As a result, in this experimental task, motion and shape processing assume complementary properties, in accordance to the widely accepted organization of the visual system (Ungerleider & Mishkin, 1982).

Brain areas along the dorsal visual stream have been reported to be specialized for processing motion information, such as V3A, MT+/V5 (Tootell et al., 1997; Tootell et al., 1995), IPS (Grefkes & Fink, 2005) and V6 (Pitzalis, Fattori, & Galletti, 2013). On the other hand, several areas in the ventral stream are tuned to the preferential processing of specific object categories (LOC, FFA, PPA) (Epstein, Harris, Stanley, & Kanwisher, 1999; Grill-Spector, Kourtzi, & Kanwisher, 2001; Kanwisher et al., 1997).

Since SFM stimuli involve the detection of coherent motion cues to extract 3D shape information, and thus require areas along both dorsal and ventral visual streams, they assume particular interest for the study of impaired coherent perception in WS given the well known dorsal-ventral visual stream dissociation described in this condition.

The visual integration type of ability needed to achieve holistic perception of the whole 3D shape from local information was formerly described as impaired in this disorder

(Bernardino et al., 2012, described in chapter 3). The disrupted visual integration in WS is in line with our previous behavioural findings demonstrating impairments in 3D SFM perception into a larger extent than those found in 2D motion tasks (Mendes et al., 2005). In a previous EEG study (Bernardino, Castelhana, Farivar, Silva, & Castelo-Branco, 2013, described in chapter 5), we investigated the electrophysiological neural underpinnings of 3D coherent perception in WS. We identified atypical neural responses to 3D SFM conditions in WS revealed by distinct ERP waveform components. In particular, a novel positive component peaking around 200msec (P200) was only found for the WS group. To investigate the cortical generators of these distinct neural responses, source localization analyses demonstrated more posterior (occipital) sources in the WS group as compared to controls, who showed more parietal sources. These findings suggest reorganization of responses to 3D SFM stimuli in WS. The neural correlates of such reorganization are best dissected by the superior spatial resolution of fMRI, which is the topic of the current chapter.

In the current study, we do therefore extend our prior EEG/ERP findings by conducting an fMRI study employing a 3D SFM visual integrative task (similar to that described in Chapter 5) in which motion cues drive 3D shape perception. The research literature into the neural correlates of SFM perception in healthy development demonstrated that it is carried out in an extended network of cortical regions spanning the occipital, posterior parietal and also posterior temporal cortices (Graewe, Lemos et al., 2012; James, Humphrey, Gati, Menon, & Goodale, 2002; Klaver et al., 2008; Orban, Sunaert, Todd, Van Hecke, & Marchal, 1999; Paradis et al., 2000; Peuskens et al., 2004). Areas along the intraparietal sulcus (IPS) and the lateral occipital complex (LOC) have been typically identified across studies as showing increased activation in response to SFM objects (James et al., 2002; Klaver et al., 2008; Orban et al., 1999). Less consistent findings have been reported in areas V1, V3A and V5/MT possibly due to distinct task requirements and the fact that these regions underlie lower level motion processing (Murray et al., 2003; Paradis et al., 2000). The identified areas reflect the complementary properties of motion (dorsal pathway) and shape processing (ventral pathway) in SFM perception. Given the reported dorsal vs. ventral dissociation in WS characterized by dorsal stream vulnerability in contrast to relative preservation of ventral stream (Atkinson et al., 2003; Paul et al., 2002), we expected to observe distinct neural networks in WS in response to 3D SFM stimulus characterized by differential activation in dorsal visual regions with possible further

implications for the organization of the ventral visual stream regions that are connected to the dorsal stream. To better assess the nature and specificity of the neural substrates of 3D SFM perception in WS, high-level visual stimuli (static faces, places, objects and scrambled) and simple motion stimuli (2D coherent moving dots and static dots) were also presented to the participants. This approach helps elucidate whether how the neural network recruited by SFM stimulation responds to lower level stimuli and if is also separately recruited for the processing of shape and motion. In summary, we aimed to better understand separate dorsal and ventral visual functioning in WS as well as the cross-talk between these visual streams when their integrated processing is required for 3D SFM perception (Farivar, 2009; Farivar et al., 2009).

Methods

Participants

A total of 20 participants took part in the study, namely 10 WS patients and 10 healthy control participants. Due to exclusion criteria concerning excessive movement during the fMRI acquisition (see details below) or inability to remain inside the scanner until the end of the acquisition, 4 participants (3 WS and 1 control) were excluded from the analysis. As a result, 7 WS patients aged between 15 and 37 years (mean \pm SE = 21.57 ± 3.01) and 9 chronological age matched control participants aged between 15 and 29 years (mean \pm SE = 21.22 ± 1.61) were included for the final analysis.

The WS participants were identified from a large sample of participants who had previously participated in our studies (Bernardino, Castelhana et al., 2013; Bernardino et al., 2012; Bernardino, Mouga et al., 2013, described in chapters 3, 4 and 5). The selection was based on the age (≥ 15 years of age) and on the ability to cooperate in the fMRI acquisition. The diagnosis was confirmed by genetic examinations including the FISH analysis, which demonstrated the typical hemizygous 7q11.23 deletion (~ 1.55 Mb) in all patients. None of the WS participants was diagnosed with Attention Dysfunction Hyperactivity Disorder (ADHD) or was taking medication to control for attention and behavioural problems or depression symptoms. The Social Communication Questionnaire which is a screening test for ASD symptoms was completed by the participants' parents to exclude co-morbidity with ASD (Rutter et al., 2003). The positive cut-off for ASD is 15 and all participants scored below. All WS patients underwent a complete ophthalmologic examination performed by

an experienced ophthalmologist, including best-corrected visual acuity (Snellen optotypes), complete oculomotor examination, stereopsis evaluation using the Randot test, slit lamp examination of anterior chamber structures and fundus examination. No abnormalities that could affect vision were identified. When necessary, the correction to normal vision was ensured using specific eyeglasses compatible with the magnetic field. Given that WS patients exhibited high levels of anxiety and hypersensitivity to the sound, a research staff member worked with each patient so they were previously familiarized with the MRI sounds and were able to attend and perform experimental tasks inside the scanner. A research assistant remained close to patients holding their hand in order to ensure that participants feel safe and stayed calm during the fMRI acquisition.

The control group included 9 typically developing participants who were matched for chronological-age (Mann-Whitney U test, $p > 0.05$), gender and handedness with the WS group. Two WS patients and one control participant demonstrated left-hand dominance as it was measured using the Edinburgh Inventory (Oldfield, 1971). The exclusion criteria for all participants included the presence of psychiatric or neurological pathologies, abnormal ophthalmological conditions and the use of medication for treating depression.

All participants included in the study received the Portuguese adapted version of the Wechsler Intelligence Scale for Children – 3rd edition (WISC-III) (Wechsler, 2003) or the Wechsler Adult Intelligence Scale– 3rd edition (WAIS-III) (Wechsler, 2008), according to the participant's age. The demographic characterization of both groups is summarized in Table 6.1.

This study was conducted in accordance to the Declaration of Helsinki and was approved by the local Ethics Committees of the Faculty of Medicine of the University of Coimbra. Parents of participants or, when appropriate, the participants themselves provided verbal and written informed consent.

Table 6.1. Demographic characteristics

	WS (n=7)		Control (n=9)	
	Mean (SE)	Range	Mean (SE)	Range
Chronological Age (years)	21.57 (3.01)	15-37	21.22. (1.61)	15-29
FSIQ (WISC-III or WAIS-III)	54.29 (4.57)	42-75	120.79 (3.26)	106-136
Handedness (left: right)	2:5		1:8	
Gender (masculine: feminine)	3:4		5:4	

NOTE. WS = Williams Syndrome group; Control= control group; FSIQ = Full-scale intellectual quotient; WISC-III = Wechsler Intelligence Scale for Children, 3rd. ed.; WAIS-III = Wechsler Adult Intelligence Scale, 3rd ed; SE= Standard Error of the mean.

Materials and Procedure

In the present study, an experimental task using 3D SFM stimuli (similar to that described in Chapter 5) was conducted as well as separate runs presenting high-level visual categorical stimuli and simple motion stimuli. The SFM and the high-level visual object runs were presented using Presentation 15.0 software (Neurobehavioural systems) and the simple motion run was presented using Matlab® (R2009b). Stimuli were projected with an LCD projector (SilentVision 6011, Avotec Inc, Florida USA) onto a rear-projection Fujitsu Siemens type screen (1024 x 768, refresh rate 60 Hz). The screen was viewed at a distance of 45.5 cm with an angled mirror positioned on the head-coil and subtended 30.3° width and 23.1° height of visual angle.

During the fMRI acquisition, the participants' eye movements were monitored using a video recording system in order to ensure compliance, safety and verify that wakefulness was maintained (RealEye 5721, Avotec Inc, Florida, USA).

Experimental SFM stimuli and design

The experimental stimuli consisted of videos of SFM defined faces and chairs with the duration of 980ms (for further details, see Bernardino, Castelhana et al., 2013; Farivar et al., 2009; Graewe, De Weerd et al., 2012). Face stimuli consisted of three-dimensional laser-scanned heads from the Max-Planck Face Database and chair stimuli were selected from a chair model database. Both face and chair stimuli were rendered using a unique texture mapping technique (Troje & Bulthoff, 1996) and rotated in a cycle from -22.5 degrees to

22.5 degrees centered at the frontal plane. Stimulus depth information was parametrically manipulated at two different levels resulting in an overall 2 (stimulus category) x 2 (depth levels) design. The depth levels were parameterized in terms of anterior-posterior range in which “full” and “flat” depth conditions had 10% and 90% less depth, respectively, using the posterior plane as a reference (see Figure 6.1B).

The experimental task consisted of 3 separate runs with the duration of approximately 4 minutes each. A slow event-related design was employed in which 4 experimental conditions (Full Face, Full Chair, Flat Face and Flat Chair) were randomly presented. A total of 12 trials per condition were obtained. The participants viewed a fixation cross followed by the SFM animation and were required to press a button whenever the presented stimulus was a face (see Figure 1b). Responses were provided using a button box (right hand index finger) after stimulus disappearance, during the variable inter-stimuli fixation interval (7.5, 10, 12.5 sec).

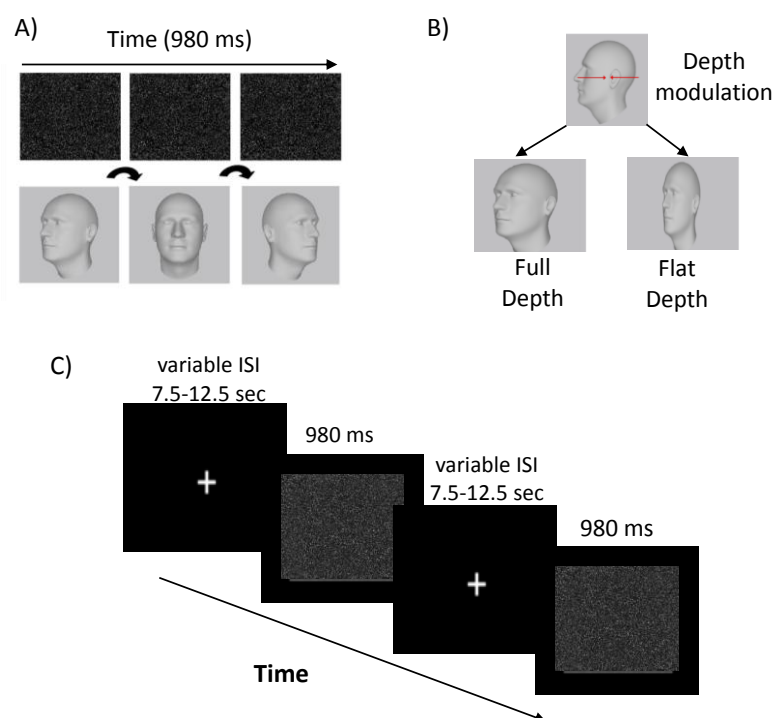


Figure 6.1. Stimuli and paradigm (adapted from Graewe, Lemos et al., 2012). A) SFM faces and chairs rotated from left to right in one cycle and were shown during 980 msec. Object perception is rendered possible by integration of the moving dot pattern, the object being physically absent when the rotation/motion is absent; B) The depth modulation resulted in SFM stimulus conditions with 2 different depth levels (full and flat depth) parameterized in terms of anterior-posterior range. C) Face and Chair stimuli were presented randomly at one of the 2 depth levels separated by a variable 7.5-12.5 sec ISI in which participants were asked to fixate a cross in the centre of the screen. **NOTE.** The images of the heads included in the figure just illustrate the structure in the SFM stimuli and do not represent (because they are physically absent and not visible in static images) the exact percept during the movies' presentation.

High-level visual categorical stimuli and design

During the high-level visual categorical run, subjects viewed static gray-scale photographic images of faces, places (landscapes, skylines), objects (tools, cars, chairs), and scrambled versions of objects (9.5° by 9.5°). Stimuli were presented on a dark background centered at fixation (fixation cross with radius 0.15° in middle of display). Each stimulus category (faces, places, objects, scrambled images) was presented during three pseudo-randomly ordered blocks performing a total of 12 blocks. Each block lasted 20s separated by 10s fixation baseline interval. Images (20 per block) were presented during 800ms with 200ms of inter-stimulus intervals. Subjects were instructed to fixate on each image and were asked to press a button whenever an image was identical to the previous one (“one-back task”). This task was administered to ensure stable attention levels.

Motion stimuli and design

In the motion run, participants viewed coherently moving texture patterns alternated with the same static pattern. Both moving and static patterns (12.6° by 12.6°) were composed of arrays of 600 dots with 0.3° diameter. The dots were white and were shown in a dark background. In the moving patterns, dots could be moving in four directions (left, right, up down) at a constant speed of 5°/s. The run lasted 4.18min and consisted of 30 sec-blocks for each type of stimulus. In each block 6 stimuli with 4.5 sec duration were included and separated by 500ms of inter-stimulus-interval. The blocks were separated by 10 sec periods of fixation. To maintain participants engaged, they were instructed to watch attentively to the centre of the screen.

Imaging data acquisition and pre-processing

Scanning was performed in a 3T Siemens Trio scanner at the Portuguese Brain Imaging Network using a 12 channel head coil. For structural whole brain images two high-resolution T₁ – weighted MPRAGE (magnetization-prepared rapid-acquisition gradient echo) sequences (1x1x1 mm voxel size, 160 slices, repetition time (TR) 2.3s, echo time (TE) 2.98ms, flip angle (FA)9° and field of view (FOV) 256x256) were conducted. Standard T₂*-weighted gradient-echo planar imaging was used for functional task runs (echo planar imaging - EPI, interleaved slice acquisition order, voxel size 2x2x4 mm, 29 slices, TR 2.5s, TE 49ms, in-plane matrix 128x128, FA 90°, FOV=256 mm) covering the entire brain. Functional images for face- and motion localizers were acquired using a gradient echo T₂* -

weighted echo-planar (2.5x2.5x3.5 voxel size, 25 slices, TR 2s, TE 47ms in-plane matrix 102x102, FA 90°, FOV=256mm) .

The data were pre-processed and analyzed using Brainvoyager QX 2.4. We applied slice scan time correction, temporal high-pass filtering (2 cycles per run) and correction for small within-run head movements. Participants exceeding 3 mm were excluded from further analysis (n=2 WS, 1 control). Before group analysis the images were spatially smoothed using 4mm (for experimental SFM runs) and 5 mm (for face/object and motion localizer) full-width-half-maximum Gaussian kernel and then were transformed into Talairach coordinates which have been extensively used in studies in WS (Boddaert et al., 2006; Eckert et al., 2006; Meyer-Lindenberg et al., 2004; O'Hearn et al., 2011).

Data Analysis

All the statistical analyses were performed using IBM SPSS Statistics 19 (IBM, USA, <http://www.ibm.com/software/analytics/spss/>) and the BrainVoyager QX 2.4 software (Brain Innovation, Maastricht, the Netherlands).

Behavioural data

Nonparametric statistics (Mann-Whitney U tests) were carried out for all statistical analyses to avoid biases due to deviations from normality and variance heterogeneity.

Functional data

First, a three-way random-effects (RFX) ANOVA with within-factors “depth” (full vs. flat) and “category” (face and chairs) and between-factor “group” (control vs. WS) was conducted. Then, whole brain statistical maps for group effect were computed. This map revealed areas for which there are fundamental differences between groups irrespective of other factors. Additionally, we computed an interaction “depth” x “group” map to assess regions for which, across groups, flat and full conditions are differentially affected. Resulting *F* maps were thresholded at $p < 0.05$ corrected for multiple comparisons through cluster-level statistical threshold estimation based on Monte Carlo simulation with 1000 iterations. Further analysis of the identified regions was performed with a ROI-based random effects general linear model (GLM) to identify the task conditions which drove the significant RFX ANOVA interaction and group effects. In addition, for each identified region, a ROI-based

ANOVA was performed to assess its response to both high-level visual and motion runs. Post-hoc t -tests were also computed whenever significant group or interaction effects were found. These latter ANOVAs were conducted to assess if the areas of differential processing between groups identified with the SFM stimuli were restricted to that paradigm or already exhibited differences for lower-level stimuli such as static images or unstructured motion.

Additionally, correlation analyses were performed between fMRI SFM-defined objects responses and IQ in order to understand if the intelligence level were correlated with the pattern of activation found in WS. A whole-brain RFX ANOVA with the covariate IQ was computed. The resulting statistical maps did not show any region in which the β weights and the IQ scores correlated significantly.

Results

Behaviour

Behavioural analysis revealed that WS and control groups achieved similar categorization performance in the SFM task for all categorical stimuli and depth conditions ($p > 0.05$, Mann-Whitney U). In sum, both groups are performance-matched under the conditions of our experiment.

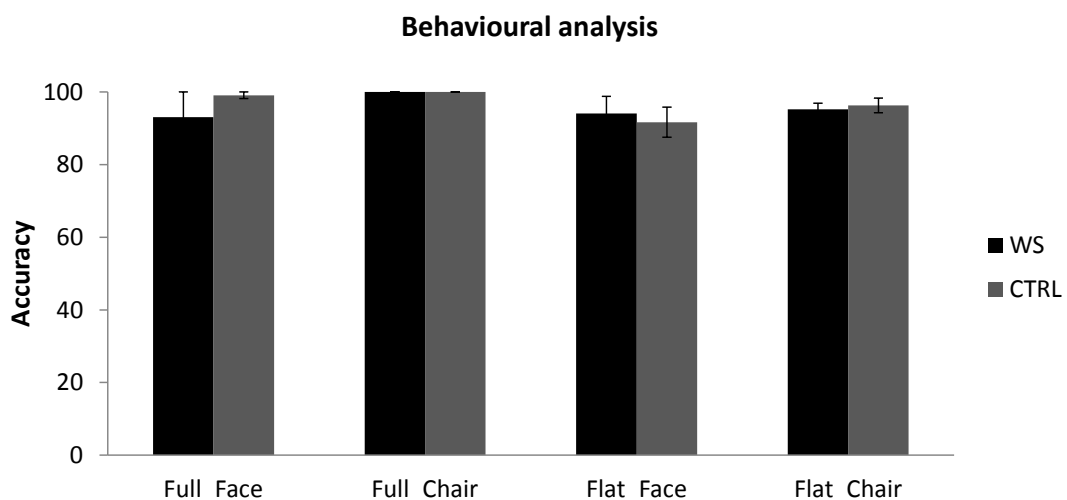


Figure 6.2. Performance across SFM category and depth conditions in WS and typical developing controls. Groups are performance matched under the conditions of our experiment (Mann-Whitney test, $p > 0.05$). **NOTE.** Error bars show the SEM., WS = Williams Syndrome group, CTRL = chronological age-matched typical developing control group.

fMRI: Whole-brain analysis of between group effects in SFM task

The whole-brain RFX ANOVA revealed significant group effects in bilateral caudal intraparietal sulcus (cIPS) and lateral occipital cortex/ hMT+ (larger activation for control subjects, see below) as well as in cuneus, precuneus, and retrosplenial cortex (larger activation for WS subjects, see below). This contrast between the pattern observed in controls and the more medial activation seen in WS is summarized in Table 6.2. ($F \geq 12.84$; $p < 0.05$, corrected for multiple comparisons) and further highlighted in Figure 6.3. There was no significant group x depth interaction effect. ROI-based post-hoc t tests confirmed higher fMRI and more medial activation for WS compared with controls in response to Flat depth (10%) stimuli in the right cuneus, right precuneus, left retrosplenial cortex as well as left middle temporal gyrus (MTG), and left frontal operculum. Interestingly, Full depth (90%) conditions showed increased activation in WS only for the MTG. The same analysis revealed enhanced neural responses for controls compared to WS in bilateral caudal intraparietal sulcus (cIPS) and right lateral occipital cortex (LO/hMT+) for both Full and Flat depth levels (for further details on statistical significance, see Table 6.2). Somatosensory areas were also observed due to sensory stimulation (see Methods for details).

Table 6.2. Whole brain RFX ANOVA analysis: summary of RFX-GLM contrasts, outputs and statistics

	Peak			No of voxels	<i>F</i> value	Full condition		Flat condition	
	Talairach					<i>t</i> value	<i>p</i>	<i>t</i> value	<i>p</i>
	Coordinates	X	Y						
WS>CTRL									
RH cuneus	14	-77	24	1323	14.24	-0.77	0.458	-2.52	0.025
RH precuneus	11	-62	42	2988	25.02	-1.20	0.251	-2.67	0.019
LH middle temporal gyrus (MTG)	-56	9	1542	21.97	-2.68	0.018	-4.40	0.001	
RH retrosplenial cortex	23	-59	15	831	19.46	-1.03	0.321	-1.06	0.309
LH retrosplenial cortex	-65	15	1038	12.84	-0.74	0.474	-2.45	0.028	
LH frontal operculum	13	9	2370	23.23	-1.25	0.232	-3.08	0.008	
CTRL>WS									
RH caudal intraparietal sulcus (cIPS)	23	-50	30	2121	20.64	5.08	<0.001	4.15	<0.001
LH caudal intraparietal sulcus (cIPS)	-65	42	784	17.50	0.392	0.001	2.724	0.016	
RH lateral occipital cortex/ hMT+	29	-74	9	350	13.54	3.871	0.002	2.421	0.030

◀NOTE Brain regions showing significant whole brain RFX-ANOVA group effect ($p < 0.05$, corrected for multiple comparisons) and ROI-based GLM-RFX contrasts for group differences between responses to Full and Flat depth conditions. Negative t tests indicate higher β values for the WS group than for controls. Positive t tests indicate higher β values for the control group than for WS. X, Y and Z represent Talairach coordinates. Significant comparisons are marked in bold. WS= Williams syndrome, CTRL= chronological age-matched typical developing control group, RH=right hemisphere, LH=left hemisphere;

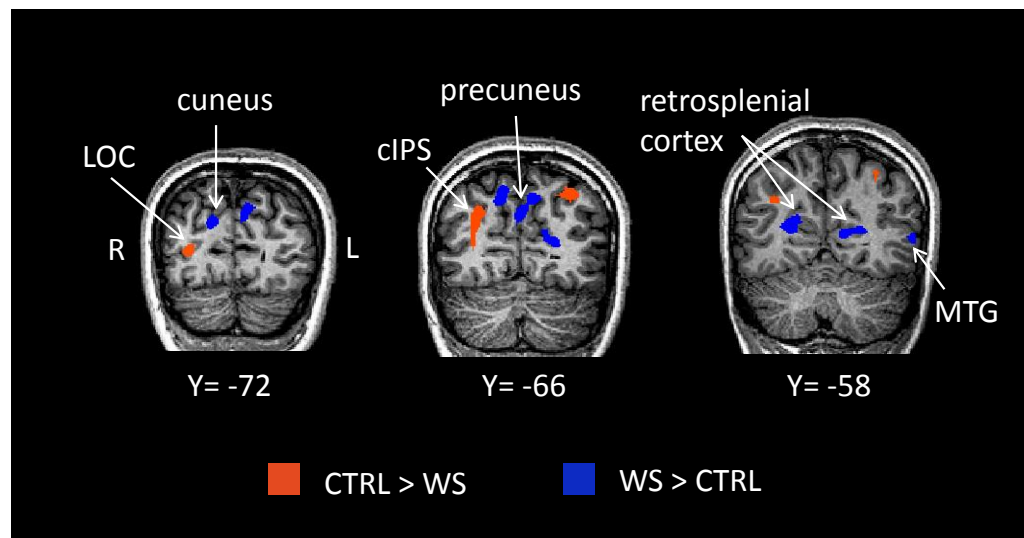


Figure 6.3. RFX ANOVA group effects for SFM categorization. Note the more dorsolateral activation pattern in controls and shift to the midline observed for SFM responses in WS. Statistical maps overlaid on coronal slices of a representative subject. Blue clusters depict regions where activation was higher for individuals with WS than controls. Orange clusters depict regions where activation was lower for individuals with WS than controls. Slice locations are given in Talairach coordinates. NOTE. WS= Williams syndrome, CTRL= chronological age-matched typical developing control group, LO= lateral occipital cortex, cIPS= caudal intraparietal sulcus, MTG= middle temporal gyrus, R= right, L= left.

Interestingly, ventral stream category specific areas traditionally defined by functional localizers did not show significant differences between controls and WS. This may indicate that these areas presented a relatively spared function in WS. However, we may also not identify group difference in these regions because these they are characterized by high anatomical variability or because the small patches of activation did not survive to the rigorous correction for multiple comparisons applied. In order to further elucidate the differences in activation in these areas, we show the pattern of activation in response to SFM stimulation for each group separately (see Fig. 6.4). We observe that individuals with

WS show activation of similar areas along the ventral stream as compared to controls, even though with a more widespread pattern of activation than the one found in the control group and which might deserve a more detailed follow up study.

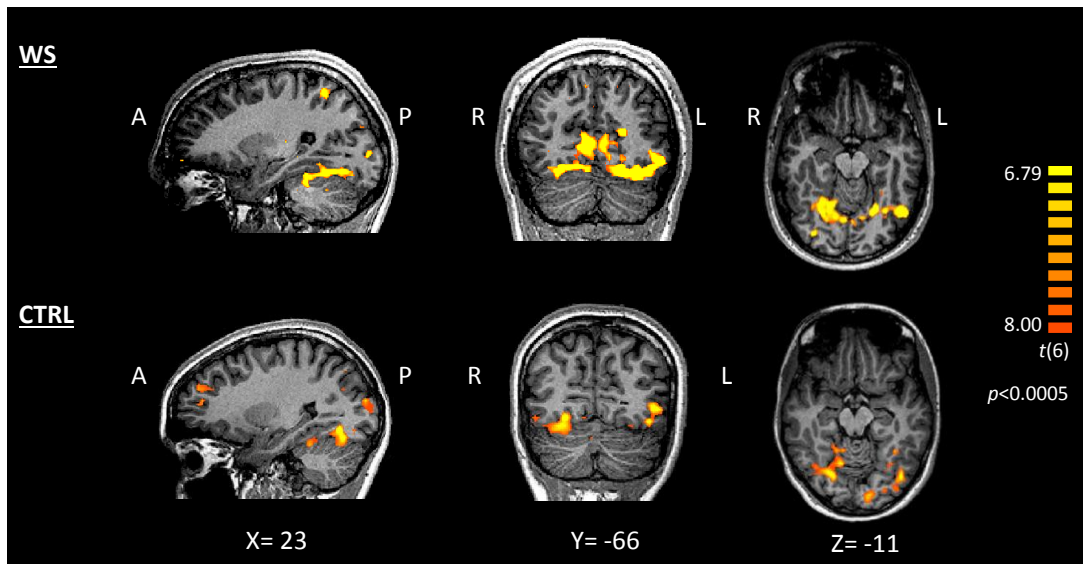


Figure 6.4. Pattern of activation of WS and control groups in the SFM task. Statistical maps overlaid on coronal, sagittal and axial slices of representative WS and control subjects. Slice locations are given in Talairach coordinates. **NOTE.** WS= Williams syndrome, CTRL= chronological age-matched typical developing control group, A=anterior, P=posterior, R= right, L= left.

Since ventral stream category specific localized regions did not show significant differences in the whole brain RFX ANOVA, we did therefore only focus on the regions that showed group differences (listed in Table 6.2 and illustrated in Fig 6.3). These areas can be driven by different processing of motion extraction, shape processing, or other processes exclusive to 3D SFM that require the integration of these features. In this manner, to assess their specificity, we analyzed the responses of these regions to our high-level categorical and simple motion localizer stimuli. We found that, in most cases, the altered response of these areas to 3D SFM stimuli shows already significant between group differences for either (or both) simple motion coherence or static images of high-level categories. Most importantly, the medial (WS) vs. more lateral (controls) occipito-parietal pattern of activity was also replicated for these stimulus conditions.

Regarding the responses to *static images of high-level visual categories* (faces, places, objects, scrambled), we found significant group effects in the right cIPS and in the right LO/hMT+

and significant interaction effect in right precuneus, left MTG, and right LO/hMT+. Post-hoc *t*-test analyses allowed us to investigate the differential response of these regions to these static stimuli categories (faces, objects, places and scrambled). We found increased activation in WS compared to controls in the right precuneus for place stimuli and in the left MTG for face and places stimuli. On the other hand, controls revealed, as expected, enhanced activity in right cIPS and in right LO/hMT+ for all high-level visual categories as compared with WS (see Table 6.3 for further details on statistical significance).

Concerning the *simple motion coherence stimuli* (2D coherent moving dots vs. static dots), we found significant group effect in the right cuneus, bilateral retrosplenial cortex (increased in WS, see below), right cIPS and right LO/hMT+ (decreased in WS) and significant interaction effect in the left MTG, and right retrosplenial cortex. Post-hoc *t*-tests allowed us to investigate the differential response of these regions to the alternating coherent dot motion and static dot stimuli. Accordingly, we found significantly increased activation in WS compared to controls in the cuneus, bilateral retrosplenial cortex in response to coherent 2D motion stimuli and in the right cuneus and left MTG for static dot stimuli. On the other hand, controls revealed, as expected, significantly enhanced activity in right cIPS for motion stimuli and in the right LO/hMT+ for both stimuli as compared with WS (for further details on the statistical significance, see Table 6.4).

Table 6.3. ROI-based ANOVA: High-level visual localizer

	Group effect		Interaction effect		Faces		Objects		Places		Scrambled	
	<i>F</i>	<i>p</i>	<i>F</i>	<i>p</i>	<i>t</i>	<i>p</i>	<i>t</i>	<i>p</i>	<i>t</i>	<i>p</i>	<i>t</i>	<i>p</i>
WS>CTRL*												
RH cuneus	1.10	0.314	0.84	0.478	----	----	----	----	----	----	----	----
RH precuneus	0.84	0.375	3.506	0.024	0.11	0.914	-1.91	0.078	-2.25	0.04	0.496	0.628
LH middle temporal gyrus (MTG)	3.93	0.070	3.49	0.025	-2.81	0.015	-1.55	0.145	-2.50	0.026	-0.85	0.412
RH retrosplenial cortex	0.458	0.510	2.28	0.094	----	----	----	----	----	----	----	----
LH retrosplenial cortex	1.59	0.230	1.48	0.236	----	----	----	----	----	----	----	----
LH frontal operculum	0.65	0.435	1.46	0.240	----	----	----	----	----	----	----	----
CTRL > WS*												
RH caudal intraparietal sulcus (cIPS)	41.230	<0.001	1.62	0.200	5.97	<0.001	6.03	<0.001	7.95	<0.001	5.00	<0.001
LH caudal intraparietal sulcus (cIPS)	3.50	0.084	1.86	0.153	----	----	----	----	----	----	----	----
RH lateral occipital cortex/hMT+	25.70	<0.001	2.641	0.063	3.29	0.005	4.85	<0.001	5.85	<0.001	5.15	<0.001

NOTE. ROI-based ANOVA and GLM-RFX contrasts for group differences between responses to high-level visual categories in the regions revealed by SFM stimulation. Negative *t* tests indicate higher β values for the WS group than for controls. Positive *t* tests indicate higher β values for the control group than for WS. Significant comparisons are marked in bold. WS= Williams syndrome, CTRL= chronological age-matched typical developing control group, RH=right hemisphere, LH=left hemisphere; * evidence from the SFM task analyses;

Table 6.4. ROI-based ANOVA: Motion localizer

	Group effect		Interaction effect		No motion		Motion	
	<i>F</i>	<i>p</i>	<i>F</i>	<i>p</i>	<i>t</i>	<i>p</i>	<i>t</i>	<i>p</i>
WS>CTRL*								
RH cuneus	9.39	0.008	1.53	0.236	-3.53	0.003	-2.96	0.010
RH precuneus	0.95	0.347	0.88	0.365	----	----	----	----
LH middle temporal gyrus (MTG)	3.93	0.069	3.49	0.025	-3.14	0.007	0.28	0.235
RH retrosplenial cortex	6.22	0.026	9.37	0.009	-1.08	0.299	-3.34	0.005
LH retrosplenial cortex	5.39	0.036	3.48	0.083	-1.18	0.133	-3.10	0.008
LH frontal operculum	0.23	0.638	4.25	0.058	----	----	----	----
CTRL > WS*								
RH caudal intraparietal sulcus	5.09	0.041	0.96	0.344	1.82	0.090	2.58	0.022
LH caudal intraparietal sulcus	0.00	0.977	0.27	0.609	----	----	----	----
RH lateral occipital cortex/hMT+	9.43	0.008	0.04	0.940	2.76	0.015	3.11	0.008

NOTE. ROI-based ANOVA and GLM-RFX contrasts for group differences between responses to motion localizer runs in the regions revealed by SFM stimulation. Negative *t* tests indicate higher β values for the WS group than for controls. Positive *t* tests indicate higher β values for the control group than for WS. Significant comparisons are signalled with bold, RH=right hemisphere, LH=left hemisphere, * evidence from the SFM task analyses;

Discussion

The current work is, to our knowledge, the first fMRI study examining dorsal and ventral visual function underlying 3D visual coherent perception in WS. We used 3D SFM stimuli to assess object and depth perception from motion cues and to investigate how dorsal and ventral stream signals are integrated to solve this task. We found that a distinct neural network is recruited in WS in response to the performance matched 3D SFM task as compared to the control group. Under such conditions we could confirm the reorganization hypothesis suggested by our EEG study (Chapter 5) and provide a more trustworthy localization of its neural correlates. Interestingly, WS participants activated more medial parieto-occipital areas (cuneus, precuneus and retrosplenial cortex) when perceiving 3D SFM stimuli whereas control participants preferentially recruited areas in the cIPS and the LO/hMT+.

The areas of increased activation in the control group are in close agreement with the neural correlates of SFM perception found in prior studies. In fact, the cIPS area found in our study (see also, James et al., 2002) is likely to correspond to POIPS (located at the intersection of IPS and parieto-occipital sulcus, Orban et al., 1999), parieto-occipital junction (Klaver et al., 2008; Paradis et al., 2000) or PSA (parietal shape area, Murray et al., 2003). Across studies, this area also exhibited stronger responses for coherent motion than incoherent/random motion. In addition, our findings revealed that in typically developing participants, the cIPS strongly responds to relatively simple motion as well as to high level visual categorical stimuli. These findings are in accordance with the notion that cIPS is involved in analysis of surface pattern orientation, in orientation discrimination tasks and in coding 3D features of objects (Grefkes & Fink, 2005). In fact, Murray and colleagues (2003) found that the area they described as PSA (equivalent to our cIPS) albeit activating for SFM stimuli also responds to 3D line drawings which led authors to suggest the involvement of this area in shape perception.

Importantly, our results indicated that WS participants fail to activate the cIPS area in the same way control participants do. Previous fMRI studies also demonstrated hypoactivation in regions in the dorsal stream immediately adjacent to the IPS in visuospatial tasks (Meyer-Lindenberg et al., 2004; Sarpal et al., 2008). Such findings may be explained by previous evidence of morphological abnormalities in the IPS in this disorder (Meyer-Lindenberg et al., 2006).

The involvement of LO/hMT+ area in SFM perception was also previously reported in typical developing adults (Murray et al., 2003; Orban et al., 1999). In this study, we found increased activation in the control group as compared with the WS group, suggesting that the latter fails in recruiting this area in the lateral part of the dorsal stream to process coherent motion stimuli.

Previous studies have also reported ventral stream correlates of 3D SFM perception in typically developing adults (James et al., 2002; Klaver et al., 2008; Orban et al., 1999). However, it is important to note that we did not find major between group differences in this visual processing stream. This finding suggests that areas along the ventral stream may be relatively preserved in the WS group, at least when compared with the dorsal stream. This is in line with our model of dorsal-ventral dissociation in this disorder, which postulates the dorsal node as the main source of impairment. Indeed, analyzing the pattern of activation for each group, we verified that individuals with WS activated similar areas to the controls within the ventral pathway in response to SFM stimuli. However, we can also observe that the activation in the WS has a more broadly distributed character (including ventral temporo-occipital regions as well as the MTG), whereas the activation in the control group is more circumscribed and possibly indicates higher cortical specialization.

These observations are in accordance with the slightly different pattern of functional activation of ventral areas such as in FFA region observed in the WS group (Golarai et al., 2010; O'Hearn et al., 2011) despite performance on ventral stream tasks achieving normal or near-normal levels (Deruelle et al., 2006; Paul et al., 2002).

Concerning the pattern of brain activation found in the WS group in response to SFM, we verified a surprising occipito-parietal shift of brain activity patterns to the midline cortex, especially pronounced in the cuneus, precuneus and retrosplenial cortex. Interestingly, we observed the involvement of retrosplenial cortex and cuneus in simple motion processing in the clinical group. These results show that the shift to the midline in the areas activating for the SFM stimuli in the WS is already driven by the differential pattern of motion processing in this disorder. These results may be framed into the recent findings of Pitzalis and colleagues (2013) who demonstrated in EEG and fMRI experiments that motion signals flow in parallel from the occipital pole to the medial and lateral motion areas V6 and Mt+, respectively. The fact that WS participants recruit more medial areas (cuneus – V6 and retrosplenial cortex) to process coherent motion suggest that they predominantly use the medial pathway for motion coherence computations whereas controls favour the lateral pathway (hMT+). Thus, our results support the evidence of parallel flow of information in

medial and lateral parts of the dorsal visual stream for motion processing as proposed by Pitzalis and colleagues (2013). Such hypothesis is strengthened by a previous case study of our group that demonstrated damage in dorsal stream areas, V3A and V6, in a patient with unilateral parieto-occipital lesion while area hMT+ showed normal responses to motion contrast (Castelo-Branco et al., 2006). The present study extends these findings to a clinical neurodevelopmental model of dorsal stream vulnerability and suggests that in the presence of dorsal stream dysfunction, the medial pathway is the one preferentially recruited to partly compensate for the resulting impairments. In fact, it may be the existence of this parallel pathway in medial parts of the dorsal stream that facilitates the occurrence of this reorganization in WS.

In sum, the present study investigates dorsal and ventral visual functioning in WS by exploring the neural responses to a 3D SFM task. We found a substantial reorganization of the dorsal visual stream in WS with the pattern of activation in this group (cuneus, precuneus and retrosplenial cortex) following an occipito-parietal shift to the midline as compared to controls (cIPS and LO/hMT+). In contrast, areas along the ventral visual stream in WS appear to exhibit subtle differences in the pattern of activation comparing to that found in the control group which deserves further detailed examination in a follow-up study. Our findings may be interpreted in the light of recent evidence for parallel motion processing in medial (V6) and lateral (hMT+) parts of the dorsal stream (Pitzalis, Bozzacchi et al., 2013).

References

- Atkinson, J., Braddick, O., Anker, S., Curran, W., Andrew, R., Wattam-Bell, J., et al. (2003). Neurobiological models of visuospatial cognition in children with Williams syndrome: measures of dorsal-stream and frontal function. *Dev Neuropsychol*, *23*(1-2), 139-172.
- Atkinson, J., Braddick, O., Rose, F. E., Searcy, Y. M., Wattam-Bell, J., & Bellugi, U. (2006). Dorsal-stream motion processing deficits persist into adulthood in Williams syndrome. *Neuropsychologia*, *44*(5), 828-833.
- Bernardino, I., Castelhana, J., Farivar, R., Silva, E. D., & Castelo-Branco, M. (2013a). Neural correlates of visual integration in Williams syndrome: Gamma oscillation patterns in a model of impaired coherence. *Neuropsychologia*, *51*(7), 1287-1295.
- Bernardino, I., Mouga, S., Almeida, J., van Asselen, M., Oliveira, G., & Castelo-Branco, M. (2012). A direct comparison of local-global integration in autism and other developmental disorders: implications for the central coherence hypothesis. *PLoS One*, *in press*.
- Bernardino, I., Mouga, S., Castelo-Branco, M., & van Asselen, M. (2013b). Egocentric and allocentric spatial representations in Williams syndrome. *J Int Neuropsychol Soc*, *19*(1), 54-62.
- Boddaert, N., Mochel, F., Meresse, I., Seidenwurm, D., Cachia, A., Brunelle, F., et al. (2006). Parieto-occipital grey matter abnormalities in children with Williams syndrome. *Neuroimage*, *30*(3), 721-725.
- Castelo-Branco, M., Mendes, M., Sebastiao, A. R., Reis, A., Soares, M., Saraiva, J., et al. (2007). Visual phenotype in Williams-Beuren syndrome challenges magnocellular theories explaining human neurodevelopmental visual cortical disorders. *J Clin Invest*, *117*(12), 3720-3729.
- Castelo-Branco, M., Mendes, M., Silva, M. F., Januario, C., Machado, E., Pinto, A., et al. (2006). Specific retinotopically based magnocellular impairment in a patient with medial visual dorsal stream damage. *Neuropsychologia*, *44*(2), 238-253.
- Deruelle, C., Rondan, C., Mancini, J., & Livet, M. O. (2006). Do children with Williams syndrome fail to process visual configurational information? *Res Dev Disabil*, *27*(3), 243-253.
- Eckert, M. A., Galaburda, A. M., Karchemskiy, A., Liang, A., Thompson, P., Dutton, R. A., et al. (2006). Anomalous sylvian fissure morphology in Williams syndrome. *Neuroimage*, *33*(1), 39-45.
- Epstein, R., Harris, A., Stanley, D., & Kanwisher, N. (1999). The parahippocampal place area: recognition, navigation, or encoding? *Neuron*, *23*(1), 115-125.
- Farivar, R. (2009). Dorsal-ventral integration in object recognition. *Brain Res Rev*, *61*(2), 144-153.
- Farivar, R., Blanck, O., & Chaudhuri, A. (2009). Dorsal-ventral integration in the recognition of motion-defined unfamiliar faces. *J Neurosci*, *29*(16), 5336-5342.
- Golarai, G., Hong, S., Haas, B. W., Galaburda, A. M., Mills, D. L., Bellugi, U., et al. (2010). The fusiform face area is enlarged in Williams syndrome. *J Neurosci*, *30*(19), 6700-6712.
- Graewe, B., De Weerd, P., Farivar, R., & Castelo-Branco, M. (2012a). Stimulus dependency of object-evoked responses in human visual cortex: an inverse problem for category specificity. *PLoS One*, *7*(2), e30727.
- Graewe, B., Lemos, R., Ferreira, C., Santana, I., Farivar, R., De Weerd, P., et al. (2012b). Impaired Processing of 3D Motion-Defined Faces in Mild Cognitive Impairment and Healthy Aging: An fMRI Study. *Cereb Cortex*.
- Grefkes, C., & Fink, G. R. (2005). The functional organization of the intraparietal sulcus in humans and monkeys. *J Anat*, *207*(1), 3-17.
- Grill-Spector, K., Kourtzi, Z., & Kanwisher, N. (2001). The lateral occipital complex and its role in object recognition. *Vision Res*, *41*(10-11), 1409-1422.
- Hubel, D. H., & Wiesel, T. N. (1968). Receptive fields and functional architecture of monkey striate cortex. *J Physiol*, *195*(1), 215-243.
- James, T. W., Humphrey, G. K., Gati, J. S., Menon, R. S., & Goodale, M. A. (2002). Differential effects of viewpoint on object-driven activation in dorsal and ventral streams. *Neuron*, *35*(4), 793-801.
- Kanwisher, N., McDermott, J., & Chun, M. M. (1997). The fusiform face area: a module in human extrastriate cortex specialized for face perception. *J Neurosci*, *17*(11), 4302-4311.
- Klaver, P., Lichtensteiger, J., Bucher, K., Dietrich, T., Loenneker, T., & Martin, E. (2008). Dorsal stream development in motion and structure-from-motion perception. *Neuroimage*, *39*(4), 1815-1823.

- Mendes, M., Silva, F., Simoes, L., Jorge, M., Saraiva, J., & Castelo-Branco, M. (2005). Visual magnocellular and structure from motion perceptual deficits in a neurodevelopmental model of dorsal stream function. *Brain Res Cogn Brain Res*, 25(3), 788-798.
- Meyer-Lindenberg, A., Kohn, P., Mervis, C. B., Kippenhan, J. S., Olsen, R. K., Morris, C. A., et al. (2004). Neural basis of genetically determined visuospatial construction deficit in Williams syndrome. *Neuron*, 43(5), 623-631.
- Meyer-Lindenberg, A., Mervis, C. B., & Berman, K. F. (2006). Neural mechanisms in Williams syndrome: a unique window to genetic influences on cognition and behaviour. *Nat Rev Neurosci*, 7(5), 380-393.
- Murray, S. O., Olshausen, B. A., & Woods, D. L. (2003). Processing shape, motion and three-dimensional shape-from-motion in the human cortex. *Cereb Cortex*, 13(5), 508-516.
- Newsome, W. T., & Pare, E. B. (1988). A selective impairment of motion perception following lesions of the middle temporal visual area (MT). *J Neurosci*, 8(6), 2201-2211.
- O'Hearn, K., Roth, J. K., Courtney, S. M., Luna, B., Street, W., Terwillinger, R., et al. (2011). Object recognition in Williams syndrome: uneven ventral stream activation. *Dev Sci*, 14(3), 549-565.
- Oldfield, R. C. (1971). The assessment and analysis of handedness: the Edinburgh inventory. *Neuropsychologia*, 9(1), 97-113.
- Orban, G. A., Sunaert, S., Todd, J. T., Van Hecke, P., & Marchal, G. (1999). Human cortical regions involved in extracting depth from motion. *Neuron*, 24(4), 929-940.
- Paradis, A. L., Cornilleau-Peres, V., Droulez, J., Van De Moortele, P. F., Lobel, E., Berthoz, A., et al. (2000). Visual perception of motion and 3-D structure from motion: an fMRI study. *Cereb Cortex*, 10(8), 772-783.
- Paul, B. M., Stiles, J., Passarotti, A., Bavar, N., & Bellugi, U. (2002). Face and place processing in Williams syndrome: evidence for a dorsal-ventral dissociation. *Neuroreport*, 13(9), 1115-1119.
- Peuskens, H., Claeys, K. G., Todd, J. T., Norman, J. F., Van Hecke, P., & Orban, G. A. (2004). Attention to 3-D shape, 3-D motion, and texture in 3-D structure from motion displays. *J Cogn Neurosci*, 16(4), 665-682.
- Pitzalis, S., Bozzacchi, C., Bultrini, A., Fattori, P., Galletti, C., & Di Russo, F. (2013a). Parallel motion signals to the medial and lateral motion areas V6 and MT+. *Neuroimage*, 67, 89-100.
- Pitzalis, S., Fattori, P., & Galletti, C. (2013b). The functional role of the medial motion area V6. *Front Behav Neurosci*, 6, 91.
- Reiss, J. E., Hoffman, J. E., & Landau, B. (2005). Motion processing specialization in Williams syndrome. *Vision Res*, 45(27), 3379-3390.
- Rutter, M., Bailey, A., & Lord, C. (2003). *Social Communication Questionnaire*. Los Angeles: Western Psychological Services.
- Sarpal, D., Buchsbaum, B. R., Kohn, P. D., Kippenhan, J. S., Mervis, C. B., Morris, C. A., et al. (2008). A genetic model for understanding higher order visual processing: functional interactions of the ventral visual stream in Williams syndrome. *Cereb Cortex*, 18(10), 2402-2409.
- Tootell, R. B., Mendola, J. D., Hadjikhani, N. K., Ledden, P. J., Liu, A. K., Reppas, J. B., et al. (1997). Functional analysis of V3A and related areas in human visual cortex. *J Neurosci*, 17(18), 7060-7078.
- Tootell, R. B., Reppas, J. B., Kwong, K. K., Malach, R., Born, R. T., Brady, T. J., et al. (1995). Functional analysis of human MT and related visual cortical areas using magnetic resonance imaging. *J Neurosci*, 15(4), 3215-3230.
- Troje, N. F., & Bulthoff, H. H. (1996). Face recognition under varying poses: the role of texture and shape. *Vision Res*, 36(12), 1761-1771.
- Ungerleider, L. G., & Mishkin, M. (1982). Two cortical visual systems. In D. J. Ingle, M. A. Goodale & R. J. W. Mansfield (Eds.), *Analysis of visual behavior*(pp. 549-586). Cambridge: MIT Press.
- Wallach, H., & O'Connell, D. N. (1953). The kinetic depth effect. *J Exp Psychol*, 45(4), 205-217.
- Wechsler, D. (2003). *Manual for the Intelligence Scale for Children*. Lisbon: Cegoc-Tea.
- Wechsler, D. (2008). *Manual for the Intelligence Scale for Adults*. Lisbon: Cegoc-Tea.

CONCLUDING REMARKS

CHAPTER 7

Discussion and Conclusions

Discussion

In the current thesis a combination of psychophysics, electrophysiological and neuroimaging tools was employed with the purpose to better understand the nature and the extent of dorsal visual pathway dysfunction in Williams syndrome (WS).

The comprehension of dorsal stream impairments in WS benefits from the examination of important cognitive dissociations described in this clinical population. In fact, since the pioneering studies of Bellugi and colleagues, WS cognitive profile was established as comprising a few clear-cut dissociations rendering this genetic condition as a representative model of the modularity of mind perspective (Bellugi et al., 2000; Bellugi et al., 1988a). The intriguing WS cognitive profile is characterized by preserved language and facial perception abilities contrasting with severe visuospatial impairments (Mervis et al., 2000). Within the visuospatial domain a major dissociation regarding local and global information processing emerged and has dominated the research on the WS cognitive profile.

Importantly, the examination of these cognitive dissociations goes hand in hand with the investigation of the functional dichotomy between dorsal and ventral visual pathways at the neural level. Once again, a dysfunction in one pathway (dorsal stream) contrasted with the relative preservation on the other (ventral stream) (Atkinson et al., 1997; Paul et al., 2002). Using a novel approach to the study of dorsal-ventral dissociation in WS, a dichotomy between processing of egocentric and allocentric spatial representations was also explored. In sum, the work presented in this thesis addressed multiple levels of visual processing along dorsal and ventral visual pathways in WS, from the point of view of the aforementioned functional dissociations (lobal-local/ dorsal-ventral/ego-allo) and their interconnections. The implications of the current findings for the understanding of the disease mechanisms underlying visuospatial impairments as well as for the proper understanding of the visual streams functioning will be pointed out in this chapter.

Global-local visual dissociation in WS

The first research question investigated in this work focused on the visual coherence deficits in WS and was addressed in relation to a global-local visual processing dichotomy. It is widely accepted that individuals with WS exhibit a tendency to visually process the parts or the details of an image and fail to construct the whole configuration (Bellugi, Sabo, & Vaid,

1988b). Nevertheless, the influence of perceptual and visuoconstructive task demands on the observed impairments remains to be established (E. K. Farran & Jarrold, 2003). Moreover the distinction between truly global impairment from a merely locally-focused cognitive style remains to be done in the same study, using multiple comparison groups and cognitive models of weak central coherence. The work described in Chapter 3 addressed these points. Given that a detailed focused cognitive style and global visual impairment in the presence of dorsal stream dysfunction has been also described in autism spectrum disorders (ASD) (Uta Frith, 1989; Happe, 1996; Spencer et al., 2000), it was in our opinion mandatory to design an experiment whereby a direct comparison between the two neurodevelopmental conditions could be performed. The results of our study demonstrated the presence of a locally-focused cognitive style in addition to a global processing impairment in both perception and memory conditions, specifically and dominantly in WS. Moreover, visual integration as was measured by our visuoconstructive task was also found to be severely impaired in the WS group. Our results are in line with the hypothesis arguing that individuals with WS have particular difficulty in using spatial relations when integrating parts of an image (E. K. Farran & Jarrold, 2003) as was highlighted in our visuoconstructive task. Indeed, our study provided strong evidence of visual integration deficits in WS unravelling the difficulties of these patients in integrating local information to construct the global configuration.

Surprisingly, the results found in the ASD participants go in the opposite direction under the matched conditions of our experiment, since they demonstrated unexpected general global preference and were able to process visual information at a global level. The fact that visual coherence is more impaired in WS than in ASD suggests that higher levels of impaired visual integration seem to be associated with larger dorsal stream dysfunction. In this study we proposed a new approach to understand visual coherence deficits in WS raising the hypothesis that these impairments may be a marker of dorsal stream dysfunction and are distinctive in WS. This hypothesis is supported by fMRI evidence of reduced activity in occipito-parietal areas in the WS group as compared to the control group in a task using the same Navon hierarchical figures (Mobbs, Eckert, Menon et al., 2007). In sum, this study proposed WS as a clinical model of impaired visual coherence associated with dorsal stream dysfunction.

Egocentric-allocentric dissociation in WS (as a measure of dorsal-ventral dissociation)

The study of dorsal-ventral dissociation has been so far limited to the contrast between behavioural and neuronal responses to visuospatial (dorsal stream) and face recognition (ventral stream) experimental tasks (Meyer-Lindenberg et al., 2004; Paul et al., 2002). This approach is far from optimal since face recognition is highly dependent of motivational features. Motivation to faces is indeed naturally enhanced in individuals with WS given their social phenotype characterized by the drive to socialize even with unfamiliar people and to recognize faces (O'Hearn, Courtney, Street, & Landau, 2009). This fact brings to light the need to investigate dorsal and ventral visual function through multiple levels of visual processing specially those related to functions that have significant impact on the daily life of these patients. An interesting dissociation in this context lies on the dichotomy between egocentric (self-centred) and allocentric (world-centred) spatial frames of reference which are essential for the development of wayfinding and spatial navigation abilities shown to be highly disrupted in this condition.

In the study presented in Chapter 4 we investigated the egocentric (dorsal stream) and allocentric (ventral stream) spatial representations in WS. Surprisingly both egocentric and allocentric spatial processing were found to be impaired in WS in a computerized spatial judgment task. Importantly, in a more ecological paradigm (board task), WS participants achieved similar results to those found in participants with the same intellectual level and non-verbal mental age. This suggests that performance improves when a more ecological approach is used which constitutes an important clue to the development and validation of rehabilitation strategies.

The deficits found in egocentric spatial judgments are in line with the studies reporting dorsal stream dysfunction in WS (Atkinson et al., 2003; Castelo-Branco et al., 2007; Meyer-Lindenberg et al., 2004). The unexpected impairments in the allocentric task conditions are, in turn, in accordance with abnormal activation of hippocampal and parahippocampal formations in WS (Meyer-Lindenberg, Mervis et al., 2005) and point out the existence of atypical functioning within the ventral visual stream. The latter hypothesis is at odds with the traditionally characterization of WS indicating preserved ventral visual stream. It is instead in line with the increasing evidence that areas along the ventral visual stream have a different pattern of activation as compared to normal brain functioning (Golarai et al., 2010; O'Hearn et al., 2011).

This study also suggests the need to analyse the interdependencies of egocentric and allocentric representations reflected in the known interconnections between dorsal and ventral streams. Indeed, it was demonstrated that the allocentric representations develop late in the ontogenesis and based on the egocentric coding (Zaehle et al., 2007). They share some neural sources such as precuneus which was found in our fMRI study (Chapter 6) to exhibit an abnormal pattern of activation in response to visual coherence in WS as compared to the control group. Increased evidence suggested that some dependencies between the two reference frames occur and that they work together to process complex representations of environment (Burgess, 2006). There is a brain area, the retrosplenial cortex, which has been described to be involved in spatial navigation and have an important role in translating information between allocentric and egocentric reference frames (for a review, see Vann, Aggleton, & Maguire, 2009). However, in the WS group, this area was found (in our fMRI study, Chapter 6) to be involved in other cognitive processes such as motion processing. This may suggest that the reorganization within the dorsal visual stream may have impact in the neural mechanisms underlying the interconnections between allocentric and egocentric frames of reference. This point draws attention to the need of studying dorsal-ventral interconnections to comprehensively understand the visuospatial deficits in WS.

Dorsal-ventral dissociation vs. dorsal-ventral integration

The aforesaid findings gather evidence supporting the notion that WS is a clinical model of visual coherence impairment associated with dorsal stream dysfunction (and subtle alterations in the ventral stream). Additionally, the clues into the need to study dorsal-ventral interconnections in order to fully dissect the visuospatial impairments in the WS group, led us to investigate the neural substrates of 3D visual coherence using an experimental paradigm (three-dimensional structure-from-motion - 3D SFM) requiring both dorsal and ventral visual stream involvement. Both EEG and fMRI studies described in Chapter 5 and Chapter 6, respectively, evidenced differential neural correlates underlying 3D object and depth perception from motion cues in WS. This suggests a distinct organization of the neural networks responding to 3D SFM coherence in this condition. More specifically, WS participants showed a more medial (cuneus, precuneus and retrosplenial cortex) pattern of activation contrasting with the healthy participants who exhibited more lateral activations

(cIPS and LO/hMT+) in response to 3D coherent motion, 2D simple motion and high-level visual categories.

The results of our studies can be framed in the context of the recent model proposed by Pitzalis and colleagues (2013) stating the existence of parallel motion processing in medial (V6) and lateral (hMT+) parts of the dorsal stream. Indeed, our EEG and fMRI findings are highly concordant with their observations. The authors observed that coherent motion elicited three important components which have distinct neural sources. Component P130 is generated in mid-temporal activations which might be assigned to the motion sensitive area hMT+. On the other hand, components N140 and P230 appear to originate from the area V6. Interestingly, the P230 component described as originating in area V6 seems to be the same that we observed exclusively in the WS group in our EEG/ERP study (described in Chapter 5). Accordingly, in our EEG experiment WS subjects showed lower P100 amplitude than control participants followed by an earlier N150 component and showed a novel component peaking positive at 200ms - P200- that was virtually absent in controls. Control participants, in turn, exhibited the expected positive P100 early visual component, followed by a negative peak - N170 – the putative face component. These observations provide a framework to understand the likely neural generators of the novel P200 component exclusively found in the WS group and integrate those findings with the matching pattern of medial activation found in the fMRI study.

An additional point highlighted by the fMRI study relates to the ventral stream activation in the WS group. In our study we were not able to detect significant differences in activation in areas along the ventral visual pathway possibly due to our small sample size or to the use of strict cluster-threshold correction. In any case dorsal stream deficits are disproportionately larger than any ventral stream impairment that might have gone undetected. Nevertheless, by examining the statistical maps of brain activation in both WS and control groups we verified a more broadly distributed activation of the ventral region evidencing less specialization in the WS group as contrasted with the control group. Based on these evidences, we may hypothesize that the substantial reorganization observed in the dorsal visual pathway in WS has implications on the pattern of activation along the ventral visual pathway. It remains however to identify which brain areas are underlying the integration of information from the two pathways and what mechanisms are involved in such processes.

Implications for models of disease mechanism

The work presented in this thesis provides important hints regarding the mechanisms underlying the most predominant type of dysfunction in the WS cognitive profile, namely the visuospatial deficits. The improvement in the understanding of these deficits is particularly relevant since they have important impact in the daily life of WS patients.

We established WS as a model of impaired visual coherence with predominant difficulties in visual integration. These deficits were linked to the dorsal stream dysfunction which has been frequently described in this clinical population. In spite of our reduced sample sizes, the combination of our EEG/ERP data with our fMRI findings resulting from random effects analyses provided strong evidence in favour of a substantial reorganization in the dorsal visual stream in this clinical model.

Interestingly, these studies provided evidence of a new dissociation in the WS group, this time related to the dorsal stream functioning (medial vs. lateral routes within of dorsal stream) which should be further tested in future studies. This evidence extends our knowledge regarding the nature and the extent of dorsal visual stream impairment in WS. So far, fMRI studies have reported altered activations in occipital and parietal (IPS) areas to support the notion of dorsal stream dysfunction in this condition (Meyer-Lindenberg et al., 2004). However, it was unknown whether an alternative neural network was recruited in the WS brain to compensate the abnormal pattern of activation in areas typically involved in coherent perception. These results open a new window of opportunity to investigate the role of the areas predominantly activated by the WS group (cuneus, precuneus and retrosplenial cortex) in other functions also affected in this disorder. Such an example is the role of retrosplenial cortex in the combined use of information from egocentric and allocentric spatial reference frames in WS.

Besides giving new input regarding dorsal visual stream function in WS, our studies also provided helpful evidence concerning the ventral visual stream functioning and the interconnections between both. The function of ventral visual pathway was found to be slightly altered as was demonstrated by behavioural assessment (ego-allo spatial judgments described in Chapter 4) as well as by neuroimaging patterns (in Chapter 6). These findings are concordant with new increasing perspective that ventral stream is not “totally preserved” as was initially defined. Since the ventral stream was not the main subject of interest in the present studies, subsequent work should be conducted in order to dissect the functioning of

areas within this pathway. The use of high-level functional localizers will be important to disentangle the specific role of each category-sensitive area within the ventral visual pathway.

Finally, it remains to be referred the role of the intellectual disability present in the WS population (Martens et al., 2008) in the observed deficits. In our studies this was tested by including control groups matched for intellectual quotient (IQ) or computing correlations between our functional measures and IQ. Interestingly, we did not find a relation between IQ and our behavioural and functional measures. We may conclude that the visuospatial deficits found in WS as were assessed by our studies might not be explained by generalized cognitive deficits and are distinctive in the WS cognitive phenotype.

Implications for typical brain functioning

The comprehension of mechanisms underlying visuospatial dysfunction in WS brings new insight into the knowledge of the cognition in general and particularly regarding the relation between genes, brain and behaviour. In this thesis, we provide some contributions to this point.

First, we provided evidence supporting the notion that the dorsal visual stream (occipito-parietal areas) should be considered as being part of the neural network involved in global integration since we established the link between visual coherence deficits and dorsal stream dysfunction in WS. Additionally, our first study also pointed out the need to investigate the brain areas underlying the integration of both local and global levels of organization. Given that unlike the findings concerning WS, we did not find integration impairments in the ASD, we propose that these ‘integrative’ areas may be preserved in this disorder. This stresses the effectiveness of directly compare these two neurodevelopmental disorders who share some visual features while being in the opposite pole of the socio-emotional continuum.

Secondly, we found evidence of two different gamma sub-bands accounting for the construction of coherent percepts (Chapter 5): a low-frequency gamma band (20-40 Hz) and a high-frequency gamma band (40-90Hz). Such findings are in line with studies stating that there is a frequency specialization in the gamma-band activity domain with distinct sub-bands contributing to distinct cognitive processes (Buschman & Miller, 2007; Vidal et al., 2006).

Additionally, our results supported the evidence of two parallel pathways within the dorsal visual stream processing motion information: the medial part involving the contribution of area V6 and the lateral part including motion sensitive areas hMT+. This is a recently proposed model that receives important input from studies like ours on neurodevelopmental disorders of dorsal stream dysfunction.

Finally, the study of functional dichotomies in WS (local-global, ego-allo, dorsal-ventral) demonstrated that the existence of dissociation between some cognitive functions and their associated neural networks may disrupt the integration mechanisms essential to reach the best possible level of performance in terms of effective brain functioning. On the other hand, the fact that in a given dissociation mechanism one level is more spared than other enables the possibility of reorganization through the more preserved pathway. In this way, the redistribution of activity allows the use of more intact regions which may contribute to partially compensate the deficits observed in other areas. The research in the WS functional dissociations also suggested the need to taking into account the possible interconnections between the different dissociation nodes. The idea that independent functioning cognitive modules can be identified in neurodevelopmental disorders has been modified in order to incorporate findings suggesting the interdependency of different cognitive functions and the contributions of a given brain region to multiple cognitive, sensory and motor processes.

Conclusions

The work presented in this thesis, confirmed the dorsal stream dysfunction in WS from the point of view of different functional dissociations (local-global / ego-allo / dorsal-ventral). We went further in the understanding of these impairments by demonstrating a substantial reorganization within the dorsal visual pathway in WS involving a more medial neural network in response to visual coherence. This reorganization may implicate alterations in the ventral stream functioning changing the notion of “totally intact” ventral visual stream in this genetic disorder. These findings improve our understanding of the neural mechanisms underlying visuospatial impairment in WS and provide additional knowledge into the functional organization of the dorsal visual pathway.

References

- Atkinson, J., Braddick, O., Anker, S., Curran, W., Andrew, R., Wattam-Bell, J., et al. (2003). Neurobiological models of visuospatial cognition in children with Williams syndrome: measures of dorsal-stream and frontal function. *Dev Neuropsychol*, *23*(1-2), 139-172.
- Atkinson, J., King, J., Braddick, O., Nokes, L., Anker, S., & Braddick, F. (1997). A specific deficit of dorsal stream function in Williams' syndrome. *Neuroreport*, *8*(8), 1919-1922.
- Bellugi, U., Lichtenberger, L., Jones, W., Lai, Z., & St George, M. (2000). I. The neurocognitive profile of Williams Syndrome: a complex pattern of strengths and weaknesses. *J Cogn Neurosci*, *12 Suppl 1*, 7-29.
- Bellugi, U., Sabo, H., & Vaid, J. (1988a). Dissociation between language and cognitive functions in Williams syndrome. In D. Bishop & K. Mogford (Eds.), *Language development in exceptional circumstances*. (pp. 177-189). London: Churchill-Livingstone.
- Bellugi, U., Sabo, H., & Vaid, J. (1988b). Spatial deficits in children with Williams syndrome. In U. Stiles-Davis, U. Kritchvshy & U. Bellugi (Eds.), *Spatial cognition: brain bases and development*. (pp. 273-297). Hillsdale: Lawrence Erlbaum Associates, Inc.
- Burgess, N. (2006). Spatial memory: how egocentric and allocentric combine. *Trends Cogn Sci*, *10*(12), 551-557.
- Buschman, T. J., & Miller, E. K. (2007). Top-down versus bottom-up control of attention in the prefrontal and posterior parietal cortices. *Science*, *315*(5820), 1860-1862.
- Castelo-Branco, M., Mendes, M., Sebastiao, A. R., Reis, A., Soares, M., Saraiva, J., et al. (2007). Visual phenotype in Williams-Beuren syndrome challenges magnocellular theories explaining human neurodevelopmental visual cortical disorders. *J Clin Invest*, *117*(12), 3720-3729.
- Farran, E. K., & Jarrold, C. (2003). Visuospatial cognition in Williams syndrome: reviewing and accounting for the strengths and weaknesses in performance. *Dev Neuropsychol*, *23*(1-2), 173-200.
- Frith, U. (1989). *Autism : explaining the enigma*. Oxford, UK ; Cambridge, MA, USA: Basil Blackwell.
- Golarai, G., Hong, S., Haas, B. W., Galaburda, A. M., Mills, D. L., Bellugi, U., et al. (2010). The fusiform face area is enlarged in Williams syndrome. *J Neurosci*, *30*(19), 6700-6712.
- Happe, F. G. (1996). Studying weak central coherence at low levels: children with autism do not succumb to visual illusions. A research note. *J Child Psychol Psychiatry*, *37*(7), 873-877.
- Martens, M. A., Wilson, S. J., & Reutens, D. C. (2008). Research Review: Williams syndrome: a critical review of the cognitive, behavioral, and neuroanatomical phenotype. *J Child Psychol Psychiatry*, *49*(6), 576-608.
- Mervis, C. B., Robinson, B. F., Bertrand, J., Morris, C. A., Klein-Tasman, B. P., & Armstrong, S. C. (2000). The Williams syndrome cognitive profile. *Brain Cogn*, *44*(3), 604-628.
- Meyer-Lindenberg, A., Kohn, P., Mervis, C. B., Kippenhan, J. S., Olsen, R. K., Morris, C. A., et al. (2004). Neural basis of genetically determined visuospatial construction deficit in Williams syndrome. *Neuron*, *43*(5), 623-631.
- Meyer-Lindenberg, A., Mervis, C. B., Sarpal, D., Koch, P., Steele, S., Kohn, P., et al. (2005). Functional, structural, and metabolic abnormalities of the hippocampal formation in Williams syndrome. *J Clin Invest*, *115*(7), 1888-1895.
- Mobbs, D., Eckert, M. A., Menon, V., Mills, D., Korenberg, J., Galaburda, A. M., et al. (2007). Reduced parietal and visual cortical activation during global processing in Williams syndrome. *Dev Med Child Neurol*, *49*(6), 433-438.
- O'Hearn, K., Courtney, S., Street, W., & Landau, B. (2009). Working memory impairment in people with Williams syndrome: effects of delay, task and stimuli. *Brain Cogn*, *69*(3), 495-503.

- O'Hearn, K., Roth, J. K., Courtney, S. M., Luna, B., Street, W., Terwillinger, R., et al. (2011). Object recognition in Williams syndrome: uneven ventral stream activation. *Dev Sci*, *14*(3), 549-565.
- Pani, J., Mervis, C. B., & Robinson, B. F. (1999). Global spatial organization by individuals with Williams syndrome. *Psychological Science*, *10*(5), 453-458.
- Paul, B. M., Stiles, J., Passarotti, A., Bavar, N., & Bellugi, U. (2002). Face and place processing in Williams syndrome: evidence for a dorsal-ventral dissociation. *Neuroreport*, *13*(9), 1115-1119.
- Pitzalis, S., Bozzacchi, C., Bultrini, A., Fattori, P., Galletti, C., & Di Russo, F. (2013). Parallel motion signals to the medial and lateral motion areas V6 and MT+. *Neuroimage*, *67*, 89-100.
- Spencer, J., O'Brien, J., Riggs, K., Braddick, O., Atkinson, J., & Wattam-Bell, J. (2000). Motion processing in autism: evidence for a dorsal stream deficiency. *Neuroreport*, *11*(12), 2765-2767.
- Vann, S. D., Aggleton, J. P., & Maguire, E. A. (2009). What does the retrosplenial cortex do? *Nat Rev Neurosci*, *10*(11), 792-802.
- Vidal, J. R., Chaumon, M., O'Regan, J. K., & Tallon-Baudry, C. (2006). Visual grouping and the focusing of attention induce gamma-band oscillations at different frequencies in human magnetoencephalogram signals. *J Cogn Neurosci*, *18*(11), 1850-1862.
- Zaehle, T., Jordan, K., Wustenberg, T., Baudewig, J., Dechent, P., & Mast, F. W. (2007). The neural basis of the egocentric and allocentric spatial frame of reference. *Brain Res*, *1137*(1), 92-103.

List of Publications

Bernardino, I., Mouga, S., Almeida, J., van Asselen, M., Oliveira, G. & Castelo-Branco, M. (2012). A Direct Comparison of local-global integration in autism and other developmental disorders: implications for the central coherence hypothesis. *PLoS One*. 7:(6) e3935.

Bernardino, I., Castelo-Branco, M. & van Asselen, M. (2013). Egocentric and allocentric spatial representations in Williams syndrome. *Journal of the International Neuropsychological Society*, 19, 1-9.

Bernardino, I., Castelhana, J., Farivar, R., Silva, E. & Castelo-Branco, M. (2013). Neural correlates of visual integration in Williams syndrome: gamma oscillation patterns in a model of impaired coherence. *Neuropsychologia*, 51, 1287-1295.

Violante, I.R., Ribeiro, M.J., Edden, R.A.E., Guimarães, P., **Bernardino, I.**, Rebola, J., Cunha, G., Silva, E. & Castelo-Branco, M. (2013). GABA deficit in the visual cortex of patients with neurofibromatosis type 1: genotype-phenotype correlations and functional impact. *Brain*, 136, 918:25.

Violante, I.R., Ribeiro, M.J., Cunha, G., **Bernardino, I.**, Duarte, J.V., Ramos, F., Saraiva, J., Silva, E. & Castelo-Branco, M. (2012). Abnormal brain activation in neurofibromatosis type 1: a link between visual processing and the default mode network. *PLoS One*. 7:6, e38785.

Ribeiro, M.J., Violante, I.R., **Bernardino, I.**, Ramos, F., Saraiva, J., Reviriego, P., Upadhyaya, M., Silva, E. & Castelo-Branco, M. (2012). Abnormal achromatic and chromatic contrast sensitivity in neurofibromatosis type 1. *Invest Ophthalmol Vis Sci*. 53:1, 287-293.

Agradecimentos

Os “números arriscados” são aqueles que mais nos põem à prova. São os que nos fazem testar os nossos limites. São os que nos fazem evoluir. São aqueles que nos fazem sustentar a respiração. São também os que nos fazem vibrar. São principalmente os que nos mostram quem temos incondicionalmente ao nosso lado e que, de uma forma ou de outra, são parte muito importante do resultado final. Este trabalho de doutoramento foi, para mim, um “número arriscado” unicamente possível porque partilhado com pessoas excepcionais que me ensinaram que vale a pena arriscar e ir mais além. É a todas essas pessoas que dedico estas páginas.

Começo por dirigir um profundo agradecimento ao Professor Miguel Castelo-Branco, a pessoa que esteve sempre nos “bastidores”, na base deste trabalho e cujo contributo científico e pessoal foi infindável. Agradeço todas as aprendizagens, o entusiasmo e paixão pela ciência que me transmitiu, o incentivo à criatividade e ao espírito crítico e, sobretudo, todo o apoio e confiança que depositou em mim.

Agradeço à Marieke, por todos os ensinamentos, pelas palavras sensatas, de amizade e encorajamento e pela confiança que me transmitiu. Por ser, para mim, um exemplo de rigor e profissionalismo que vou sempre guardar.

Um agradecimento especial a todos os ‘meus’ meninos e jovens com Síndrome de Williams e às suas famílias pelo sorriso permanente, pela incansável colaboração e pela constante luta a que se propõem. Eles foram o motor deste trabalho e com eles aprendi que o amor pode transformar os ‘enganos’ da genética. Acredito nestas crianças, no seu potencial e no amor das suas famílias. Acredito, também, que valerá sempre a pena continuar a olhar para elas com o intuito de descortinar os enigmáticos mecanismos que as tornam tão especiais.

Um agradecimento importante a todas as pessoas e instituições que tiveram uma participação fundamental nestes trabalhos. Agradeço à escola “Rumo ao Futuro”, aos seus alunos e professores e especialmente à sua diretora, a minha Titi Luísa, pela forma como me acolheram e pela disponibilidade permanente. Agradeço ainda à Associação Portuguesa de Pais e Amigos do Cidadão com Deficiência Mental” (APPACDM) de Coimbra e à “Associação Paralisia Cerebral Coimbra (APCC)/ Quinta da Conraria” pela sua valiosa colaboração.

A todos os meus colegas e amigos do IBILI, por serem únicos e singulares, por me proporcionarem momentos profundos de partilha e de amizade e por constituírem uma base sólida e segura que me permitiu arriscar e ir mais além. Agradeço à Susana, por me ter ensinado que as primeiras impressões podem falhar, por ser a minha rede de segurança sempre que a corda dançou em demasia, pela amizade, pelos sorrisos e risos incontrolláveis e pelos olhares cúmplices e encorajadores, obrigada por tudo! Ao Zé, por ser um ‘bocado de mim’, pelo carinho e cumplicidade, pelos ‘bons dias’, por me ajudar a acreditar e por ter sido a mão tão preciosa que me segurou nos últimos passos deste caminho. À Inês Almeida, companheira de gabinete e de percurso, amiga e confidente, pelos momentos intensos de partilha, por ter sido a mão que ajudou a manter o equilíbrio. À Inês Violante, pelo seu pragmatismo e determinação, por saber sempre determinar as funções certas, pelo seu exemplo e por me ter incentivado sempre a dar o próximo passo. Ao Castelhana, pela

disponibilidade incondicional, pela tranquilidade e simplicidade que põe em tudo o que faz. À Filipa, pela determinação e pelas palavras sempre sinceras, maduras e encorajadoras. À Ana pelo sorriso, à Andreia pela ternura, à Raquel pela boa-disposição, ao João Meneses pelas boas conversas e partilhas, ao Carlos Amaral pelo incentivo (e grande ajuda com os cabeçalhos do word!), ao Marco pelas brincadeiras, ao João Duarte pelo companheirismo, à Britta pelos bons momentos. A todos por terem deixado uma marca na minha vida, por terem vivido comigo as pequenas conquistas e as inevitáveis quedas que fizeram parte deste percurso.

Agradeço ao João, pela pessoa fantástica que é, pela amizade genuína e eterna, por ter sido o primeiro a acreditar e nunca ter desistido de mim e por continuar de mão dada comigo até ao fim, obrigada por tudo (e mais alguma coisa)! Aos “fantastic” Susana, Gonçalo e Alex. À Susana por ser a minha cúmplice, ao Gonçalo por ser sempre ‘Team Inês’ no sentido mais genuíno e afectuoso do termo, ao Alex pelo bons momentos vividos, sempre no “bom sentido”. Aos três pela amizade, pelos momentos de diversão e de cumplicidade que vivemos e que foram a lufada de ar fresco que tornou mais leve cada passo arriscado. À Marta e à Catarina, à Inês, à Dora e à Ana por serem as amigas de sempre e por me acompanharem incondicionalmente, sustendo a respiração a cada desequilíbrio e suspirando de alívio a cada passada certa.

Agradeço à minha família por estar sempre na primeira fila a torcer pela caçula. Aos meus pais por todo o Amor e por serem o meu porto seguro. Aos meus irmãos, Ana e João, por serem os melhores irmãos e amigos do Mundo, pelos “gritos de incentivo”, pelos “aplausos”. Por vibrarem comigo mesmo quando a distância não tornou tão possível a partilha. Aos meus sobrinhos lindos que, mesmo não sabendo, foram, para mim, fonte de inspiração pela sua energia e vitalidade e pelo seu espírito curioso e traquina.

E agora que este “número arriscado” está perto da sua estreia, resta-me dizer...

Muito Obrigada!

Inês Bernardino, 2013

“Life should be lived on the edge of life. You have to exercise rebellion: to refuse to tape yourself to rules, to refuse your own success, to refuse to repeat yourself, to see every day, every year, every idea as a true challenge - and then you are going to live your life on a tightrope.” (Philippe Petit, In Man on Wire)

Curriculum Vitae

Inês Bernardino was born on July 23, 1984 in Marinha Grande, Portugal. In 2002, she completed her secondary school education at Escola Secundária Eng.º Acácio Calazans Duarte in Marinha Grande, after which she studied Psychology at the Faculty of Psychology and Educational Sciences of the University of Coimbra. For her master thesis, she did a research internship at the Visual Neuroscience Laboratory, IBILI, at the Faculty of Medicine of the University of Coimbra, under the supervision of Professor Miguel Castelo-Branco and Professor Mário Simões. In October 2007 she attained her master's degree and, at the same time, started her PhD research project on the “Investigation of the dorsal stream hypothesis in Williams syndrome” at the same laboratory, under the supervision of Professor Miguel Castelo-Branco and Professor Marieke van Asselen.